REGULATION OF THE BRANCH POINT BETWEEN THE GLYOXYLATE SHUNT AND THE TCA CYCLE IN MYCOBACTERIA

CHRISTINA MUELLER

(B.Sc. (Major in Integrative Biology), University of Basel)

A THESIS SUBMITTED

FOR THE DEGREE OF MASTER OF SCIENCE

IN INFECTIOUS DISEASES,

VACCINOLOGY AND DRUG DISCOVERY

DEPARTMENT OF MICROBIOLOGY

NATIONAL UNIVERSITY OF SINGAPORE

&

BIOZENTRUM

UNIVERSITY OF BASEL

2009

Acknowledgment

This Master thesis would not have been possible without the support of various people to whom I would like to express my sincere gratitude.

My deepest gratitude goes to my supervisor, Dr. Kevin Pethe, who introduced me to the fascinating world of research. Without his scientific guidance, encouraging support and patience I would never have been able to develop this thesis.

I also wish to express my thanks to Dr. Thomas Dick for giving me the opportunity to pursue my project in the Tuberculosis Unit of Novartis Institute for Tropical Diseases.

My acknowledgment also goes to Sylvie Alonso and Gerd Pluschke for their willingness to be co-supervisors of my thesis.

I wish to express my appreciation to all the members of the Tuberculosis Unit for their guidance, assistance and help. In particular, I thank Melvin for introducing me to protein-work and for never getting tired in giving me helpful scientific advices; Wai Yee for introducing me to the world of molecular cloning; Boon Heng for teaching me about cell culturing and setting up MIC assays; and Meera and Patricia for their kindness in proof reading parts of my thesis. Thank you all for making the lab an enjoyable place to work in.

Special thanks goes to the other Master students in the TB Unit, Boon Zhi, Martin, Meliana and Paul, who became not only valued fellow students but also dear friends.

I would also like to thank National University of Singapore, Novartis Institute for Tropical Diseases, Swiss Tropical Institute and University of Basel for making this joint Master possible. In particular I thank Prof. Marcel Tanner and Dr. Markus Wenk.

In addition my thanks goes to all the professors/lecturers, from the various Institutes involved in this program, for their encouragement and assistance.

My whole-hearted gratitude goes to my parents, who gave me this unique opportunity to come to Singapore. Their unlimited care, generous support and constant encouragement gave (and give) me an emotional "crutch" and allow me to live carefree. I also would like to thank my brother Andreas for his moral support. *Engraziel fetg per tut!*

Last but not least, I thank all my dear friends from back home. Thanks for all your visits, your phone calls, your letters, postcards and emails and for the constant chocolate and cheese supply throughout the last year. There are no words in describing how much your friendship means to me.

Singapore, January 2009 Christina Müller

Table of Contents

Summary

The TCA cycle is the midpoint of a cell's metabolism. It's amphibolic character allows on one side the production of ATP, on the other side provides precursors for many biosynthetic pathways. Although hexoses are the preferred carbon source for most organisms, many bacteria such as *Escherichia coli* and *Mycobacterium tuberculosis*, are also able to grow on fatty acids or acetate as sole source of carbon and energy. This though, requires the operation of the anaplerotic sequence of the glyoxylate shunt. Under these circumstances, the glyoxylate bypass enzyme isocitrate lyase (ICL) is in direct competition with the TCA's cycle enzyme isocitrate dehydrogenase (ICD) for their common substrate isocitrate. As was found in *E. coli*, control of the glyoxylate bypass implies the increased expression of ICL, which is accompanied by modulation of ICD activity through a reversible phosphorylation by a isocitrate dehydrogenase kinase/phosphatase (ICDK/P).

The branch point in *M. tuberculosis* is more complex compared to *E. coli*. There are two *icl* genes (*icl-1* and *icl-2*) and two *icd* genes (*icd-1* and *icd-2*). The genes are phylogenetically not related. How *M. tuberculosis* regulates the glyoxylate shunt/TCA cycle branch point is currently unknown. However, bioinformatics predicted that the branch point has to be regulated by phosphorylation of ICD-1.

The understanding of the regulation of this branch point is of major importance, since it's believed that fatty acids are the main source of carbon and energy for *M. tuberculosis* in chronically infected animals and in man.

In this project, we aimed at finding this particular kinase/phosphatase in *Mycobacterium bovis* BCG. Further, we wanted to gain some insight into the coordinate regulation of this branch point. In order to pursue these purposes, we implemented to extract the putative kinase/phosphatase using an affinity column containing resins that bind ATP-binding proteins. In context with that, we also purified the substrates of the putative kinase/phosphatase, the two *M. tuberculosis* isocitrate dehydrogenases, ICD-1 and ICD-2, and tested their enzymatic activity.

From studies in *E. coli* it is known that the involvement of the glyoxylate bypass in metabolism depends on the nature of the available carbon source(s) and further, that the direction of the carbon flux into this bypass is dependent on the phosphorylation status of isocitrate dehydrogenase. Based on this, we tried to examine the phosphoproteom of BCG when either grown on glucose or on acetate by using a column, whose beads had an affinity for phosphoproteins. Since it was known that in *E. coli* the phosphorylation/dephosphorylation of ICD was carried out at the amino acid residue serine 113, we used Ser/Thr antibodies in order to detect the Ser/Thr phosphoproteins, among which we would eventually find ICD-1 and/or ICD-2. In addition, we created a BCG mutant strain expressing a modified *E. coli* ICD enzyme, dubbed ICD_{opt}, which did not permit phosphorylation at its serine 113. With this construct we aimed in

dysregulating the branch point in BCG. This would possibly allow to proof the concept that the branch point in *M. tuberculosis* is regulated analogue to the one in *E. coli*.

During the course of this project, we were neither able to extract the putative ICDK/P in BCG, nor gaining insight into the phosphoproteom and its dependence on the carbon source. Moreover, when growing BCG expressing ICD_{opt} in either glucose or acetate based medium, we found no major phenotypic alterations in comparison to wt BCG. In order to pursue the intention of dysregulating the branch point we constructed a BCG *Δicd-1* and a BCG *Δicd-2* knockout mutant. Performing growth assays with these two constructs showed no phenotypic differences when compared to wt BCG. Furthermore, measuring ICD enzyme activity we found no major differences between BCG *Δicd-1* and wt BCG. However, no isocitrate dehydrogenase activity was detected in the BCG *Δicd-2* strain. This result was surprising since 1) it suggested that ICD-1 does not contribute to the overall isocitrate dehydrogenase activity in BCG and 2) the growth kinetic of the BCG Δ*icd-2* strain was comparable to the growth of the parental strain on all tested carbon sources. We demonstrated that the BCG *Δicd-2* knockout mutant achieved optimal growth by diverting the carbon flux through the glyoxylate shunt, even on glucose or glycerol. These results were confirmed by showing that the BCG *Δicd-2* strain is deficient for the synthesis of α-ketoglutarate (the end-product of the reaction catalyzed by ICD), thereby rendering the mutant strain auxotrophic for glutamic acid.

Overall, these results suggest that ICD-2 is the only ICD enzyme active in BCG. The reasons why ICD-1 is not enzymatically active are not clear, but it could be explained by a lack of expression or by a constitutive phosphorylation of the enzyme at the active site. Indeed, much more work needs to be done for the better understanding of the regulation of this branch point. Based on our experimental findings, we predict that ICD-1 and ICD-2 differ in their function and possibly in their form of regulation by the putative isocitrate dehydrogenase kinase/phosphatase.

List of Tables

List of Figures

List of Abbreviations

2D	Two-Dimensional
ABP	ATP-Binding Proteins
AP	Alkaline Phosphatase
ATP	Adenosine Triphosphate
AIDS	Acquired Immunodeficiency Syndrome
bp	Basepair
BCA	Bicinchoninic Acid
BCG	Bacillus of Calmette and Guérin
BCIP/ NBT	"Alkaline Phosphatase Chromogen"
BSA	Bovine Serum Albumin
C	Carbon
CoA	Coenzyme A
CV	Column Volume
DNA	Deoxyribonucleic Acid
dNTP	Deoxyribonucleotide Triphosphate
DOTS	Directly Observed Therapy, Short-Course
DTT	1,4-Dithiothreitol
EDTA	Ethylenediaminetetraacetic Acid
FAD(H)	Flavin Adenine Dinucleotide (Reduced)
BSA-FAF	Bovine Serum Albumin Fatty Acid Free

FBS	Fetal Bovine Serum
GC	Guanine and Cytosine
GS-GOGAT	Glutamine Synthetase – Glutamate Synthase
His	Histidine
HIV	Human Immunodeficiency Virus
ICD	Isocitrate Dehydrogenase
ICD_{opt}	Isocitrate Dehydrogenase Optimised
ICDK/P	Isocitrate Dehydrogenase Kinase/Phosphatase
ICL	Isocitrate Lyase
IMAC	Immobilised Metal Ion Affinity Chromatography
IFN	Interferon
IgG IgM	Immunoglobulin G
IgM	Immunoglobulin M
IL	Interleukin
INH	Isoniazid
IPTG	Isopropyl-Beta-D-Thiogalactopyranoside
hyg	Hygromycin Resistance Cassette
kDa	Kilodalton
K_m	Michaelis-Menten Constant
MAS	Malate Synthase
MAPK	Mitogen-Activated Protein Kinase
MBP	Maltose Binding Protein
MCL	2-Methylisocitrate Lyase

MDR-TB	Multidrug-Resistant Tuberculosis
MHC II	Major Histocompatibility Complex Class II
MIC	Minimum Inhibitory Concentration
Mg	Magnesium
Mn	Manganese
MTBC	*M. tuberculosis* Complex
NAD(H)	Nicotinamide Adenine Dinucleotide (Reduced)
Ni-NTA	Nickel-Nitrilotriacetate
3-NP	3-Nitropropionate
NADP(H)	Nicotinamide Adenine Dinucleotide Phosphate (Reduced)
NRP	Non-Replicating Persistence
OD_{600}	Optical Density at a Wavelength of 600 nm
o/n	Over Night
PCR	Polymerase Chain Reaction
PPD	Purified Protein Derivative
PstP	Serine/Threonine Protein Phosphatase
PVDF	Polyvinylidene Fluoride
PZA	Pyrazinamide
RIF	Rifampicin
RNA	Ribonucleic Acid
RNI	Reactive Nitrogen Intermediates
ROI	Reactive Oxygen Intermediates
rRNA	Ribosomal Ribonucleic Acid

RT	Room Temperature
SDM	Site Directed Mutagenesis
SDS-PAGE	Sodium Dodecyl Sulfate Polyacrylamide Gel Electrophoresis
Ser/Thr	Serine/Threonine
STPK	Serine/Threonine Protein Kinase
STR	Streptomycin
TACO	Tryptophan-Aspartate Containing Coat Protein
TB	Tuberculosis
TCA	Tricarboxylic Acid
TGF	Transforming Growth Factor
TNF	Tumor Necrosis Factor
TLR	Toll-Like Receptor
Trx	Thioredoxin
V_{max}	Maximum Velocity
WHO	World Health Organisation
XDR	Extensively-Drug Resistance

Introduction

PART I

1.1 Tuberculosis from a Global Perspective

1.1.1 Burden of Tuberculosis

Tuberculosis (TB) belongs with approximately 3 million annual deaths worldwide to the group of "big killer diseases". In 2006 there were according to WHO an estimated 9.2 million new cases of TB (139 per 100,000 population; Figure 1), including 0.7 million HIV-positive cases (8% of the total).

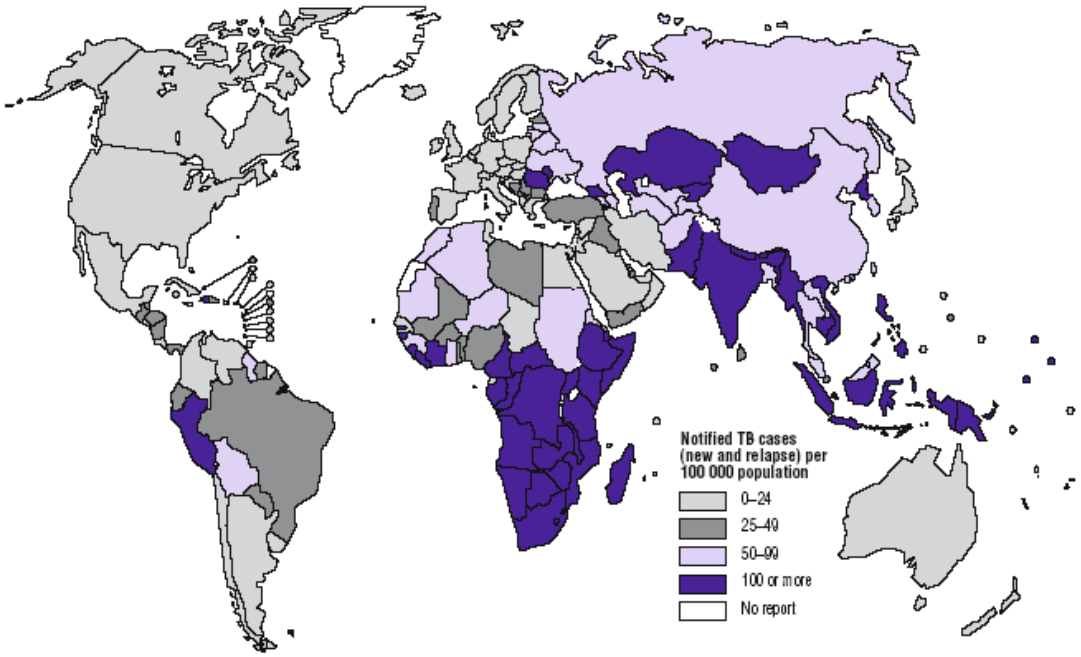

Figure 1.1 | **Global Burden.** Estimated TB incidence rates by country, 2006. (WHO/HTM/TB/2008.393)

Further, there were an estimated 14.4 million prevalent cases and an estimated 1.7 million deaths, out of which 0.2 million were HIV positive. Approximately 1.5 million cases were said to have multidrug-resistant tuberculosis (MDR-TB). The incidence of 9.1 million cases in 2005 increased to 9.2 million cases in 2006, which is most probably due to population growth. South-East Asia along with the Western Pacific regions account for 55% of global cases, and Africa accounts for 31%. Comparing the absolute number of cases; India, China, Indonesia, South Africa and Nigeria rank first to fifth respectively. Africa has the highest incidence rate per capita (363 per 100,000 population), as well as the highest incidence of HIV-related TB since TB control in Africa is dominated by the worsening HIV epidemic.

These numbers demonstrate that TB control is difficult and even though it is a curable disease, many people still die from it. In response to this situation, a global control strategy, called DOTS (Directly Observed Therapy, Short-course), was introduced by WHO. The basic five components of the DOTS strategy are:

1 Sustained political commitment with increased and sustained financing.

2 Case detection through quality-assured bacteriology, *i.e.* guarantee access to quality assured sputum microscopy.

3 Standardised short-course chemotherapy for all cases of TB under proper case management conditions, including direct observation of treatment.

4 Uninterrupted supply of quality-assured drugs in context with an effective management system.

5 Recording and reporting system, enabling outcome assessment of all patients and assessment of overall programme performance.

The DOTS approach is nowadays one of the most important "Stop TB" Strategies. WHO reported that in 2006, out of the estimated 9.2 million new cases, 54% were detected by DOTS program.

(WHO/CDS/TB/2003.313), (WHO/HTM/TB/2008.393), (www.who.int/tb/en/)

1.1.2 Global Epidemiology

The distribution of tuberculosis within different populations and/or regions depends on the transmission. The incidence rate was shown to be highest among young adults, where transmission has been stable or has increased over decades and most cases were attributable to a new infection or reinfection. In comparison, the caseload changes in older adults, where transmission is falling and most cases are due to reactivation of latent infection. In countries with low incidence rates such as Western Europe and North America, native tuberculosis patients are usually old, while immigrants from countries with high-incidence tend to be younger (Dye, 2006).

The comparatively few cases that are found among children (*i.e.* between 0-14 years old), even in countries with high transmission, may not reflect the reality due to the fact that diagnosis of childhood tuberculosis is difficult.

Also, there is a higher number of smear-positive cases found in men than in women (1.4 million compared to 775,000 in 2004). One explanation is that women have poorer access to health facilities, but it is also an indication of the real epidemiological differences in

exposure to infection and susceptibility to development of active disease between the genders (Dye, 2006).

The global increase in tuberculosis incidence is ascribable to the remarkable increase of cases in countries of Eastern Europe (principally the former Soviet Union) since 1990, and in sub-Saharan Africa since the mid-1980. The reason for the resurgence of tuberculosis in Eastern Europe can be explained by the worsening of the economical situation such as increased levels of unemployment, by the deteriorating public health systems and the general failure of tuberculosis control (Frieden et al., 2003), (Olusoji Adeyi *et al*. 2007). Interesting to mention is that from a global point of view, only 3% of all new tuberculosis cases are said to be multidrug resistant. However, the frequency is higher in so-called hotspot areas, e.g. parts of Eastern Europe. TB patients in Eastern Europe and central Asia are ten times more likely to have MDR-TB than in other parts of the world, and 5.5% of the new cases are MDR-TB (Olusoji Adeyi *et al*. 2007). Overall it seems that currently, in Eastern Europe as well as in sub-Saharan Africa, the rate of increase has slowed since the mid-1990s and in Eastern Europe it might even be in decline (Dye et al., 2005).

From 2004 onwards, the worldwide continued increase is estimated to be wholly attributable to the increase of cases in Africa, and HIV plays an important role. Worldwide, in 2004, around 13% of the new tuberculosis cases in adults were HIV infected. Regional differences where immense, with 34% in Africa but only 1.4% in the Western Pacific region. Further, it was shown that areas in Africa, where HIV infection rates were high in the general population, also had a high number of patients with tuberculosis and a high proportion of those tuberculosis patients were women between

15-24 years old. In 2004, co-infection with tuberculosis exceeded 50% in countries like Botswana, South Africa, Zambia and Zimbabwe (WHO/HTM/TB/2006.362). Overall, the increase in tuberculosis cases in Africa is slowing, most probably because HIV infection rates are stabilizing or even falling (Dye, 2006). It is also believed that HIV has a smaller impact on tuberculosis prevalence than on incidence, since life expectancy of tuberculosis patients is significantly diminished when infected with HIV (Corbett et al., 2004). Unfortunately, because HIV has had and presently still does have a big influence on tuberculosis epidemiology, other important risk factors such as chronic diseases (diabetes, undernutrition, respiratory illnesses due to tobacco and air pollution) have been somewhat neglected (Dye, 2006).

Tuberculosis kills young adults and over 80% of DALYs (disability-adjusted life years) are lost because of premature death rather than illness. Global and regional trends in tuberculosis deaths are vague, because most countries with high tuberculosis burden do not compile reliable statistics on the cause of death. Nevertheless, it has been indicated that death rates from tuberculosis, after having risen during the 1990s, might have been falling since 2000 (Dye, 2006).

In 1991, the WHO was aiming to detect 70% of all infectious cases of tuberculosis and to cure 85% of them by 2005. Unfortunately, the reality nowadays shows that although more than 80% of known cases are successfully treated, only 45% of the cases are detected. New targets were set by Millennium Development Goals and Stop TB Partnership, but in order to meet them, the generation and implementation of new information is needed (Onyebujoh et al., 2006).

1.2 History of Tuberculosis

1.2.1 The Origin

The *M. tuberculosis* complex (MTBC) includes the human and animal pathogens *M. africanum*, *M. microti*, *M. canetti*, *M. tuberculosis* and *M. bovis*. It has emerged probably some 40,000 years ago from its progenitor in East Africa, the region, where at the same time the dissemination of modern human populations started. The two main lineages of MTBC arose later, some 20,000 to 30,000 yeas ago. One of the two lineages spread exclusively among humans, whereas the other is believed to have spread from humans to animals. The latter one includes the pathogens *M. bovis* and *M. caprae.* The transition from human to animal hosts can be related to the plant and animal domestication that took place some 13,000 years ago in the fertile Crescent (Wirth et al., 2008).

The use of comparative genomics and related technologies allowed discrimination between the members of the MTBC by comparison of the distribution of RDs (deleted regions within the genome). It was found that *M. tuberculosis* strains are more closely related to the common ancestor of the MTBC than are *M. bovis* strains. It seems plausible that a separate lineage, represented by *M. africanum*, *M. microti* and *M. bovis*, evolved from the progenitor of nowadays' *M. tuberculosis* isolates and adapted to new hosts. Whether the progenitor of *M. tuberculosis* was already a human pathogen or not, remains to be determined (Brosch et al., 2001).

It is of importance to note that archeological evidence of early tuberculosis is not only found in East Africa but also in America. It is believed that the disease occurred throughout America, prior to the arrival of the first European explorers (Daniel, 2006).

1.2.2 The Great White Plague

The epidemic spread of TB was slow but urbanisation in feudal Europe, which resulted in increased population density and thus, allowed person-to-person spread of the tubercle bacilli, set off an epidemic that came to be called "The Great White Plague". From the 17th to the 18th century, almost all Western Europeans were infected and one in four deaths were due to tuberculosis. As infected Western Europeans started travelling to colonize alien lands and migrants later started to settle down, almost of all in North America, the epidemic followed them and finally, the disease spread worldwide. In the 18th and 19th century, tuberculosis peaked in West Europe and the United States and was the largest cause of death. 100-200 years later, it had disseminated to Eastern Europe, Asia, Africa and South America. (Daniel, 1994)

1.2.3 Aetiology of Tuberculosis

Tuberculosis was well-known in ancient Greece. Hippocrates recognised tuberculosis and understood the clinical manifestation of the disease. Nonetheless, nothing significant happened in the history of tuberculosis until the 9th and 10th centuries. It was around 1020, when Ibn Sina, a Persian physician and philosopher, also known by his latin name Avicenna, suggested the communicable nature of the disease. He wrote excellent descriptions of the clinical features and the pathology of tuberculosis and developed a method of quarantine (Daniel, 1994). Much later, in 1689, Dr. Richard Morton established that the pulmonary form of the disease was associated with "tubercles". As late as in the 1820s, tuberculosis was identified as a single disease and in 1839 was

termed “tuberculosis” by J.L.Schönlein. Also during that time, tuberculosis sanatoria were established (Figure 1.2) and became common throughout Europe from the end of the late 19th century onwards (Daniel, 1994). It was Robert Koch in 1882, who changed the thinking about tuberculosis. He described the tubercle bacillus *M. tuberculosis* and demonstrated it to be the cause of tuberculosis using his famous postulates, the Henle-Koch postulates. To this day, they are the standard for the demonstration of infectious etiology (Daniel, 2006). Further, he isolated a substance from tubercle bacilli that he called tuberculin. With this and other achievements such as development of staining techniques and implementation of cultures on solid media, Robert Koch can be thought as the founder of the science of microbiology (Daniel, 2006). Overall, it was the first time that a disease was directly correlated to bacteria. In 1906 Albert Calmette and Camille Guérin developed a vaccine for immunising against tuberculosis, termed BCG (Bacillus of Calmette and Guérin) vaccine, which derived from the attenuated strain of *M. bovis*. It was first used in humans in 1921 in France, but received worldwide acceptance only after World War II (Daniel, 1994).

Figure 1.2 | **The search for a cure**. At the end of the 19th century, sanatoria such as Valmora were established as a solution to the problems of tuberculosis control.

(www.unm.edu/~market/cgi-bin/archives/002658.html)

The grim and often infaust prognosis of tuberculosis changed dramatically in November 1944, when a woman, who failed to respond to the common anti-tubercular treatment at that time – rest and thoracoplasty – was treated with streptomycin, isolated only 11 months earlier by Selman Waksman, got cured. Similar were the first results with patients treated with isoniazid. With these striking results, the era of successful chemotherapy for

tuberculosis seemed to be launched, and people thought that the conquest of tuberculosis was within one's reach (Daniel, 1994).

1.3 Transmission and Progression

Worldwide, every third person is said to be latently infected with *M. tuberculosis*. Individuals with prolonged, frequent or intense contact have a particularly high chance of becoming infected; the estimated infection rate lies around 22%. A person with untreated, active tuberculosis can infect 10-15 other individuals per year. Further at risk are people, who live in areas where tuberculosis is a common disease; low-income and/or medically neglected populations; people with poor nutrition; people living in crowded or unsanitary living condition; elderly people and infants, especially when exposed to adults in high-risk categories; immunocompromised people, especially HIV/AIDS patients, persons, whose immunity is suppressed, especially those on long term steroids; diabetics; health care workers; and drug abusers.

Even though the great majority of infected individuals are latent, asymptomatic carriers of *M. tuberculosis* and do not exhibit any clinical symptoms, they represent slow-release reservoirs. Latently infected individuals have a 2-23% lifetime risk of developing reactivation of the disease and this risk increases to 10% per annum in persons with immunodeficiency states, mostly due to HIV co-infection.

Disease reactivation and the subsequent primary infection of immunocompromised individuals results in more than 3 million deaths annually. (www.infektionsbiologie.ch), (WHO/CDS/TB/2003.313), (www.who.int/tb/en/)

The spread of the disease (Figure 1.3) can occur only from people with active, but not latent tuberculosis. Individuals become infected by the inhalation of air-borne droplet nuclei containing *M. tuberculosis*. Transmission is dependent on the number of infectious droplets expelled by the carrier, the duration of exposure and the virulence of the *M. tuberculosis* strain. Since tuberculosis is spread from person to person, isolation of patients with active disease is an efficient strategy to break the chain of transmission. Subsequent anti-tubercular drug treatment of patients with active but non-resistant tuberculosis, generally results in cessation of transmission after two weeks (Zahrt, 2003).

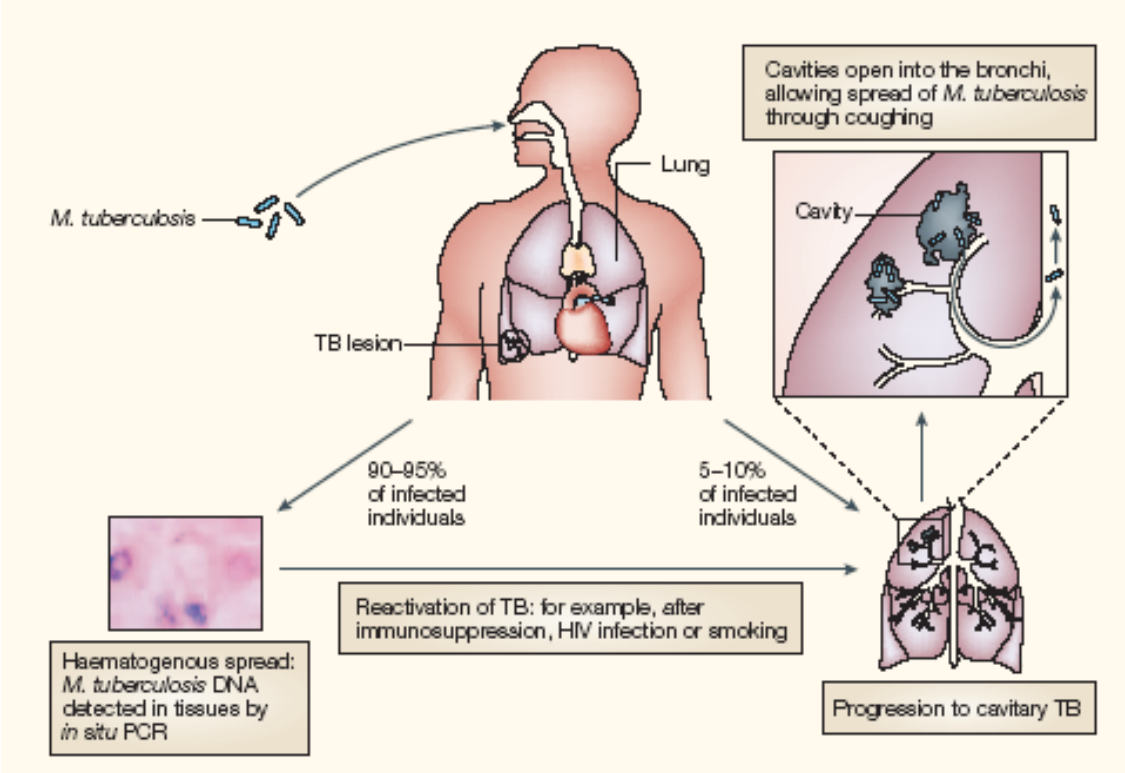

Figure 1.3 | **Transmission and progression with M. tuberculosis.** Tuberculosis is spread by aerosols and can lead to an infection, which results in the formation of a primary lesion. Around 3 weeks upon first infection of unimmunised humans, the bacilli spread haematogenously. In 90-95% the infection remains latent. 5-10% of infected individuals show a progression of the disease. Mostly, the disease remains latent for decades, but can be reactivated due to suppression of the immune system (e.g. HIV). Progression of the disease leads to cavity formation and hence, to active TB, which results in the spread of the bacilli by aerosols {Rook, 2005 #61}.

1.4 Clinical Manifestations

The disease affects primarily the lungs in "discrete consolidated foci", named granulomas. Tuberculosis can be divided into active disease, characterised by the microscopic detection of viable bacteria in a patients sputum; and latent disease, where no overt signs of disease symptoms are exhibited. In the latter case, only a delayed-type hypersensitivity reaction, provoked by challenging a patient with purified protein derivative (PPD) subcutaneously, can provide evidence of being infected with *M. tuberculosis* (Boshoff and Barry, 2005). In 75% of cases with active disease the lungs are affected (pulmonary tuberculosis). The typical symptoms include chronic cough with blood-tinged sputum, chest pain, fever, night sweats, weakness and weight loss. The other 25% of active cases develop extrapulmonary tuberculosis, also termed disseminated tuberculosis or milliary tuberculosis. It spreads via the blood system and can attack the central nervous system (meningitis), the circulatory system, the lymphatic system (scrofula), the gastrointestinal system, the genitourinary system, bones (Pott's disease), joints and the skin (lupus vulgaris); (Frieden et al., 2003), (Smith, 2003). Infection at these sites provokes a variety of different symptoms. It appears as complication in 1-3% of all tuberculosis cases and occurs more frequently in people with weakened immune system, in people that had known tuberculosis with inadequate treatment, and infants. Although not contagious, it may co-exist with pulmonary tuberculosis, which in turn is infectious (Smith, 2003).

1.5 Pathogenesis

Infection of *M. tuberculosis* occurs via inhalation of the bacillus into a pulmonary alveolus. The first contact is thought to be with resident, alveolar macrophages and with dendritic cells. Dendritic cells play a very important role in this early stage of infection, since they are much better antigen presenting cells than are macrophages. They are also said to be essential in terms of T cell activation and dissemination of the bacilli due to their migratory feature (Smith, 2003).

M. tuberculosis is phagocytosed upon binding to a macrophage mannose and/or complement receptor. Within the host macrophage, the bacterium initially resides within an endocytic vacuole. The normal progression of the phagosome is characterised by phagosome-lysosome fusion, along with various alterations in the environment. The milieu becomes very hostile and the bacilli encounter acidic pH, reactive oxygen intermediates (ROI), lysosomal enzymes, toxic peptides and reactive nitrogen intermediates (RNI). RNIs were shown to be very effective against virulent mycobacteria in mouse macrophages and it was observed that resistance to RNIs correlates with virulence of *M. tuberculosis* (Smith, 2003).

Although macrophages in general provide an effective initial barrier against pathogens, *M. tuberculosis* has evolved many evasion strategies that allow survival within the phagocytic cell. One evasion mechanism is the inhibition of phagosome-lysosome fusion, thereby preventing *M. tuberculosis* from degradation. It has been observed that phagosomes containing pathogenic mycobacteria differ from the ones harbouring non-pathogenic strains (Koul et al., 2004). For example are many characteristics of early

endosomes retained in phagosomes harbouring pathogenic bacilli. The pH fails to acidify below pH 6.2 and the endosomal compartment remains positive for a range of early endosomal markers. One of them is rab5, a member of the small GTPases. It was found that the persistence of rab5 and the absence of rab7, a marker of the late endosome, is consistent with the arrest of the maturation from early to late endosome (Pethe et al., 2004), (Pieters, 2001). Another protein, termed TACO, was found to be associated with infected cells and is actively retained at the mycobacterial phagosome membrane and thus, prevents phagosome-lysosome fusion. Interesting to mention is the finding that the Kupffer cells in the liver, which is the major clearance site for mycobacterial infections, lack TACO (Pieters, 2001). Overall, how the tubercle bacilli achieve the arrest of phagosomal maturation is currently not known. Data from different groups suggest that more than one mechanism may be responsible for the process of arrest (Pethe et al., 2004).

Other evasion strategies include the inhibition of apoptosis and stimulation of bactericidal responses by interfering with signalling pathways that involve MAPKs, IFN-γ and calcium signalling (Koul et al., 2004). Antigen presentation seems also to be altered due to interactions of bacterial components with TLR2, which results in a decreased expression of MHC class II molecules. On the other hand, the production of inhibitory cytokines like IL-10 and TGF-β is increased (Smith, 2003).

Alveolar macrophages, which are not able to eliminate the ingested bacilli, eventually burst, because of continuous multiplication of the pathogen. This results in the release of the bacilli into the surrounding environment and to further ingestion by other alveolar macrophages and by inactivated monocytes, lymphocytes and neutrophils recruited from

the peripheral blood. Unfortunately, none of these immune cells kill the bacteria very efficiently (Dannenberg, 1994). At that stage, a primary lesion (Figure 1.4), usually in the mid-region of the lung, composed of macrophage-derived giant cells and lymphocytes, begins to form. This lesion along with the draining and affected lymph nodes is referred to as the Ghon Complex and is thought to enable the spread of bacteria through the draining lymphatic system into the bloodstream. This in turn leads to reinfection of apical pulmonary regions and to the formation of secondary lesions, small tubercles with caseous centres (Boshoff and Barry, 2005).

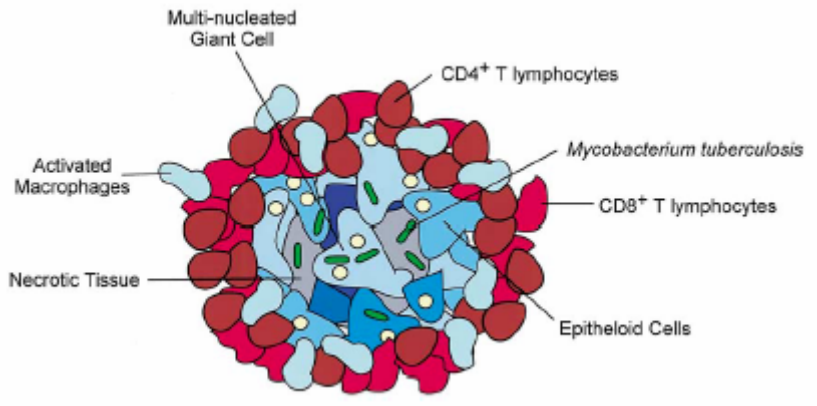

Figure 1.4 | **Composition of granulomas.** The granuloma is the site of infection, persistence and pathology. It is also the site of protection {Kaufmann, 2001 #65}. The centre of a granulomas is composed mainly of necrotic tissue, multinucleated giant cells (fused macrophages) and epitheloid-like cells. The periphery consists of activated macrophages and T lymphocytes {Zahrt, 2003 #10}.

The onset of a cell mediated immune response, which is characterised by the migration of T lymphocytes to the site of infection, kills the infected macrophages. However, it also results in tissue-damaging due to the release of lysozyme and TNF-α from activated macrophages. As a consequence, caseous necrosis develops within the centre of the

lesion. Bacilli are able to survive in the caseum but cannot multiply, because of the hostile environment (anoxic conditions, acidic pH, toxic fatty acids). In this foci the bacteria are able to persist for decades (Smith, 2003). Along with the events stated above, the host becomes tuberculin positive, due to the tuberculin-like products of the bacilli. It is to remark that the local tissue damage is necessary in order to control bacillary multiplication. After such control is established, activated macrophages can accumulate around the caseous and prevent the extension of the disease.

A cell mediated immune response produces antigen specific T cells, which attract monocytes from the bloodstream and activate them. This is important since only activated macrophages are capable of degrading the bacilli. Macrophage activation occurs also upon interaction with lymphokines, endotoxin-like bacillary products and ingestion of dead cells and tissue debris (Dannenberg, 1994).

Importantly, it is the strength of the adaptive immune response that determines the fate of the infection. In individuals with effective cell mediated immunity, the infection may be arrested permanently at this point. The granulomas heal and only small fibrous and calcified lesions are left. Although the infection is arrested, it is believed that the bacilli are not eliminated but persist throughout a person's lifetime in an asymptomatic and non-transmissible state. This enclosed infection is referred to as latent or persistent tuberculosis (Smith, 2003). In contrast, individuals that fail to control the initial infection in the lung or alternatively, experience reactivation of the tubercle bacillus from latency, develop active disease. Thereby, granuloma centres enlarge and the bacilli may spread hematogenously. Further, they develop multiple uncontrolled tubercles with caseation in not only the lungs, but also in extrapulmonary sites (Dannenberg, 1994). The progression

of primary tuberculosis, an unknown process till date, leads to the liquefaction of the caseous lesions. The liquefied material serves as growth medium for the bacilli and this allows them to multiply extracellular, which they do often in great quantity and thus overcome the cell mediated immune response.

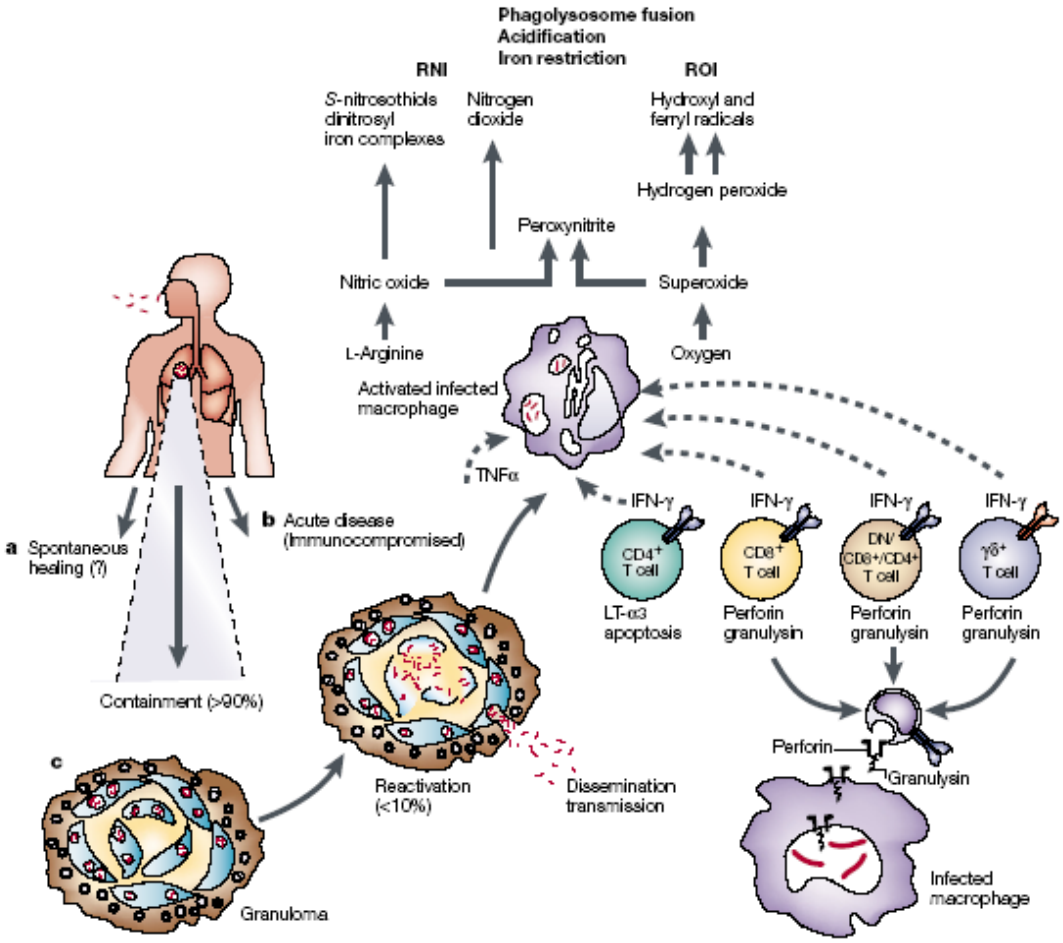

Figure 1.5 | **Main characteristics of tuberculosis.** In this picture the three potential outcomes of a TB infection are depicted. **a** | The spontaneous healing of a TB infection is not known but is assumed to be minute. **b** | Development of disease can occur directly after infection in immunocompromised hosts. **c** | In the majority of cases, disease develops much later after infection as a result of reactivation. The key players of the adaptive immune response are the different effector T cell populations and the macrophages. Macrophages are activated by IFN-γ and TNF-α, which are both released by T cells. Activation leads to phagosome-lysosome fusion and to the production of antibacterial molecules such as RNI and ROI {Kaufmann, 2001 #65}.

Macrophages don't survive in liquefied (or even solid) caseous material. Hence, activated macrophages are ineffective in controlling the extracellular multiplication of tubercle bacilli. Host sensitivity towards tuberculin-like products of the bacillus has a toxic effect to the tissue, resulting in necrosis and rupture of nearby bronchi. This finally results in the formation of a cavity (Dannenberg, 1994).

A cavity consists of an external zone that encapsulates the cavity and a liquefying internal zone, where the high oxygen content from the ambient air allows bacterial growth. Via this cavity, bacilli and the liquefied caseous material can be discharged, e.g. by coughing, into the airways and thus, reach other parts of the lungs and the external environment. The infected host becomes a source of infection and can spread tubercle bacilli to other persons. As for a caseous focus, a "healed" cavity is rarely completely free of bacteria, meaning that bacteria may also persist in this ambit for many years (Dannenberg, 1994), (Smith, 2003). The main characteristics of tuberculosis are depicted in Figure 1.5.

1.6 Diagnostics

Tuberculosis can be diagnosed using different methods, as for instance X-ray, staining of sputum smear and immunoassay tests. An abnormal chest X-ray can provide an indication of tuberculosis. However, chest X-ray findings often resemble findings from other diseases.

The gold standard though is still the direct demonstration of the tubercle bacilli from a patients sputum in Löwenstein-Jensen culture medium. Unfortunately, this method requires usually 3 to 8 weeks due to the slow growing nature of *M. tuberculosis*.

Microscopic examination is much faster but also less accurate. Staining methods include fluorochrome staining, Ziehl-Neelesen staining with carbon-fuchsin, also referred to as acid-fast staining, and Kinyoun staining method. Sputum does generally provide an adequate sample from the lung. Occasionally, bronchoscopy is necessary in order to obtain samples of mucus or lung tissue and to examine the bronchial tubes. Smear staining followed by microscopy is time consuming due to the slow growth of the bacteria. PCR technologies nowadays allow identification of pathogenic DNA within a day. (Andersen et al., 2000), (www.infektionsbiologie.ch)

The tuberculin skin test, also known as Mantoux test, uses PPD to provoke a so-called delayed hypersensitivity response. It displays a T cell activation. Although an important tool to diagnose tuberculosis, it only indicates that a bacterial infection has taken place some time in the past. It does not reveal if the infection is currently active. More over, this test has poor specificity and shows cross-reactivity with BCG vaccination. At present, the tuberculin skin test is used to diagnose latent infection in non-immunised individuals. (Andersen et al., 2000), (Frieden et al., 2003)

The Quantiferon test is a new *in vitro* diagnostic test that measures the release of IFN-γ from peripheral blood T lymphocytes, following stimulation with a specific *M. tuberculosis* antigen (ESAT-6). This test has good sensitivity and specificity and is also applicable after a BCG vaccination. However, this test is very expensive and hence, is of limited use in developing countries. Further, it is still unknown how well this test can measure the risk of reactivation of a latent infection (Andersen et al., 2000).

1.7 Prevention

One main aspect of controlling tuberculosis is: stopping the spread of the disease by early case searching and treatment of an early infection before development of active disease. Further, monitored treatment (DOTS) of active tuberculosis cases over 6 months is unremitting. Other essential control strategies include socio-economic improvements in living standards and exposure prophylaxis, e.g. for relatives of a tuberculosis case. (www.infektionsbiologie.ch), (WHO/HTM/TB/2008.393)

The BCG vaccine is still much in use in developing countries, especially to prevent development of the deadly form of the disease in children (meningitis and miliary tuberculosis). It is very safe and cheap and offers a good protection to children in terms of dissemination, but is of limited use in adults due to inefficient protection. Even though new vaccines have been developed, none of them have shown to be significantly better than the BCG vaccine (Frieden et al., 2003).

Since tubercle bacilli are spread from person to person, early recognition and subsequent treatment (including isolation) of active disease is very important.

1.8 Treatment

Treatment of Tuberculosis has several aims, which are to cure a patient from tuberculosis, to prevent death from active disease or from its late effects, to prevent relapse, to reduce transmission and to prevent the development of acquired drug resistance (WHO/CDS/TB/2003.313).

1.8.1 First-Line Antituberculosis Drugs

The first line antituberculosis drugs are isoniazid, rifampicin, pyrazinamide, streptomycin and ethambutol. These drugs are the most efficient bactericidal drugs and active against all populations of tuberculosis bacilli. Their main properties are their bactericidal and sterilizing activity and the prevention of resistance (WHO/CDS/TB/2003.313).

Isoniazid (INH) is a prodrug and is activated by KatG, a catalase-peroxidase hemoprotein. INH inhibits InhA, a NADH-specific enoyl-acyl carrier protein reductase. This process inhibits the synthesis of mycolic acids required for the mycobacterial cell wall. In humans, INH shows a high early bactericidal activity that kills actively growing bacteria. For the first two weeks of treatment, INH causes rapid decrease in sputum bacilli. Afterwards, the decrease slows down for non-growing bacterial populations. Concerning adverse effects in humans, it is to mention that INH crosses the placental barrier. This requires strict observations of the neonate of an INH-treated mother for any anomalous effects (Brennan et al., 2008).

Rifampicin (RIF) inhibits the activity of the β-subunit of DNA-dependent RNA polymerase, which acts early in transcription. By binding the β-subunit in close proximity to the RNA/DNA channel, the transit of the growing RNA chain is physically blocked. RIF is the most efficient drug in terms of sterilising activity since it is very effective against persistent bacilli in the continuation phase of treatment. Potential toxic effects in humans include hepatotoxicity, though is generally rare with RIF alone. However, pre-existing conditions can have an intensifying effect. For RIF (10 mg/kg) it was reported

that clinically apparent liver toxicity occurred in 2-5% of cases and altered liver function tests in 10-15% of cases (Brennan et al., 2008).

Pyrazinamide (PZA) and streptomycin (STR) are also bactericidal, but only against certain bacteria populations or rather, pyrazinamide is only active in an acidic environment and streptomycin is active against fast multiplying tubercle bacilli. The mechanism of action of PZA is poorly understood. It was found that it inhibits different functions at acid pH. PZA is essential in the treatment of tuberculosis meningitis since it crosses inflamed meninges. Concerning adverse effects in humans, PZA should not be used for treatment of latent tuberculosis, because the rate of hepatotoxicity is unacceptably high. The mode of action for streptomycin (STR) is the inhibition of protein synthesis by binding to the conserved A site of the 16S rRNA in the 30S ribosomal subunit. STR shows rapid development of resistance in humans and has the potential to cause serious neurotoxic effects in humans (Brennan et al., 2008).

Ethambutol (ETH) inhibits cell-wall biosynthesis by inhibiting arabinosyl transferases. This drug is effective against actively growing mycobacteria, including *M. tuberculosis*. It is used in combination with other first-line drugs in order to avoid the emergence of genetic resistance to the drugs. The most severe toxic effects of the drug found in humans include optic neuropathy and occasional hepatotoxicity (Brennan et al., 2008).

1.8.2 Regimen

Tuberculosis treatment regimen is divided into an initial phase, lasting two months and a continuation phase, lasting four or six months. The initial phase consists of the drugs isoniazid, rifampicin pyrazinamide and ethambutol, all having the effect of killing the tubercle bacilli rapidly. Within approximately two weeks infectious patients become non-infectious, symptoms decrease and most of the sputum smear-positive patients become smear-negative within two months. The drugs used during the continuation phase are fewer but have to be taken for a longer time. They have a sterilizing activity, *i.e.* they eliminate the remaining bacilli and prevent a relapse. Usually, short-course chemotherapy consists of a drug combination treatment, *i.e.* four drugs regimen during the initial phase and two drugs regimen during the continuation phase, in order to prevent drug resistance. Drug combination treatment is especially important in patients with high bacterial load since the risk of developing resistance is increased (WHO/CDS/TB/2003.313).

Re-treatment of tuberculosis patients due to failure, relapse or return after default, have a higher chance of drug resistance that might have been acquired during the prior, insufficient drug therapy. Those patients are also at high risk of developing MDR-TB (WHO/CDS/TB/2003.313).

Treatment of extrapulmonary tuberculosis is, from a public health of view, not of significant importance since patients are non-infectious, unless their lungs are infected as well (WHO/CDS/TB/2003.313).

TB treatment for HIV-infected patients is principally the same as for non-HIV infected TB patients. However, it was found that response to tuberculosis treatment and survival is better in HIV-infected individuals when RIF was included in the short-course treatment (Frieden et al., 2003).

A patient with MDR-TB is defined as having active tuberculosis with bacilli resistant to at least rifampicin and isoniazid. It is observed more frequently in re-treatment cases, especially in failure cases. Short-course chemotherapy in MDR-TB patients is ineffective and patients need to be treated intensively and for up to 24 months. Treatment of MDR-TB requires the use of so called second-line antibiotics, which are more expensive and often toxic. Second-line drugs include ethionamide, cycloserine, para-aminosalicylic acid, quinolones (moxifoxacin, ciprofoxacin), and injectable antibiotics such as amikacin, kanamycin or capreomycin. Furthermore, lung resection is frequently needed; although it has to be added that in developing countries the facilities for pulmonary surgery are not available. In general, the mortality rate among individuals with MDR-TB is high (WHO/CDS/TB/2003.313).

Extensively-drug resistance (XDR tuberculosis) has been observed so far only in HIV co-infected patients. The bacilli are resistant to at least rifampicin and isoniazid, a quinolone and one injectable second-line antibiotic (WHO/CDS/TB/2003.313).

1.9 Persistence, Latency and Dormancy

1.9.1 Clinical Aspects

Despite the ability of *M. tuberculosis* to generate a productive cell-mediated immune response, *M. tuberculosis* is capable of persisting within the host and to cause a long-term asymptomatic (latent) infection. Latency, persistence and dormancy are the terms associated with the description of chronic TB (Gomez and McKinney, 2004).

Latency, generally, is a clinical term describing the asymptomatic, chronic stage of a human infection. In relation to TB it was defined by Amberson as "the presence of any tuberculous lesion, which fails to produce symptoms of its presence". Latent cases are typically PPD-positive by skin test, but are not contagious to others. Without antibiotic treatment, a latent infection is thought to be the classic outcome of a TB infection (Gomez and McKinney, 2004).

Given that *M. tuberculosis* causes a latent infection, it has the ability to persist within the host. The manifestation of persistence is due to the capacity of the pathogen to reside within macrophages, to avoid elimination by the human hosts immune response and to slow the rate of clearance by anti-tuberculosis drugs (Young, 2005).

Persisting tubercle bacilli may be in a state of dormancy, a term that is described as "a reversible state of low metabolic activity, in which cells can persist for extended periods without division" (Young, 2005). Important to mention is that dormant bacilli are only able to resume growth subsequent to their recovery (Young, 2005).

1.9.2 Laboratorial Aspects

"The question of how bacteria survive for decades in immunologically educated hosts without causing disease has puzzled microbiologists for a century" (Stewart et al., 2003). The difficulty to define the precise location of persistent bacilli within the host is a substantial obstacle to develop and perform *in situ* studies. Further, the limited understanding about the bacterial determinants that allow for persistence, makes it very difficult to experimentally recreate the conditions encountered by the pathogen during latency. Nonetheless, a variety of *in vitro* and *in vivo* systems have been established to address the question cited above. Although these systems are limited in their ability to fully recapitulate host and bacterial characteristics, they are able to mimic certain aspects of latent infection (Young, 2005).

1.9.2.1 In vivo Models – Cornell Mouse Model and Low-Dose Murine Model

Cornell Mouse Model. Developed at Cornell University in the 1950s, the Cornell mouse model (Figure 1.6) was the first model using a surrogate animal host to display latency of tuberculosis. In this model, mice are infected with virulent *M. tuberculosis* and subsequently treated with antimycobacterial drugs. This results in "clinically sterile" animal tissue. Albeit clinically sterile, after a three-month period without antibiotics, infection resumes in about one third of the mice and the number of relapses is even higher when mice are subjected to immunosuppressive therapy (Young, 2005).

Although this model has the advantage to achieve and maintain low or undetectable bacterial number in infected tissues, it is debatable how close this model reflects a human

latent infection. This, because anti-tubercular drugs are actually used to achieve latency (Honer zu Bentrup and Russell, 2001).

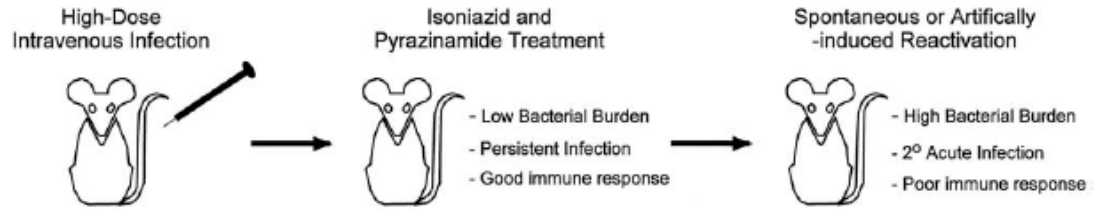

Figure 1.6 | **The Cornell mouse model.** This model is used to evaluate *in vivo* persistence of *M. tuberculosis* {Zahrt, 2003 #10}.

Low-dose Murine Model. The low-dose mouse model (Figure 1.7) stands in contrast to the Cornell mouse model since mice are infected with a low-dose inoculum of *M. tuberculosis*. It is an alternative method to recap many characteristics of *M. tuberculosis* during infection. Upon infection, the animals develop a strong cell-mediated immune response, leading to the natural formation of persistent bacilli. Furthermore, the mice remain competent to reactivation of the disease, either spontaneously or artificially (*i.e.* after treatment with immunosuppressive drugs) (Zahrt, 2003).

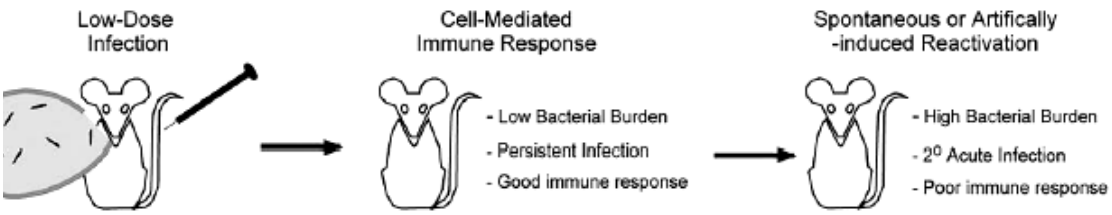

Figure 1.7 | **The low-dose murine model.** This model is applied for evaluation of *in vivo* persistence of *M. tuberculosis* {Zahrt, 2003 #10}.

1.9.2.2 In vitro Models – Wayne Model and Nutrient Starvation Model

The Wayne Non-Replicating Persistence Model. During clinical latency, *M. tuberculosis* possibly resides within granulomatous lesions in the host lung tissue. "The non-replicating persistence" model (Figure 1.8), developed by Lawrence Wayne, is based on the assumption that within these lesions, the bacilli encounter hypoxic or anaerobic conditions (Young, 2005).

In this model, *in vitro* grown bacteria cultures are subjected to a gradual depletion of oxygen thus, adapting to microaerophilic and, eventually, anaerobic conditions in the medium. The cells progress through two stages of non-replicating persistence: NRP-1, a brief microaerophilic state characterised by cessation of DNA synthesis, and NRP-2, an anoxic stationary phase. In this latter phase, bacilli are in a state of oxygen starvation-induced growth arrest and protein expression is shut down. Synchronous cell division occurs after transferring the bacilli into an oxygen-rich medium (Boshoff and Barry, 2005), (Honer zu Bentrup and Russell, 2001). In the non-replicative state, the bacilli exhibit resistance to the drugs isoniazid and rifampicin but become sensitive to metronidazole, a drug active against anaerobically growing organisms (Young, 2005).

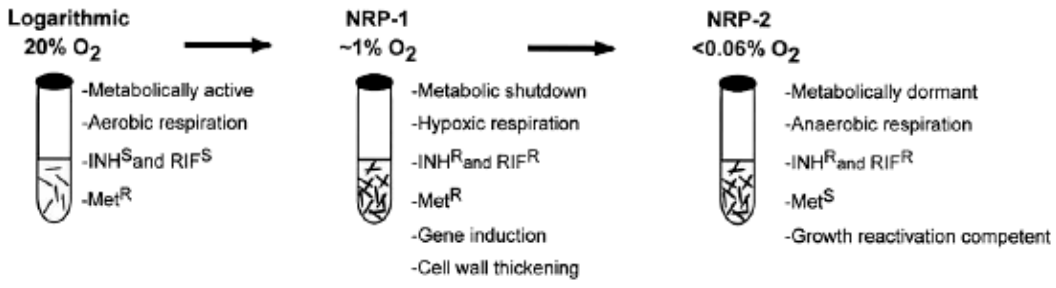

Figure 1.8 | **The Wayne non-replicating persistence model.** This NRP model system is used to assess the growth behavior of *M. tuberculosis* in hypoxic conditions {Zahrt, 2003 #10}.

The Nutrient Starvation Model. The nutrient starvation model (Figure 1.9) was established to investigate the effect of nutrients, predicted to be encountered by *M. tuberculosis* in a granuloma, on the bacilli's metabolism. The model assumes that within granulomas, the availability of nutrients and other essential cofactors is likely to be limited. For *M. tuberculosis* it is crucial to metabolically adapt to this environment in order to survive and persist.

The model is initiated by transferring cultures from a nutrient-rich medium to a nutrient-limiting medium. Subsequently, the cultures are incubated under these conditions for a prolonged period. Nutrient starvation results in a gradual decrease of respiration to minimal levels, increased resistance to isoniazid and rifampicin, continued resistance to metronidazole, an altered colony morphology (cell wall thickening) and altered staining properties (loss of acid fast staining). On a genetic level, a global downregulation in gene expression can be observed. The bacilli remain viable and their recovery is observed when shifting to rich medium.

The effect of nutrient starvation on the growth of *M. tuberculosis in vivo* is presently unclear, but changing to secondary metabolism systems might be fundamental in order to ensure the survival within host tissues (Betts et al., 2002).

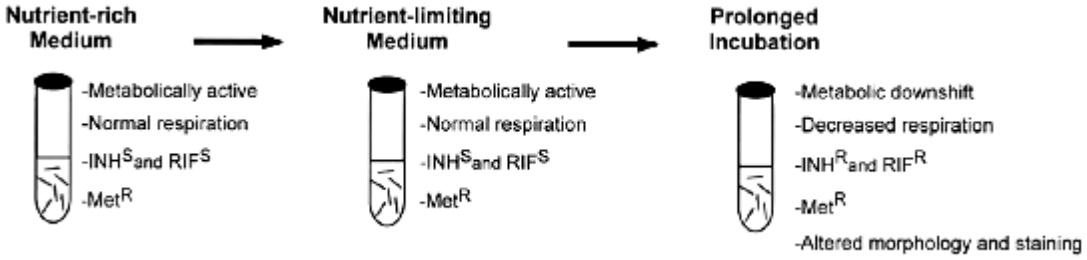

Figure 1.9 | **The nutrient starvation model.** This *in vitro* model is used to assess the growth behavior of *M. tuberculosis* in nutrient-limiting conditions {Zahrt, 2003 #10}.

1.10 Genomics and Proteomics

1.10.1 Genomics

The study of mycobacterial genetics has blossomed in recent years due to the development of several new genetic approaches and to the DNA sequencing of the *M. tuberculosis* H37Rv genome. Annotation of this genome that consists of 4.4 x 10^6 base pairs and contains around 4000 genes, revealed some unique features. For example, over 200 genes (*i.e.* 6% of the total genome) are annotated as encoding enzymes involved in fatty acid metabolism, and out of the 200, 100 are predicted to function in the β-oxidation pathway. Comparatively, *E. coli* has only 50 enzymes for fatty acid metabolism (Cole et al., 1998), (Smith, 2003). Another distinctive feature is the presence of the unrelated PE and PPE families of acidic, glycine-rich proteins, which make up 4% of the entire genome (172 genes in total). Similar levels of abundance is also observed in other members of the *M. tuberculosis* complex and further, they are also found in non-pathogenic mycobacteria. Various of them could be localized in the cell wall and cell membrane. In addition, they were shown to be antigenic. Size variation in members of a PE subfamily (PE-PGRS subfamily) has been found in clinical TB strains. These data suggested that some of the PE and PPE proteins might be involved in antigenic variation of *M. tuberculosis* during infection. However, up to the present their function remain unclear (Tundup et al., 2006).

Nonetheless, most of the in *M. tuberculosis* annotated groups of genes and their products are also found in other microorganisms.

Various new genetic techniques have been invented in order to study the physiology and pathogenicity of *M. tuberculosis*. Current developed methods include gene disruption, complementation and antisense methods.

Gene disruption techniques are divided into directed and global methods, which all result in gene inactivation and which all require a selectable marker, usually an antibiotic resistance cassette. Directed gene disruption achieves gene inactivation by insertion of an antibiotic resistance cassette into the middle of a gene of interest. Subsequently, this DNA (linear or circular) is transformed into mycobacteria via electroporation. In the course of allelic replacement, the chromosomal gene will be substituted with the mutated one (Smith, 2003). In contrast, global gene inactivation entails the insertion of foreign DNA (generally a transposable element) into various sites of the bacterial genome. But, as for the direct method, only one gene is inactivated.

Genetic complementation can be used to identify virulence genes of *M. tuberculosis*. Since antisense RNAs reduce specific gene expression, they can also be used for this purpose.

There are other, non-genetic methods, which allow to study the properties of *M. tuberculosis* on a genetic basis. They include reporter gene technology and promoter trap systems, hybridization-based methods and proteomics (Smith, 2003).

1.10.2 Proteomics

Proteomic tools (e.g. micro array) can be used to measure protein levels during different stages of *M. tuberculosis* infection (e.g. during macrophage infection or during growth on fatty acids) and provide global information on gene expression. Two-dimensional gel

electrophoresis technology is used to resolve high numbers of proteins and if desired, subsequent isolation of the major ones. Further, this technology also allows the comparison of protein levels among related samples. In combination with mass spectrometry, the proteins can be identified. Determination of individual protein levels on a global scale is very important in complementing results from micro arrays, because it reflects protein levels, which have undergone posttranslational modification steps. Posttranslational modifications can modulate protein levels.

Further, protein activity can be controlled by covalent modifications. They include phosphorylation of two-component systems or activation of DNA binding proteins by electrostatic binding of divalent metals (Smith, 2003).

PART II

1.11 Biochemistry – Tricarboxylic Acid Cycle

Most eukaryotic cells and many bacteria are aerobic and oxidise organic fuels such as glucose or fatty acids, completely to CO_2 and H_2O in order to obtain energy. Energy can also be produced under anaerobic conditions via fermentation, though this pathway is much less efficient in terms of energy production. The molecular processes involved in O_2 consumption and CO_2 formation by cells is called cellular respiration (Berg, 2003).

Cellular respiration can be divided into three major stages. The first stage results in a breakdown of organic fuels to yield C_2 fragments in form of acetyl coenzyme A (acetyl-CoA). The second stage is characterised by the activity of the tricarboxylic acid cycle (TCA cycle, also termed citric acid cycle or Krebs cycle), which enzymatically oxidises the acetyl-CoA molecules produced in the first stage. The energy released by the oxidative steps within the cycle is conserved in the reduced electron carriers NADH and $FADH_2$. These carriers are oxidized themselves in the third stage of respiration, a process defined as oxidative phosphorylation, and release protons (H^+) and electrons. The electrons are transferred along a chain of membrane proteins, called respiratory chain, to O_2, which in turn is reduced to H_2O. The electron transfer produces a proton gradient over the mitochondrial membrane. The protons flow through the ATP-synthase and produce ATP from ADP and inorganic phosphate. In prokaryotes, the electron transport

system is located in the cytoplasmic membrane since mitochondria are absent (Lehninger, 1993), (Berg, 2003).

The TCA cycle is the midpoint of a cell's metabolism and in aerobic organisms, serves in both catabolic and anabolic processes (amphibolic pathway). Organic fuels are built up of carbon bonds, which lose electrons during oxidative processes. The TCA cycle consists of a range of oxidative-reductive reactions that end with the oxidation of an acetyl group to CO_2. Apart from its function in the oxidative catabolism of carbohydrates, fatty acids and amino acids, it also provides precursors for many biosynthetic pathways such as for amino acids, nucleotides, cholesterol and porphyrin (Lehninger, 1993), (Berg, 2003).

The cycle (Figure 1.10) begins with the condensation of oxaloacetate (C_4 unit) with an acetyl unit of two carbon atoms to form a citrate (tricarboxylic acid with six carbon atoms). An isomer of citrate is converted via two oxidative decarboxylation steps, first into α-ketoglutarate (C_5 unit) and further into succinate (C_4 unit). From succinate, further enzymatic reactions result again in the formation of oxaloacetate. Two carbon atoms enter the cycle in form of acetyl-CoA and two carbon atoms leave the cycle in form of CO_2. Three hydride ions (*i.e.* six electrons) are transferred to three molecules of NAD, while a pair of hydrogen atoms (*i.e.* two electrons) are transferred to one molecule FAD. These reactions demonstrate that the role of the TCA cycle consists of gaining electrons of high energy from organic fuels (Lehninger, 1993), (Berg, 2003).

The TCA cycle, along with the oxidative phosphorylation, deliver the vast majority of energy used by aerobic cells, in humans, this is more than 95%. One acetyl unit produces approximately ten molecules of ATP. In contrast, anaerobic glycolysis of glucose produces only two molecules ATP. The cycle is highly efficient since a minor number of molecules produce a big amount of NADH and $FADH_2$. Oxaloacetate, as an example, takes part in the oxidation of acetyl groups but gets regenerated itself. This means that one molecule of oxaloacetate can take part in the oxidation of many acetyl molecules (Lehninger, 1993), (Berg, 2003).

Acetyl-CoA, which enters the cycle, is derived from the breakdown of fats, amino acids and glycogen. Though, breakdown of glycogen in bacteria seems to be found only under certain circumstances (Jones et al., 2008). It is of importance in this context to highlight pyruvate, produced via glycolysis, which is a significant source of acetyl-CoA. The oxidative decarboxylation of pyruvate to acetyl-CoA is the connecting link between glycolysis and the TCA cycle (Lehninger, 1993), (Berg, 2003).

Within the TCA cycle only one step will be mentioned here, *i.e.* the oxidation and decarboxylation of isocitrate to α-ketoglutarate, catalysed by isocitrate dehydrogenase (ICD). The oxidation produces the first NADH of the cycle. In eukaryotes, isocitrate dehydrogenase exists in two forms: as NAD-linked enzyme, found only in mitochondria and displaying allosteric properties, and as NADP-linked enzyme that is found in both, mitochondria and cytoplasm and showing no allosteric properties (Lehninger, 1993), (Berg, 2003). It is believed that in eukaryotes NAD-dependent ICD is involved in the

TCA cycle. However, it has been hypothesised that NADP-linked ICD might substitute for loss-of function mutations of NAD-linked ICD (Munnich, 2008).

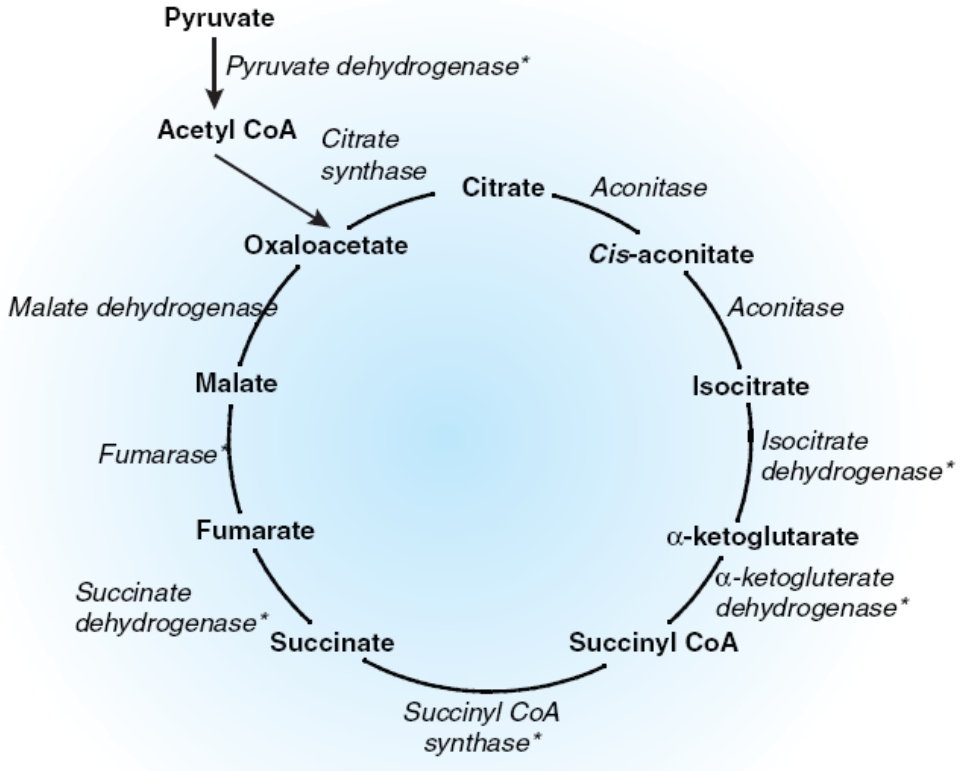

Figure 1.10 | **The TCA cycle.** This cycle begins with the condensation of oxaloacetate and acetyl-CoA. The subsequent oxidative steps release energy, which is conserved in the reduced electron carriers NAD(P)H and $FADH_2$. Apart from ATP production, the cycle provides precursors for many biosynthetic pathways. Enzymes are indicated in italic {Munnich, 2008 #46}.

In contrast with eukaryotic systems, most bacteria possess an NADP-linked ICD involved in the TCA cycle. Phylogenetic analyses revealed that genomes with only an NAD-dependent ICD never encode isocitrate lyase (ICL), an enzyme essential for growth on acetate. Those with an NADP-dependent ICD do encode ICL. Hence, the NADP dependency of prokaryotic ICD appears to be an adaptation to anabolic demand for reduced NADP during growth on acetate (Zhu et al., 2005).

1.12 Escherichia coli and its Behaviour during Growth on Acetate and Fatty Acids

Most pathogenic bacteria are heterotrophs, harbouring the ability to survive on a series of different carbon substrates such as carbohydrates, lipids, glycolipids, dicarboxylic acid and amino acids. Carbon catabolism supplies the bacterial cell, not only with energy in form of reducing agents and ATP, but also with intermediates, including acetyl-CoA, propionyl-CoA and oxaloacetate, all of which are fundamental for biosynthesis. The preferred carbon and energy source for many bacteria are hexoses. There are different pathways, which result in catabolism of these sugars. Glycolysis and pentose phosphate pathway are among the best characterised (Munoz-Elias and McKinney, 2006).

1.12.1 Growth on Acetate and Fatty Acids

In *E. coli*, when acetate is the sole source of carbon and energy, it first has to be converted into acetyl-CoA. In this form it becomes usable for replenishing intermediates of the TCA cycle via the glyoxylate shunt, which constitutes the dominant anaplerotic pathway (Munoz-Elias and McKinney, 2006). In comparison, in humans, acetate cannot be converted directly to acetyl-CoA, but is introduced into the metabolic pathways that lead to the production of pyruvate.

Degradation of fatty acids is directed via the β-oxidation cycle and results in their complete conversion into either acetyl-CoA or propionyl-CoA, depending on the nature of the fatty acids. As a consequence, bacteria are able to grow on fatty acids as sole

source of carbon by operating through the same pathways as those required for growth on acetate (Cozzone, 1998).

Upon degradation of fatty acids, ATP is formed via production of $FADH_2$ and NADH. In contrast, the conversion of acetate to acetyl-CoA does not produce ATP and thus, growth on fatty acids is energetically more favourable per carbon atom than growth on acetate (Cozzone, 1998).

1.12.2 Glyoxylate Shunt

Plants, certain invertebrates and some microorganisms such as *E. coli* and *M. tuberculosis* use for energy production and for biosynthesis a metabolic pathway called glyoxylate pathway (also dubbed glyoxylate shunt or glyoxylate bypass). When acetate or fatty acids are the sole carbon source, the operation of the glyoxylate cycle as an anaplerotic pathway is required (Wendisch et al., 2000). The reason behind is that for each molecular unit of acetate that enters the TCA cycle, two molecular units of CO_2 are lost. By this mean, no net assimilation of carbon can occur and therefore, growth on acetate or fatty acids implicitly need this separate pathway to enable biosynthesis of cellular components (Cozzone, 1998). The bypass also provides some energy since it involves two oxidative steps. Nonetheless, most energy is derived from the TCA cycle and whenever there is access to a more easily metabolisable carbon source, the glyoxylate shunt is turned off, because of catabolite repression (Cozzone, 1998).

1.12.3 Regulation of the Shunt

Upon growth on acetate, the two unique enzymes of the glyoxylate bypass, isocitrate lyase (ICL) and malate synthase (MAS) are induced. The former enzyme catalyzes the aldole cleavage of isocitrate to succinate and glyoxylate. It thus bypasses the two steps in the TCA cycle, in which carbon is lost in the form of CO_2 (Cozzone and El-Mansi, 2005). The catalytic condensation of acetyl-CoA and glyoxylate by MAS leads to the formation of malate and free-CoA, thus fulfilling its anaplerotic function (Cozzone and El-Mansi, 2005). To note is that both, succinate and malate, are intermediates of the TCA cycle and hence, lead to the production of oxaloacetate. Oxaloacetate can be converted into phosphoenolpyruvate, which serves as a precursor of glucose and gluconeogenesis (Berg, 2003).

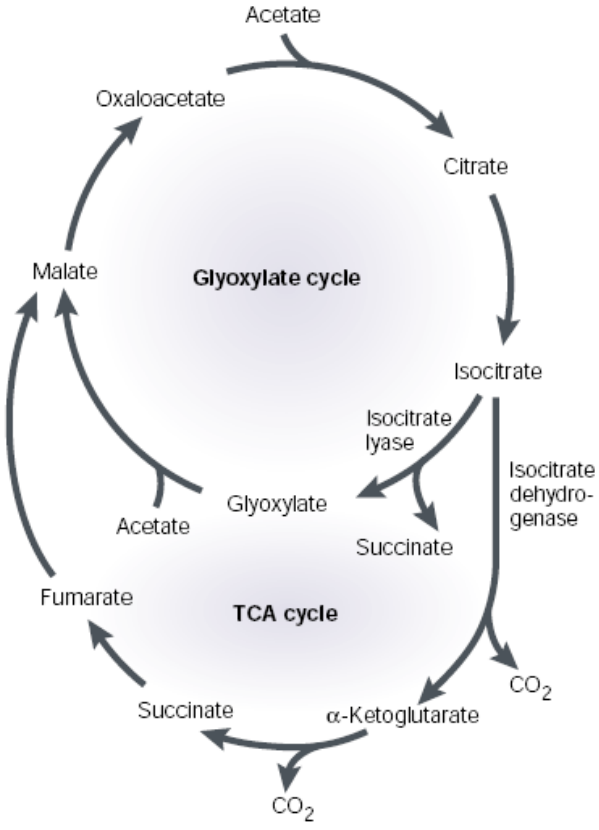

Figure 1.11 | **The glyoxylate shunt.** This pathway is mobilised when bacteria are grown on acetate or fatty acids. Whether the carbon flux is directed into the glyoxylate shunt or continues in the TCA cycle is determined at the branch point. There, isocitrate lyase and isocitrate dehydrogenase compete for their common substrate, isocitrate. It is believed that the glyoxylate shunt is the first step that directs the carbon flux into gluconeogenesis. This is the only way, by which the bacteria can acquire and retain carbon from acetate or fatty acids {Russell, 2001 #64}.

The TCA cycle and the glyoxylate bypass are coordinately regulated. When bacteria are grown on acetate or fatty acids, ICL is in direct competition with ICD for their common substrate isocitrate. It was shown that mutants deficient in isocitrate lyase are unable to grow on acetate. Control of the glyoxylate bypass concerns the increased expression of ICL, which is accompanied by modulation of ICD activity through a reversible phosphorylation (Cozzone, 1998).

1.12.4 Isocitrate Dehydrogenase

Isocitrate dehydrogenases, also known as ICDs, are a large, ubiquitous, and very ancient family of enzymes that play a central role in the TCA cycle. As mentioned earlier, most ICD family members require NAD for substrate oxidation, but yet most bacteria including *E. coli*, use NADP instead. Bacteria with NAD-dependent ICDs are unable to grow on acetate, in contrast to bacteria with NADP-dependent ICDs. NADP dependence appears to be an adaptation of the bacteria to grow on acetate. It is important to note that all enzymes require an integrated Mg^{2+} or Mn^{2+} ion and that most of them are dimers, specifically homodimers (Cozzone, 1998), (Zhu et al., 2005).

Bacterial ICDs show similarity in structure and function. This led to the assumption that the structure and the active site among most prokaryotic ICDs is conserved. Eukaryotic NADP-dependent ICDs have been shown to have diverse important biological functions; however, their regulatory mechanism remains unclear (Yasutake et al., 2003).

Each dimer ICD has two active sites and each of them binds a NAD^{+}/$NADP^{+}$ molecule and a Mg^{2+} or Mn^{2+} metal-ion. Within the active site, isocitrate binds through the formation of hydrogen bonds to a conserved sequence of about eight amino acids. Mg^{2+}

or Mn^{2+} binds to three aspartate residues through hydrogen bonds. $NAD^+/NADP^+$ binds four regions within the active site. Although these regions may vary among ICDs, their properties are similar (Fedoy et al., 2007).

E. coli has only one NADP-linked, Mg^{2+} dependent ICD, consisting of two identical subunits with a molecular mass of about 45 kDa per subunit. Sequencing of the corresponding gene *icd* showed that the enzyme has no significant sequence homology with other ICDs or nucleotide binding proteins. Further, investigation of the intracellular localization of ICD showed its dispersion in the cytoplasm (Yasutake et al., 2003).

1.12.5 Reversible Phosphorylation

The inactivation of ICD by reversible phosphorylation was first observed in a study, where acetate was added to a stationary phase culture of *E. coli* in glycerol medium containing ^{32}P-labeled orthophosphate. The result was a rapid loss of ICD activity associated with incorporation of radioactivity into the enzyme.

Further, it was shown that when bacteria are grown on acetate, about 75% of ICD is inactivated by phosphorylation and that the phosphorylated form of ICD is completely inactive. The inactivation of the enzyme forces isocitrate through the glyoxylate shunt and reroute some of the carbon flux from the TCA cycle. This form of regulation is necessary since ICL has a much lower affinity for isocitrate (K_m = 604 μM) than does ICD (K_m = 8 μM). Inhibition of ICD restricts the flux through the TCA cycle and allows the intracellular concentration of isocitrate to rise to a level, high enough to assure the flux through isocitrate lyase .

Dephosphorylation of ICD, as for example through addition of glucose to an *E. coli* culture grown in acetate medium, leads to the inhibition of the glyoxylate shunt. The explanation here is that the enzyme recovers the capability to bind isocitrate and so directs the carbon flux through the TCA cycle. By doing so, the isocitrate pool declines considerably. This decreases the probability that isocitrate lyase binds to isocitrate.

Concerning growth, it is important to mention that a precise balance between the two competing cycles is essential (Cozzone, 1998).

1.12.6 Mode of Inactivation

Inactivation and reactivation of ICD is achieved by phosphorylation and dephosphorylation of its amino acid residue serine 113. Phosphorylation prevents isocitrate from binding to the active site, because hydrogen bonds cannot form between the substrate and the enzyme. Further, the binding is inhibited by the negatively charged phosphate group of serine 113, which creates an electrostatic repulsion towards the negatively charged γ-carboxylate of isocitrate (Cozzone and El-Mansi, 2005).

It was suggested that ICD changes its conformation upon phosphorylation since it was found that the phosphorylated form of ICD was much less susceptible to proteolysis than the native form (Cozzone and El-Mansi, 2005).

1.12.7 Isocitrate Dehydrogenase Kinase/Phosphatase

Isocitrate dehydrogenase kinase/phosphatase (ICDK/P) is the bifunctional enzyme that catalyses both, the phosphorylation and the dephosphorylation of ICD (Miller et al.,

2000). Only one active site has been found on the enzyme and ICD is the only substrate recognized by ICDK/P. Its activity determines the amount of phosphorylated, and thus inactivated, ICD. Inactivation of ICD is thought to facilitate the flux through ICL since the affinity of ICL for isocitrate is much lower in comparison to ICD. In other words, the higher the concentration or activity of ICDK, the more ICD is phosphorylated/ inactivated. This lowers the carbon flux through ICD and therefore, leads to a higher concentration of intracellular isocitrate. The high concentration of isocitrate increases the chance of ICL binding to isocitrate and thus, directs the carbon flux into the glyoxylate shunt. In summary, it is believed that ICDK/P controls the partitioning of the carbon flux at this particular branch point by phosphorylation/dephosphorylation of ICD (Cozzone and El-Mansi, 2005).

Interestingly, studies using mathematical models revealed that ICD is not the "rate-controlling" step during growth on acetate. Above a certain threshold concentration of ICL, the TCA cycle and the glyoxylate shunt work in concert without need for ICD phosphorylation or dephosphorylation. It is thought that the role of ICDK/P is to facilitate the flux through ICL by inactivating approximately 75% of total ICD (Cozzone, 1998).

1.13 Insight into the Metabolism of Mycobacterium tuberculosis

1.13.1 Metabolic Flexibility

With the onset of cell-mediated immunity along with the activation of macrophage antimicrobial mechanisms and the appearance of the mycobacterial vacuole as a nutrient-

poor compartment, *M. tuberculosis* faces a very hostile environment. It seems probable that survival under these harsh circumstances might lead to changes in *M. tuberculosis* metabolic pathways and the therein occurring substrates. Unfortunately, the metabolic alterations during the process of infection are largely unknown (Munoz-Elias and McKinney, 2006).

Nevertheless, *M. tuberculosis* behaves like most other bacteria with regard to carbohydrate metabolism, energy production and biosynthesis of intermediates for macromolecules (Wheeler Paul R., 1994). The prototrophic feature and metabolic flexibility of *M. tuberculosis* permit the bacilli to oxidize a variety of carbon substrates such as sugars, tricarboxylic acids (e.g. citric acid), fatty acids and amino acids (Munoz-Elias and McKinney, 2006). The findings that this bacterium can be grown on a wide range of carbon compounds in laboratories implies that when acting as a pathogen within host tissues, it also might be able to assimilate a range of host tissue metabolites for its own purpose, notably the assimilation of the many glycans and lipids characteristic for mycobacteria (Wheeler Paul R., 1994), (Wheeler, 2005).

1.13.2 Gene Redundancy

Findings based on genetic analysis revealed that throughout the entire metabolism of *M. tuberculosis* more than one gene is predicted for a certain function. This gene redundancy or paralogy is apparent for instance for phosphofructokinase, citrate synthase, isocitrate dehydrogenase, pyruvate dehydrogenase, isocitrate lyase and lactate dehydrogenase (Wheeler Paul R., 1994), (Wheeler, 2005). Gene redundancy in *M. tuberculosis* may reflect an ability to survive and grow in very different environments within the host. As

example, one compares the centre of a caseous lesion with an active, alveolar macrophage. In contrast, it has been suggested that the loss of redundancy in the *M. leprae* genome reflects a specialized "life-style" (Wheeler, 2005).

1.13.3 THE Carbon Source

Host lipids appear to be the primary carbon source for *M. tuberculosis in vivo* during infection (Figure 1.12)**.** This is further supported by the findings that i) bacteria harvested from infected tissues preferentially metabolize fatty acids over carbohydrates, and ii) the *icl-1* and *icl-2* genes, which were shown to be essential when lipids are the sole source of carbon, are required for growth *in vivo* (Jain et al., 2007**)**.

1.13.4 Fatty Acids

Although during growth *in vitro*, *M. tuberculosis* rapidly metabolises glucose and glycerol from the medium (Figure 1.12), emerging evidence implies that during infection fatty acids are the dominant carbon substrates (Boshoff and Barry, 2005a). If so, this could explain the high abundance of genes (>150) found in the genome of *M. tuberculosis*, which encode for enzymes involved in the pathway of β-oxidative fatty acid degradation (Honer zu Bentrup and Russell, 2001). Further, it was shown that bacteria isolates from lungs of chronically infected mice preferentially oxidized fatty acids (Bloch and Segal, 1956). Also, analysis of genome sequences revealed an extensive gene redundancy for genes encoding enzymes of fatty acid degradation and further, their upregulation during infection of macrophages and mice (Munoz-Elias and McKinney,

2006). 36 homologues of *fadE* genes (encoding the fist step of the β-oxidation pathway) and 36 paralogues of *fadD* (encoding acyl-CoA ligase) were found. These genes together with the rest of the β-oxidation complex are required for catabolism of exogenous fatty acids.

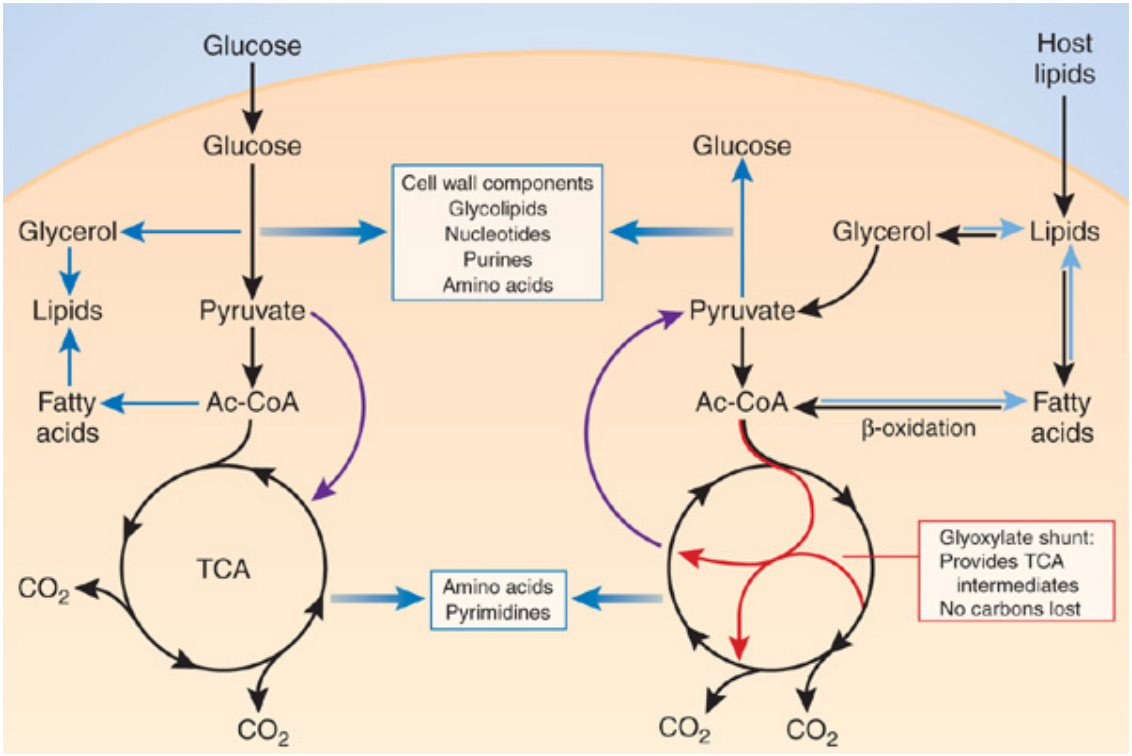

Figure 1.12 | **Major pathways of biosynthesis in *M. tuberculosis*.** The glucose-based routes are believed to function during growth of *M. tuberculosis in vitro*, whereas the lipid based routes are believed to be the ones encountered *in vivo*. Black arrows highlight pathways that generate reducing equivalents; violet arrows indicate reactions that replenish TCA and glyoxylate cycles intermediates; blue arrows show gluconeogenetic and biosynthetic pathways; red arrows show the glyoxylate shunt. This pathway replenishes both, intermediates of the TCA cycle and the glyoxylate shunt itself. The blocks highlight the different cellular components that are biosynthesised via the different biosynthetic pathways {Boshoff, 2005 #47}.

Exogenous lipids, in general, can have a big impact on the cell's economy since the amount of lipids available for assimilation is in excess compared to the quantity of carbohydrates. This, together with the bacilli's ability to simultaneously catabolise and anabolise fatty acids and the detection of lipolytic enzymes supported the view, of *M.*

tuberculosis being rather lipolytic than lipogenic. Repression, like in this case the repression of lipid synthesis enzymes, is also predicted for enzymes involved in biosynthesis of amino acids, fatty acids, purines and pyrimidines, as they can all be supplied from the host (e.g. blood plasma). Nevertheless, *M. tuberculosis* still has the ability to synthesis all metabolites from one specific carbon source since it isn't an obligate intracellular pathogen and since, under laboratory conditions, it is able to grow on only one carbon substrate (Wheeler Paul R., 1994), (Wheeler, 2005).

1.13.5 The Influence of the Immune System

Carbon source utilisation seems to depend on the immune status of the host. The onset of acquired immunity two weeks after infection, which leads to IFN-γ dependent activation of macrophages, encounters the bacilli with a change of environment in the lungs. Nutrient starvation within the phagosome forces the bacilli to shift their primary carbon source to fatty acids, which are present in the endosomal-lysosomal network of the host cell. Genes involved in β-oxidation, glyoxylate shunt and gluconeogenesis are found to be induced during survival within the phagosome of activated macrophages (Boshoff and Barry, 2005b).

Concomitant with the finding that the ability to adopt a persistent phenotype involves a metabolic shift in the carbon source used by *M. tuberculosis,* McKinney et. *al* (Munoz-Elias and McKinney, 2005) established that the two isoforms of ICL are jointly required for bacterial growth and persistence in activated macrophages and mice. Along with the upregulation of the *icl* gene, phosphoenolpyruvate carboxykinase gene *pckA*, a gene encoding for an important enzyme of gluconeogenesis pathway, was also found to be

upregulated (Boshoff and Barry, 2005b). Increased levels of ICL expression were shown to correlate directly with the activation status of the macrophage. Deletion of *icl-1* or *icl-2* attenuated bacterial persistence and virulence in mice, but showed little effect on bacterial growth in macrophages and mice during the acute phase of infection. However, deletion of both, *icl-1* and *icl-2* genes, resulted in a complete impairment of intracellular replication in activated (but not in resting) macrophages and a rapid elimination from the lungs (Munoz-Elias and McKinney, 2005).

1.13.6 At the Branch Point between the Glyoxylate Shunt and the TCA cycle

The glyoxylate shunt is, as already described earlier, a secondary metabolic pathway, which allows the bacteria to utilise fatty acids (*i.e.* C2 substrates) in times when primary carbon sources are limiting, as for instance in the phagosome, and the generation of pyruvate from glycolysis is reduced. The net incorporation of carbon replenishes the concentration of the two intermediates, succinate and malate, which have the overall effect of maintaining oxaloacetate levels. The production of oxaloacetate via pyruvate is restricted due to limitation in carbohydrate availability. The upholding of oxaloacetate levels permits acetyl-CoA to continuously enter the TCA cycle and this in turn ensures the maintenance of the cycle (Gould et al., 2006).

The branch point between the glyoxylate shunt and the TCA cycle shows differences comparing *E. coli* and *M. tuberculosis*. Some characteristics are described below.

1.13.7 Isocitrate Dehydrogenase

The *Mycobacterium tuberculosis* genome has two isoforms of isocitrate dehydrogenase. The two isoenzymes only share around 14% identity at amino acid level. *M. tuberculosis* ICD-1 is more similar to eukaryotic NADP-dependent ICDs, whereas *M. tuberculosis* ICD-2 groups with prokaryotic ICDs. Little is known so far about their enzymatic properties (Banerjee et al., 2005).

As in *E. coli*, *M. tuberculosis* isocitrate dehydrogenase is said to allosterically regulate the conversion of oxidative decarboxylation of D-isocitrate to α-ketoglutarate and CO_2 in presence of a cofactor and a metal ion. ICD-1 is a homodimer. ICD-2, although annotated as a monomer, is present in higher oligomeric forms, the dimer being the most stable one (Banerjee et al., 2005).

Furthermore, it was found that both genes encode functional TCA cycle enzymes with identical enymatic function but different physio-chemical and kinetic properties. They differ in their affinity for coenzyme NADP, pH tolerance and thermostability (Banerjee et al., 2005). By comparing V_{max}(NADP)/K_m(NADP) ratios for the two enzymes, ICD-2 was shown to be the more efficient one. ICD-1 was shown to be more robust in terms of pH tolerance and thermostability. Overall, these findings suggest that even with identical metabolic function, expression of the two ICDs could be differential during different stages of growth (Banerjee et al., 2005).

Using a pathway modelling system, it has been demonstrated that flux through the glyoxylate shunt was only allowed when both, ICD-1 and ICD-2, were more than 70% inactivated. In absence of ICL-1, more than 90% inactivation of the two enzymes is required (Singh and Ghosh, 2006).

1.13.8 Homologue of E. coli Isocitrate Dehydrogenase Kinase/Phosphatase

ICDK/P has been found neither for *M. tuberculosis* ICD-1 nor for ICD-2. Since ICDK/P in *E. coli* was shown to be a serine protein kinase/phosphatase, it seemed reasonable to examine the genome of *M. tuberculosis* for such enzymes. So far, 11 predicted eukaryotic-like serine/threonine protein kinases (STPKs) and one serine/threonine phosphatase (PstP) were found. Nine of them are predicted as transmembrane receptors. Initial studies have established roles for the STPKs in prokaryotic development, stress response and host-pathogen interactions. The metabolic functions, as well as the molecular mechanisms of Ser/Thr phosphorylation systems in *M. tuberculosis*, are hitherto unknown (Greenstein et al., 2005).

1.13.9 The Role of Isocitrate Lyase

The genome of *M. tuberculosis* apparently has two isoforms of isocitrate lyase, whereby the smaller gene *icl-1* encodes an enzyme closely related to isocitrate lyase in other eubacteria; the larger gene *icl-2* encodes an enzyme homologous to eukaryotic isocitrate lyases (Munoz-Elias and McKinney, 2005).

Gould et. *al* predicted a dual role for ICL-1; of it being involved in the glyoxylate shunt, as well as in the methylcitrate cycle. β-oxidation of even-chain fatty acids results in the production of acetyl-CoA, whereas β-oxidation of odd-chain or branched-chain fatty acids and also branched chain amino acids produces propionyl-CoA. High levels of either propionate or propionyl-CoA are toxic for bacteria and fungi. Two putative pathways, methylmalonyl-CoA pathway and methylcitrate cycle, were found in *M. tuberculosis* that

might ensure the metabolism of these two intermediates. This would circumvent their accumulation.

In *E. coli*, the methylcitrate cycle is the principal pathway for clearance of propionyl-CoA during growth on propionate. The methylcitrate cycle metabolises propionyl-CoA to pyruvate, possibly preventing propionate toxicity and also providing another pathway for carbon anaplerosis during growth on odd/branched-chain fatty acid substrates (Gould et al., 2006). The recent observation that ICL-deficient tubercle bacilli were unable to grow on propionate led to the hypothesis that these enzymes might have a dual role in the metabolism of fatty acids. They might participating as ICLs in the glyoxylate shunt and as MCLs (2-methylisocitrate lyase) in the methylcitrate cycle. This view is supported by the finding that *M. tuberculosis* possesses homologues for two of the three enzymes involved in the methylcitrate cycle. Homologues were found for methylcitrate synthase and methylcitrate dehydrogenase but not for MCL. Gould et. *al* demonstrated recently that the active site of *M. tuberculosis* ICL1 bound to pyruvate and succinate can accommodate the additional methyl group of 2-methylisocitrate and catalyse the MCL reaction (Gould et al., 2006).

1.14 Aims of the Project

This project was based on the purpose of better understanding the regulation of the branch point between the glyoxylate shunt and the TCA cycle by finding the so far unknown, putative *M. tuberculosis* isocitrate dehydrogenase kinase/phosphatase. In this context, we also tried to gain insight into the nature of ICD-1 and ICD-2 and their phosphorylation status based on the particular carbon substrate present in the growth medium. Obtaining a better understanding of this particular branch point is of major importance since fatty acids are believed to be the main source of carbon and energy for *M. tuberculosis* in chronically infected animals and also in humans. Furthermore, the glyoxylate bypass was shown to be crucial for *E. coli* and *M. tuberculosis* during growth on acetate or fatty acids.

During the course of this project we pursued the following goals:

i) Understanding the regulation of the branch point.

ii) Finding of the yet unknown, putative isocitrate dehydrogenase kinase/phosphatase in BCG.

iii) Purifying ICD-1 and ICD-2 and assure their activity. The purified proteins were thought to be in later use for the confirmation of the expected role of the putative kinase/phosphatase.

iv) Constructing a modified version of *E. coli* isocitrate dehydrogenase, which would not allow phosphorylation of its gene product in BCG. This construct would possibly show phenotypic differences when grown in either glucose or acetate and therefore allow predictions for the regulation of the bypass by the putative kinase/phosphatase.

v) Gaining insight into the nature of ICD-1 and ICD-2 by creating knockout mutants and characterise their phenotypes under different conditions. This would eventually reveal functional differences between the two isocitrate dehydrogenases and further, specify the expected role of the putative kinase.

Materials & Methods

2.1 Materials

2.1.1 Strains

Mycobacterium bovis bacillus Calmette-Guérin (#35734), henceforth stated as BCG, was obtained from the American Type Culture Collection (ATCC). *E. coli* Tuner (DE) cells were obtained from Novagen. *E. coli* TOP10 cells were obtained from Invitrogen. The *E. coli* strains JM109 and BMH 71-18 *mutS* were part of the GeneEditor *in vitro* Site-Directed Mutagenesis System kit from Promega. The human lung adenocarcinoma cell line (A549) was purchased from ATCC.

2.1.2 Media

E. coli cells were routinely propagated in Luria-Bertani (LB) broth (Becton Dickinson), or onto LB agar plates. BCG was propagated in Middlebrook 7H9 medium (Becton Dickinson), supplemented with 0.05% Tween-80, 0.5% bovine serum albumin (Roche; #10711454001), 0.081% NaCl, 0.2% glycerol and 0.2% glucose, or onto Middlebrook 7H11 agar plates.

For growth of *E. coli* the medium was, if necessary, supplemented with kanamycin (50 μg/ml), hygromycin (150 μg/ml), ampicillin (100 μg/ml), X-gal (40 μg/ml). For growth of BCG, the medium was, if required, supplemented with kanamycin (25 μg/ml), hygromycin (75 μg/ml), X-gal (40 μg/ml), sucrose (2% v/v). Ampicillin, kanamycin and X-gal were obtained from Sigma-Aldrich, hygromycin was obtained from Roche and sucrose from FisherScientific.

Human lung adenocarcinoma cells (A549) were cultured in filterised THP-1 growth medium, containing RPMI, heat-inactivated FBS (10% final concentration), glutamax I (10 mM final concentration), sodium pyruvate (1 mM final concentration), D-Glucose, anhydrous (1.25mg), 2-mercaptoethanol (0.05 mM final concentration), penicillin-streptomycin (10,000 U/ml penicillin and 10,000 μg/ml streptomycin); all components were from GIBCO).

2.1.3 Culture Conditions in a Defined Carbon Source

Middlebrook 7H9 medium was used as BCG culture medium with glycerol as main carbon source. BCG culture medium with glucose as a sole source of carbon consisted of 7H9 base (i.e. 7H9 broth with 0.05% Tween-80), supplemented with 0.2% glucose, 0.08% NaCl and 0.05% fatty acid-free BSA (BSA-FAF; Sigma Aldrich, #A8806). Alternatively, when acetate was the sole source of carbon, the culture medium consisted of 7H9 base, 0.2% sodium acetate, 0.08% NaCl, 0.05% BSA-FAF. For shifting BCG from complete 7H9 medium to glucose or acetate medium, the cells had to be washed twice by centrifugation (3000 rpm, 10 min, RT) with 7H9 base and resuspended in 7H9 base. The OD was measured and the cells inoculated into glucose or acetate medium. Starting OD_{600} was 0.02.

BCG culture medium without glutamic acid consisted of 7H9 base deprived of glutamic acid, supplemented with 0.1% sodium acetate, 0.1% glycerol, 0.08% NaCl, 0.1% BSA-FAF. Additionally, this medium was supplemented with 0.1% glutamic acid if growth in presence of glutamic acid was examined.

2.1.4 Materials for Purification of M. tuberculosis ICD-1 and ICD-2

Gateway LR Clonase Reaction (Invitrogen); Bug Buster Protein Extraction Reagent (Novagen); Lysonase Bioprocessing Reagent (Novagen); Ni^{2+}-nitrilotriacetate affinity chromatography spin columns (Ni-NTA spin column from Qiagen); millipore membrane filter (Sartorius); immobilised metal affinity chromatography column (IMAC column from Qiagen); Ni-NTA His-Bind agarose (Qiagen); Econo-Column flow adaptor (Bio-Rad); Econo-Gradient pump (Bio-Rad); Bradford protein assay (Bio-Rad), ultrafiltration spin columns (Vivaspin 10K and 30K MWCO; Sartorius Group); PD-10 column (GE Healthcare); PreScission Protease (Novagen); prepacked XK column designed for preparative gel filtration chromatography separations, Superdex 200 (M_r 10,000-600,000) 10/300 GL; 25 ml/CV (GE Healthcare); UNICORN software program for control and supervision of chromatography (GE Healthcare).

2.1.5 Materials for Western Blotting and Immunodetection

Immuno-blot PVDF Membrane for Protein Blotting (Bio-Rad); Phospho-threonine (isotype mouse IgG1) and phospho-serine (isotype mouse IgG1 and IgM) antibody (Qiagen); Alkaline phosphatase-conjugated AffiniPure Rabbit Anti-Mouse IgG + IgM (H+L) antibody (Jackson ImmunoResearch); BCIP/NBT-Blue Liquid substrate for membranes (Sigma-Aldrich).

2.1.6 Materials for Molecular Cloning

All restriction enzymes and the corresponding buffers were purchased from New Englands BioLabs; dNTPs (New England BioLabs); TAE buffer and ethidium bromide (Bio-Rad); plasmid vector pCR2.1-TOPO (Invitrogen); membrane filter for micro dialysis (Millipore, Sartorius Group); shrimp alkaline phosphatase (Roche); Gene Pulser cuvette and Gene Pulser Xcell (Bio-Rad); PETG Media Bottles (Nalrgene); DMSO (Acros Organics).

2.1.7 Materials for Crude Cell Extraction, Growth Assays, MIC_{50} Assays and Enzyme Assays

Protease inhibitor cocktail tablet, EDTA-free (Roche); glass beads and Mini Beadbeater (Biospec Products); the compounds Isoniazid, 3-Nitropropionate, DL-isocitrate and NADP were purchased from Sigma-Aldrich, NADPH was purchase from Merck; T25 flasks (Nalge Nunc).

2.1.8 Other Materials

SDS-PAGE was performed using NuPAGE Novex 4-12% Bis Tris mini gel 1.0 mm, along with the corresponding MES and MOPS buffer for PAGE. Novex Sharp Protein Standard was used as marker. Gels, buffers and the marker were purchased from Invitrogen. For subsequent Coomassie Blue staining Bio-safe Coomassie Blue from Bio-Rad was used.

Chemicals, which were used in the experiments, but are not mentioned in this Chapter by name, were either obtained from Sigma-Aldrich, Merck or FisherScientific.

NCBI (National Centre for Biotechnology Information) and TuberuList BLAST (Basic Local Alignment Search Tool program) programs, software program GraphPad Prism, version 4 for Windows.

2.1.9 Kits

Protein concentrations were determined by using the Protein Quantification Kit from Pierce (BCA Protein Assay Reagent Kit). The ProteoEnrich ATP-Binders Kit from Novagen was implemented for enrichment of ATP-binding proteins (ABPs) such as kinases. The Phosphoprotein Purification Kit from Qiagen was used to purify phosphoproteins. Further it was used for crude cell extraction of the cell line A549 and as a modified version for crude cell extraction of ABPs. The kit GeneEditor *in vitro* Site-Directed Mutagenesis System from Promega was used to introduce a point mutation into *E. coli* icd_{opt} gene. Plasmid DNA was purified using the QIAprep Spin Miniprep Kit from Qiagen. PCR samples were mixed with reagents from the Hot Star Taq Plus DNA Polymerase Kit from Invitrogen. PCR products were purified after gel electrophoresis with the PCR Purification Kit from Qiagen. The TOPO TA Cloning Kit from Invitrogen was used for subcloning of the knockout constructs into *E.coli* TOP10 cells. Purification of plasmids and inserts from agarose gels was carried out using the Gel Extraction Kit from Qiagen. Plasmid and insert ligation was carried out using Rapid Ligation from Roche.

2.2 Methods

2.2.1 Enrichment of ATP-Binding Proteins

In order to find the yet unknown kinase of wt BCG, which eventually phosphorylates ICD-1 and/or ICD-2, the ATP-Binders Kit was implemented. This kit is designed for enrichment of eukaryotic protein extracts with ABPs such as protein kinases.

Crude cell extraction was performed with pellets of wt BCG, which had been grown on glucose and on acetate. For the procedure a modified version of the protocol from the Phosphoprotein Purification Kit was used: The cell pellets were washed in PBS containing 0.05% Tween-80 in order to remove BSA. Next, they were resuspended in 5 ml lysis buffer containing CHAPS, 1 protease inhibitor tablet (1 tablette/50 ml) and benzonase (all provided by the kit). The cultures were bead beated at 4ºC, followed by centrifugation (10,000 g, 5 min, 4ºC). The supernatants were removed and centrifuged again (10,000 g, 30 min, 4ºC). In order to remove free endogenous ATP, extracts were dialysed, using a PD-10 column, in PBS containing 1 mM EDTA and 1 mM DTT. The crude cell extracts were loaded onto spin filters containing ATP-Binders resin, *i.e.* a polyacrylamid-based resin on which ATP is immobilized at the γ-phosphate. The resin has a high affinity for ABPs. The enrichment of ABPs was carried out according to the instructions of the manufacturer. For visualizing of the eluted ABPs a SDS-PAGE, followed by silver staining was performed. For silver staining the following reagents and solutions were used: fixing solution (40% methanol, 10% acetic acid); 0.02% sodium thiosulfate ($Na_2S_2O_3$); 0.1% silver nitrate ($AgNO_3$); developing solution (3% sodium carbonate, 0.05% formalin); 5% acetic acid.

2.2.2 Purification of Phosphoproteins

For characterisation of the phosphorylation status of Ser/Thr sites of wt BCG ICD-1 and ICD-2, the Phosphoprotein Purification Kit was used. This kit is designed for specific purification of phosphorylated proteins from eukaryotic cell lysates.

The experiment was carried out using glucose and acetate grown wt BCG. Additionally, the experiment was carried out with eukaryotic cell extracts from A549 cells. After crude cell extraction, lysates containing approximately 2.5 mg of total protein were taken and added to an affinity column, which bound the phosphorylated protein. The flowthrough was collected for analysis of unphosphorylated protein, the eluate fractions were used for analysis of phosphorylated protein.

Western transfer of the different fractions was carried out using a protocol from Qiagen (QIA*express* Detection and Assay Handbook). Blotting of a PVDF membrane was carried out in tank-blotting transfer buffer (25 mM Tris base, 150 mM glycine, 20% ethanol, pH 8.3) at 4ºC, 120 V, 400 mA, 1 hour.

For immunodetection the following buffers were used: TBS-Tween buffer [10 mM Tris-HCl, 150 mM NaCl, 0.1% (v/v) Tween-20, pH 7.5]; blocking buffer [(1.8 g BSA/60 ml TBS (10 mM Tris-HCl, 150 mM NaCl, pH 7.5)]; TBS-Tween/Triton buffer [(20 mM Tris-HCl, 500 mM NaCl, 0.05% (v/v), Tween-20, 0.2% (v/v) Triton X-100, pH 7.5)]; TBS-Tween buffer containing 0.1% BSA. The membrane was incubated with a phospho-threonine and phospho-serine antibody solution (1/100 dilution) at 4ºC, ~20 rpm, o/n. AP-conjugated Anti-Mouse antibody (1/8000 dilution) was used as secondary antibody.

Incubation was allowed for 1 hour at RT. BCIP/NBT-Blue was used for detection. Catalytic conversion of BCIP/NBT was allowed for up to 30 min.

2.2.3 Expression and Purification of M. tuberculosis ICD-1 and ICD-2 in E. coli

2.2.3.1 Small Scale Purification

Gateway LR Clonase Reaction was performed with an in-house entry vector containing the gene *icd-1* or alternatively *icd-2*, and an in-house destination vector containing one out of eight different N-terminal 6xHis sequence tags. The generated constructs were transformed into *E. coli* Tuner (DE3) cells. Colonies from each construct were first precultured in LB medium containing kanamycin, then transferred (1/100 dilution) into LB medium containing kanamycin and grown until OD_{600} of 0.6-0.8. The cells were cooled to 18ºC and temperature equilibrated for 30 min. Induction of protein expression by addition of 0.1 mM IPTG was allowed to proceed o/n at 18ºC, 200 rpm. Cells were harvest by centrifugation at 3,000 g for 10 min. The pellet of each construct was resuspended in 1 ml Bug Buster Protein Extraction Reagent that had been premixed with Lysonase Reagent (10 µl/g). The sample was incubated for 15 min and subsequently sonicated for 15 cycles at 20% amplitude (1 cycle: 1 sec on with 10 sec off interval). The solution was clarified by centrifugation at 13,200 rpm for 10 min. The cleared lysate was loaded onto Ni^{2+}-nitrilotriacetate affinity chromatography spin columns. After a washing step (20 mM Tris-HCl, 500 mM NaCl, 40 mM imidazole, pH 7.5), the recombinant protein was eluted with elution buffer (50 mM Tris-HCl, 300 mM NaCl, 250 mM imidazole, pH 7.5). The pellet was suspended in 1 ml solubilisation buffer (50 mM Tris-HCl, 8 M urea, 300 mM NaCl, 10 mM imidazole, pH 7.5) and incubated for 10 min.

With the different collected fractions (flowthrough/wash/eluate) a SDS-PAGE followed by Coomassie Blue staining was performed. For continuation, the following expression vectors were used: ICD-1 (~ 49 kDa) fused to Trx-6xHis-S-tag (17 kDa) and ICD-2 (~ 82 kDa) fused to pNAT83 His-tag (46 kDa).

2.2.3.2 Large Scale Purification

E. coli Tuner (DE) cells harbouring either ICD-1 fused to Trx-6xHis-S-tag or ICD-2 fused to MBP-6xHis-S-tag were both precultured in LB medium containing kanamycin. After transfer (1/100 dilution) into one litre of Terrific Broth MOPS medium [12 g/l Bacto Tryptone (Becton Dickinson), 24 g/l Bacto Yeast Extract (Becton Dickinson), 10 mM ammonium sulfate, 0.3 mM dipotassium hydrogen phosphate, 0.3 mM potassium dihydrogen phosphate, 100 mM MOPS (Sigma), pH 7.0], supplemented with kanamycin, growth was permitted for 3-4 hrs at 37ºC, 200 rpm till OD_{600} of 0.6-0.8 was reached. Induction of protein expression was carried out as described for small scale purification (section 2.2.3.1). Cells were harvest by centrifugation at 8000 rpm for 30 min at 4ºC. The pellet of both constructs (circa 16-20 g/litre) was resuspended in 50 ml binding buffer (50 mM Tris-HCl, 300 mM NaCl, 10 mM imidazole, pH 7.5) that had been premixed with Lysonase Reagent (10 µl/g) and incubated for 10-15 min at RT. The sample was sonicated in tubes on ice for 30 cycles at 30% amplitude (1 cycle: 5 sec on with 15 sec off interval). The sample was spun down at 17,000 rpm for 30 min at 4ºC. The filtered solution (using a 45 µm membrane filter) was subjected to immobilised metal affinity chromatography (IMAC). The IMAC column was packed with Ni-NTA agarose (Ni-NTA His-Bind resins; column volume (CV) was 3 ml). A flow adaptor was attached to the column in order to reduce the void volume above the resin. After column

equilibration with 10 CV binding buffer the filtered solution was loaded onto the column. After a washing step using 5 CV wash buffer (20 mM Tris-HCl, 500 mM NaCl, 40 mM imidazole, pH 7.5), recombinant protein was eluted with 6 CV elution buffer (20 Tris-HCl, 300 mM NaCl, 250 mM imidazole, pH 7.5) using a fraction collector (1 ml fraction/min). A rough estimation of the eluted protein fractions was carried out using 1X Bradford Reagent. The eluate fractions, displaying the highest protein concentration, were pooled and concentrated to about 2.5 ml volume using ultrafiltration spin columns at 3000 rpm, 20-30 min, 4ºC. Buffer exchange was carried out using a PD-10 column. Protein was eluted in 3.5 ml storage buffer (20 mM Tris-HCl, 300 mM NaCl, 10 % (v/v) glycerol, pH 7.5) The protein concentration was determined and a SDS-PAGE followed by Coomassie Blue staining was performed. The sample was cleaved with PreScission Protease (15 µl/mg) in order to remove the 6xHis-tag. Cleavage was permitted for 24 hrs at 4ºC, 60 rpm. The sample was concentrated to 500 µl using a ultrafiltration spin column at 3000 rpm, 20-30 min, 4ºC. Afterwards, the sample was loaded onto a prepacked XK column designed for preparative gel filtration chromatography separations. Fractions were collected (1 ml/fraction) at a flow rate of 0.4 ml/min. To determine the fractions that contained cleaved protein, the UNICORN software for control and supervision of chromatography was used and a SDS-PAGE followed by Coomassie Blue staining was carried out. The fractions containing cleaved protein were pooled and concentrated using ultrafiltration spin columns. The concentration of purified ICD-1 and ICD-2 was determined. The proteins were divided into aliquots and stored at -80ºC.

2.2.4 Enzyme Assays with Purified ICD-1 and ICD-2

Enzymatic activity of ICD-1 and ICD-2 was measured spectrophotometrically by monitoring the time dependent reduction of $NADP^+$ to NADPH at RT at 340 nm (absorbance maximum of NADPH). The reaction mixture contained the assay buffer (25 mM Tris-HCl, 5 mM $MgCl_2$, 100 mM NaCl, pH 7.5), as well as 2 mM final concentration of DL-isocitrate and 1 mM final concentration of $NADP^+$. Reactions were initiated by adding either ICD-1 or ICD-2, both at a final concentration of 70 nM. Activity of the enzymes was measured at four time points (30 min/ 60 min/ 90 min/ 120 min) and determined by using two standard curves. One standard curve displayed the concentration-dependent absorbance of NADPH at 340 nm. The concentration of NADPH ranged from 1 mM to 0.5 µM. The other standard curve allowed to determine the percentage of NADPH produced. All the obtained data was plotted using the software program GraphPad Prism, version 4 for Windows.

2.2.5 Optimisation of E. coli Isocitrate Dehydrogenase

2.2.5.1 Modification and Subcloning of E. coli icd_{opt}

The gene icd_{opt} is a modified version of the *icd* gene from *E. coli*. Modification consisted of base exchange, i.e. replacement of several bases with guanine and cytosine (GC). We purchased icd_{opt}, which was inserted in pBSK, from 1st BASE.

Figure 2.1 shows the *E. coli icd* gene and the different changes that led to the modified gene icd_{opt}. The gene sequence of the parental *E. coli icd* gene (1251 bp) is displayed in black (begins with line 1). The bases in red highlight the GC exchange, thus making the *E. coli icd* gene compatible for BCG. The green labelled T at basepair position 323 was

exchanged by site directed mutagenesis (SDM; will be described in section 2.2.5.2) to G. The sequence in bold (line 12) is the primer sequence (*i.e.* the mutagenic sequence) used for SDM.

```
1   CCGGCACAAGGCAAGAAGATCACCCTGCAAAACGGCAAACTCAACGTTCCTGAAAATCCG
    .....C..G.....................G........G..G.....G..G..G..C...
    ATTATCCCTTACATTGAAGGTGATGGAATCGGTGTAGATGTAACCCCAGCCATGCTGAAA
    ..C.....G.....C..G..C..C..C.....C..G..C..G.....G...........G
    GTGGTCGACGCTGCAGTCGAGAAAGCCTATAAAGGCGAGCGTAAAATCTCCTGGATGGAA
    .....G.....C..C..G.....G.....C..G.........C..G.....G........G
    ATTTACACCGGTGAAAAATCCACACAGGTTTATGGTCAGGACGTCTGGCTGCCTGCTGAA
    ..C........C..G..G..G..C.....G..C..C........G........G..C..G
    ACTCTTGATCTGATTCGTGAATATCGCGTTGCCATTAAAGGTCCGCTGACCACTCCGGTT
    ..C..G..C.....C..C..G..C.....G.....C..G..C...........C.....G
    GGTGGCGGTATTCGCTCTCTGAACGTTGCCCTGCGCCAGGAACTGGATCTCTACATCTGC 381bp
12  ..C.GCGGCATCCGCTCGCTGAACGTGGCG.............G.....C..G......
    CTGCGTCCGGTACGTTACTATCAGGGCACTCCAAGCCCGGTTAAACACCCTGAACTGACC
    .....C.....G..C.....C.........C..GTCG.....G..G.....G..G......
    GATATGGTTATCTTCCGTGAAAACTCGGAAGACATTTATGCGGGTATCGAATGGAAAGCA
    ..C.....G.........C..G.........G.....C..C..C..C.....G.....G..C
    GACTCTGCCGACGCCGAGAAAGTGATTAAATTCCTGCGTGAAGAGATGGGGGTGAAGAAA
    .....G..............G.....C..G.........C..G.........C.........G
    ATTCGCTTCCCGGAACATTGTGGTATCGGTATTAAGCCGTGTTCGGAAGAAGGCACCAAA
    ..C...........G..C..C..C.....C..C.........C.....G..G........G
    CGTCTGGTTCGTGCAGCGATCGAATACGCAATTGCTAACGATCGTGACTCTGTGACTCTG
    ..C.....G..C..C..C.....G.....C..C..C.....C..C.....G.....C...
    GTGCACAAAGGCAACATCATGAAGTTCACCGAAGGAGCGTTTAAAGACTGGGGCTACCAG
    ........G.........................G..C..C..C..G..............
    CTGGCGCGTGAAGAGTTTGGCGGTGAACTGATCGACGGTGGCCCGTGGCTGAAAGTTAAA
    .....C..C..G.....C.....C..G...........C..............G..G..G
    AACCCGAACACTGGCAAAGAGATCGTCATTAAAGACGTGATTGCTGATGCATTCCTGCAA
    ...........C.....G........G..C..G........C..C..C..C........G
    CAGATCCTGCTGCGTCCGGCTGAATATGATGTTATCGCCTGTATGAACCTGAACGGTGAC
    ..............C.....C..G..C..C..G........C..............C...
    TACATTTCTGACGCCCTGGCAGCGCAGGTTGGCGGTATCGGTATCGCCCCTGGTGCAAAC
    .....C..G...........C..C.....G.....C.....C........G..C..C...
    ATCGGTGACGAATGCGCCCTGTTTGAAGCCACCCACGGTACTGCGCCGAAATATGCCGGT
    .....C.....G...........C..G...........C..C..C.....G..C.....C
    CAGGACAAAGTAAATCCTGGCTCTATTATTCTCTCCGCTGAGATGATGCTGCGCCATATG
    ........G..G..C..G.....G..C..C..G..G..C..................C...
    GGTTGGACTGAAGCGGCTGACCTGATTGTTAAAGGTATGGAAGGCGCAATCAATGCCAAG
    ..C.....C..G..C..C.........C..G..G..C.....G.....C.....C......
    ACCGTAACTTATGACTTCGAACGTCTGATGGAAGGCGCTAAGCTGCTGAAATGTTCAGAG
    .....G..C..C.........G..C.........C.....C...........G..C..G...
    TTTGGTGAAGCGATCATCGAAAACATGT  1251 bp
    ..C..C..C..C.........G.......  1251 bp
```

Figure 2.1 | **Gene sequence and modifications of the *E. coli icd* gene**.

icd$_{opt}$ was subcloned into pMV262 and further into pMV306, transformed into wt BCG and plated on 7H11 agar plates containing kanamycin.

Substitution of Ser113Ala in *icd*$_{opt}$ was carried out by using the GeneEditor *in vitro* Site-Directed Mutagenesis System Kit from Promega.

2.2.5.2 Site Directed Mutagenesis of icd$_{opt}$

<u>*Preparation of pBSK as DNA Template.*</u> *icd*$_{opt}$ was inserted into pBSK using *BamH1* and *EcoR1*. The vector was transformed (heat-shock) into *E.coli* JM109 competent cells. Alkaline denaturation of purified plasmid DNA was carried out using 0.5 pmol of the pBSK vector, 2 µl of 2 M NaOH and 2 mM EDTA in a final volume of 20 µl. The reaction mix was incubated at RT for 5 min, then 2 µl of 2M ammonium acetate (pH 4.6) and 75 µl of 100% ethanol (4ºC) were added, followed by a additional incubation period of 30 min at -70ºC. The DNA was precipitated by centrifugation at 13,000 rpm for 15 min at 4ºC. The pellet was drained and washed with 200 µl of 70% ethanol (4ºC), centrifuged again and then dried under vacuum. The pellet was suspended in 100 µl of TE buffer (pH 8.0).

<u>*Mutagenesis Reaction.*</u> The mutagenesis reaction was based on the hybridization of the mutagenic sequence (Figure 2.1) and the selection sequence (provided by the kit) to the corresponding sites on pBSK containing *icd*$_{opt}$. The reaction mix contained 0.05 pmol of the pBSK *icd*$_{opt}$, 0.25 pmol of selection oligonucleotides from the top strand (phosphorylated; provided by the kit), 1.25 pmol of mutagenic oligonucleotides (phosphorylated), annealing 10X Buffer and sterile, deionised water. The final volume of the reaction mix was 20 µl. The sequence of the mutagenic oligonucleotides was 5'-

PhosphateGCGGCATCCGC***G***CGCTGAACGTGGC-3' with a substitution of serine to alanine at position 113 of the protein. The substitution within icd_{opt} affected the basepair at position 323, wherein thymine was substituted with guanine. For the annealing of the selection and mutagenic oligonucleotides to pBSK icd_{opt} the reaction mix was heated using a heating block to 75ºC for 5 min. Subsequently the heating block was cooled down to 37ºC by placing it at RT. For subsequent synthesis and ligation of the mutant strand 5 µl of sterile, deionised water, 3 µl of synthesis 10X Buffer, 1 µl of T4 DNA Polymerase (5-10u) and T4 DNA Ligase (1-3u) were added in this order to the reaction mix, yielding a final volume of 30 µl. The reaction was incubated at 37ºC for 90 min.

Transformation. 1.5 µl of the mutagenesis reaction was used to transform BMH 71-18 *mutS* competent cells, a mismatch repair minus strain of *E.coli*. 10 ng of purified plasmid DNA was transformed via heat-shock into JM109 competent cells. The mutated cells were selected on plates (growth o/n, 37ºC) containing 150 µl of the GeneEditor Antibiotic Selection Mix and 2.5 mg of ampicillin per 20 ml of media. Several clones were sent for sequencing using the universal primers M13F and M13R. For continuation one clone with only the desired point mutation 323T>G in icd_{opt} and no other mutation was used. For sequence alignment the NCBI (National Centre for Biotechnology Information) BLAST (Basic Local Alignment Search Tool program) was used.

Subcloning and Transformation into BCG. pBSK containing icd_{opt} (Ser113Ala) was digested with *BamHI* and *EcoRI* and cloned into pMV262, an *E. coli–Mycobacterium* multi-copy shuttle vector, under the transcriptional control of the T7 promoter. Digestion

of pMV262 with *XbaI* and *HindIII* allowed further subcloning of icd_{opt} (Ser113Ala) into pMV306, another *E. coli–Mycobacterium* single-copy shuttle vector. For growth in LB broth or alternatively on 7H11 plates kanamycin was used as an antibiotic selection marker.

Electroporation of the plasmids pMV262 icd_{opt} (Ser113Ala) and pMV306 icd_{opt} (Ser113Ala) were carried out using a standard protocol.

For electroporation 3 µl of the plasmids pMV306 (control) and pMV306 icd_{opt} (Ser113Ala)was used. After recovery, cells were plated on 7H11 plates containing kanamycin. The plates were incubated at 37ºC for about 3 weeks or until colonies were spotted.

icd_{opt} (Ser113Ala) from pMV262 and pMV306 was amplified by PCR with primers that allowed to check for proper insertion of the gene into the plasmid. In addition, sequencing of icd_{opt} (Ser113Ala) allowed to check for random point mutations.

2.2.6 Genetic Deletion of BCG icd-1 and icd-2 genes

The *icd-1* and *icd-2* genes were disrupted by allelic exchange method using the pYUB854 plasmid (Bardarov et al., 2002) displayed in Figure 2.2. The 5'-flank and 3'-flank of the target loci (Figure 2.3) where amplified by PCR and subcloned into pCR2.1 TOPO plasmid according to the instruction of the manufacturer. Primers used to amplify the 5'-flank and 3'-flank of the target loci are listed in table 2.1. The 5'-flank and 3'-flank were cloned on either side of *res-hyg-res* gene cassette of the pYUB854 plasmid. A *sacB-lacZ* cassette was excised from the pGOAL17 (Parish and Stoker, 2000) and ligated into

the PacI site of the pYUB854 plasmid. The final plasmids were UV-irradiated as described earlier (Hinds et al., 1999) and electroporated into BCG. The allelic exchange (Figure 2.4) was screened and confirmed by PCR in the white transformants resistant to hygromycin (Table 2.2).

Table 2.1 | **Details of the cloning procedure for the genes *icd-1* and *icd-2*.**

Gene of interest and replacement site	**Fragment description**	**Primer sequence**
icd-1 (1230 bp) replacement of the base pairs 100-1120 with *hyg*	1040bp *AflII-XbaI* fragment displaying the 5' region of *icd-1*	forward primer [5'-ATCTTAAGTGGTGGCCGAATGCACGACGA-3'] reverse primer [5'-ATTCTAGAATAAGCATGTCCTTGATGAGCTT-3']
	1011bp *HindIII-SpeI* fragment displaying the 3' region of *icd-1*	forward primer [5'-ATAAGCTTAGATGACCAAGGACCTCGCGAT-3'] reverse primer [5'-ATACTAGTTAGTGTCGGCTCTATGCGCAGT-3']
icd-2 (2238 bp) replacement of the base pairs 93-2093 with *hyg*	968 bp *AflII-XbaI* fragment displaying the 5' region of *icd-2*	forward primer [5'-ATCTTAAGTCTCGAATCCAAGTCCGGTGTT-3] reverse primer [5'-ATTCTAGAAAGGCACGCACAATCGGCAGAA-3]
	1085 bp *HindIII-SpeI* fragment displaying the 3' region of *icd-2*	forward primer [5'-ATAAGCTTAGACGTCATCGTGCGAGAGCT-3'] reverse primer [5'-ATACTAGTTGATGCCGCCAGCGCGCCA-3']

Table 2.2 | **Confirmation of allelic replacement.** The Primers depicted in this table were used to generate fragments, which indicated if an allelic replacement had taken place.

Gene *x*	**(i) internal region of gene *x***	**(ii) flanking region 5' end of gene *x***	**(ii) flanking region 3' end of gene *x***
icd-1	316 bp fragment forward primer [5'-TACGAAGAGGAATTCAAGGCGCA-3'] reverse primer [5'-TACCGGCCTGATACTGCCGGT-3']	(+/-999 bp) forward primer at the 5' end of *icd1* [5'-AGGTACTTGGTGGCCGAATGCA-3'] reverse primer sequence within *hyg* [5'-CACGAGCAGACCTCACTAGC-3']	(+/-999 bp) reverse primer at the 3' end of *icd1* [5'- TACCGGCTTTAGTGTCGGCTCT-3'] forward primer sequence within *hyg* [5'-ACGGTTGCTAGCACGCGCA-3']
icd-2	256 bp fragment forward primer [5'-ATCGACAGCATGTTCATGAGCA-3'] reverse primer [5'-AGCGACTCGATCTTGCTGTACA-3]	(+/-999 bp) forward primer at the 5' end of *icd2* [5'-TGCGGCGGTCTCGAATCCAA-3'] reverse primer sequence within *hyg* [5'-CACGAGCAGACCTCACTAGC-3']	(+/-999 bp) reverse primer at the 3' end of *icd2* [5'-TCGCGGCGGTGATGCCGCCA-3'] forward primer sequence within *hyg* [5'-ACGGTTGCTAGCACGCGCA-3']

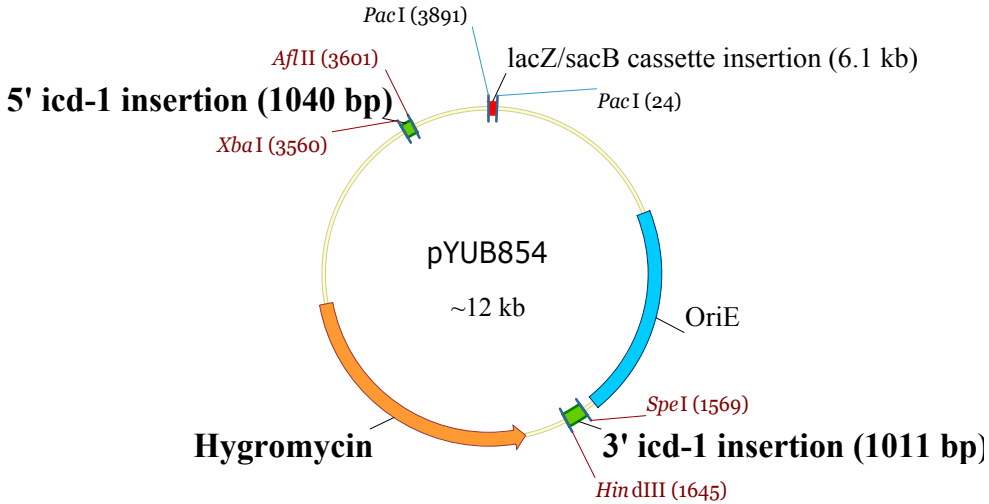

Figure 2.2 | **The final plasmid pYUB854.** This figure shows the final plasmid pYUB854 (approximately 12 kb), with the different inserts: *Hygromycin* (orange), 5' insertion and 3' insertion (green), *lacZ/sacB* gene cassette (red). The different restriction enzymes, specific for each insert, are shown in red. The origin of replication, *oriE*, is shown in blue. Again, the 5' and 3' inserts are representing *icd-1*, but could also stand for *icd-2*.

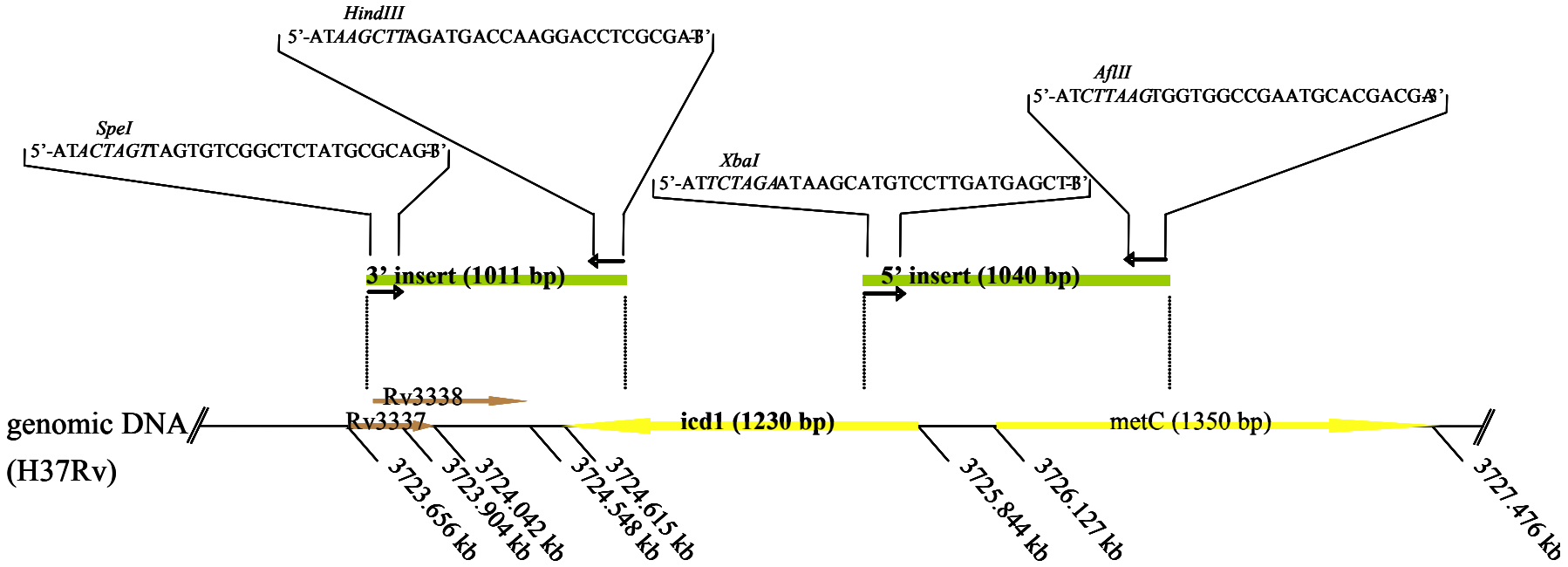

Figure 2.3 | **The location of the target gene**. The figure above shows the location of the target gene *icd-1* (yellow) on the genomic DNA of H37Rv. Also depicted are the adjacent genes *Rv3338*, *Rv3337* and *metC* (yellow and brown); the 3' and the 5' inserts (green) and the corresponding primer sequence. Sites of insertion are represented by dashed lines. In this figure, the gene of interest is represented by *icd-1*, but could also be *icd-2* since the knockout construction was the same.

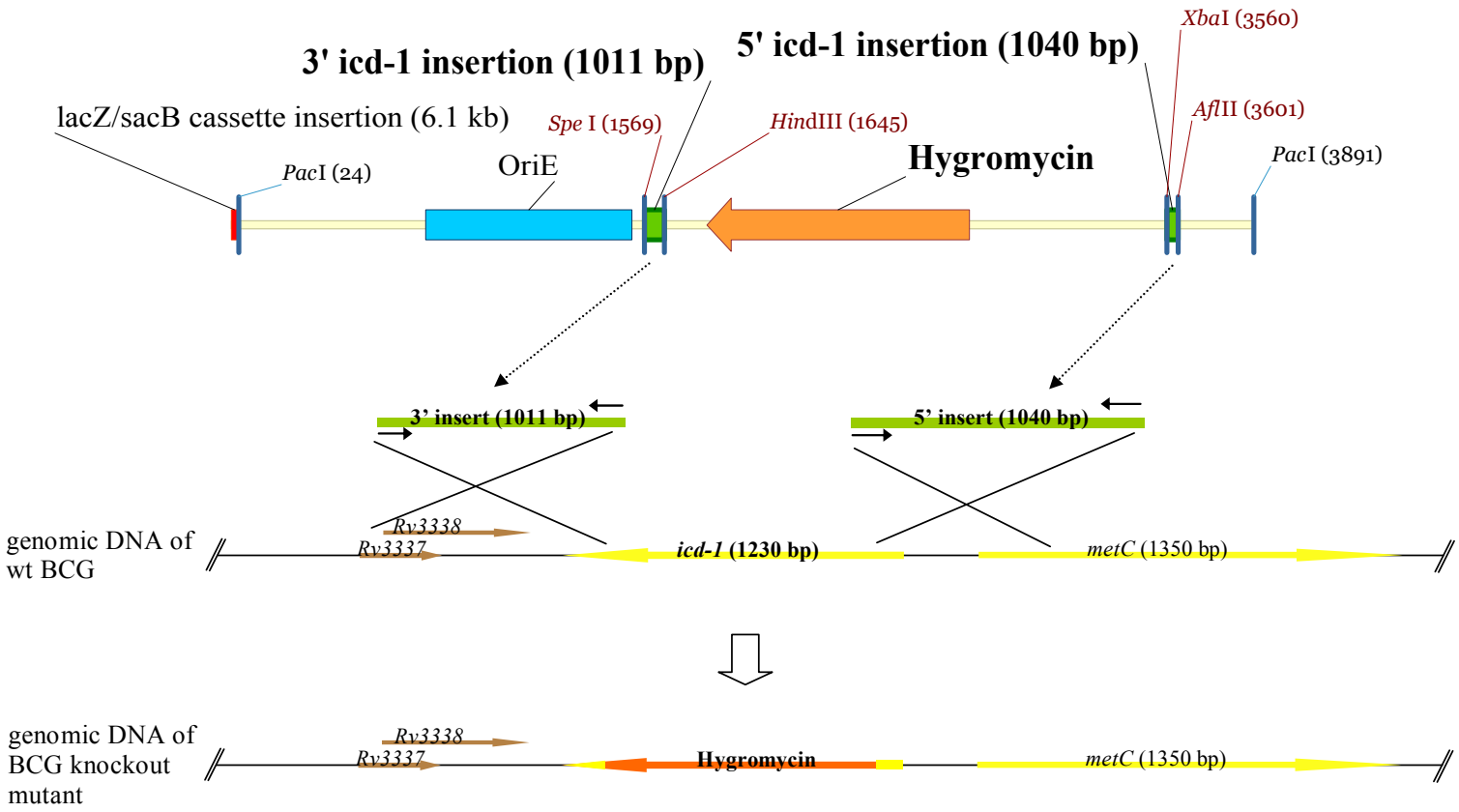

Figure 2.4 | **Homologues recombination.** pYUB854 is linearised. Dashed arrows point from the sites of the 5' and 3' inserts on the plasmid to the sites of insertion on the BCG wt genome. In the event of allelic replacement, *icd-1* is replaced by *hyg* (orange), *oriE* and the *lacZ/sacB* cassette are not inserted into the genome. As a consequence of the double crossover, the expression of the active gene is disrupted. The yellow ends of *hyg* (figure) indicate that both, the 5' and the 3' insert contained around 100 bps of *icd-1*. The homologues recombination was the same for *icd-2*.

2.2.7 ***Growth Assays***

Growth assays were performed with wt BCG, BCG pMV306 icd_{opt}, BCG pMV306 icd_{opt} (Ser113Ala), BCG *Δicd-1* and BCG *Δicd-2*. Cells were grown on glycerol, glucose and acetate. In addition, wt BCG and BCG *Δicd-2* were also grown in 7H9 base deprived of glutamic acid or alternatively, supplemented with glutamic acid. Assays were carried out using T25 flasks. Starting OD_{600} was 0.02 in a volume of 12 ml. The day of inoculation was defined as day 0. OD_{600} was measured about four times between day 1 and day 8. The first reading point was variable, starting either at day 1, 2 or 3. The data was plotted using the software program GraphPad Prism, version 4 for windows.

2.2.8 MIC_{50} Assays with the Compounds Isoniazid and 3-Nitropropionate

MIC_{50} assays were carried out with the following BCG strains: wt BCG, BCG *Δicd-1* and BCG *Δicd-2*. Stocks of the different BCG strains were grown in complete 7H9 medium until log phase. The cells were washed, OD_{600} was measured and the cells inoculated into medium containing either glycerol, glucose or acetate as sole source of carbon. Starting OD_{600} was 0.02. The compounds Isoniazid (INH) and 3-Nitropropionate (3-NP) were diluted in 90% DMSO and tested at a concentration range of 5 μM to 0.02 μM in case of INH and 1 mM to 1.95 μM in case of 3-NP for all the strains and in all the types of media mentioned above. Plates were incubated for 5 days at 37ºC. Growth inhibition was measured with an optical density at 600 nm. The data was plotted using the software program GraphPad Prism, version 4 for Windows.

2.2.9 Enzyme Assays with Crude Cell Extracts

2.2.9.1 Crude Cell Extraction

The following BCG strains were grown in glucose and acetate medium until log phase: wt BCG, BCG pMV306 icd_{opt}, BCG pMV306 icd_{opt} (Ser113Ala), BCG *Δicd-1* and BCG *Δicd-2*. Afterwards, the strains were washed twice with 7H9 base and resuspended in lysis buffer [25 mM Tris-HCl, 100 mM NaCl, 5 mM $MgCl_2$, 1 mM DTT, 1 protease inhibitor cocktail tablet, EDTA-free (1 tablet/50ml)]. The cultures were bead beated, three times for one minute at full speed and at 4ºC. The samples were centrifuged at 13,200 rpm for 10 min at 4ºC, the supernatants were removed and centrifuged again at 13,200 rpm for 10 min at 4ºC. The protein concentration was measured and the crude cell extracts were stored at 4ºC until use, but not for longer than one week.

2.2.9.2 Enzyme Assays

Enzyme assays were carried out with the cell extracts from all BCG strains mentioned above. The different cell lysates were diluted in assay buffer (25 mM Tris-HCl pH 7.5, 5 mM $MgCl_2$, 100 mM NaCl) to a final concentration of 30 µg/ml. Reactions were initiated by adding a reaction buffer containing 2 mM final concentration of DL-isocitrate and 1 mM final concentration of $NADP^+$. Enzymatic activity was monitored by measuring the production of NADPH spectrophotometrically at 340 nm at the time points 30 min, 60 min, 90 min and 120 min. As controls, 1 mM final concentration of NADPH and 70 nM final concentration of purified ICD-1 and ICD-2 were used. The assays were blanked with the lysates containing 1 mM final concentration of $NADP^+$. The different values were plotted using the software program GraphPad Prism, version 4 for Windows.

Results

3.1 In Quest of the Putative Isocitrate Dehydrogenase Kinase/Phosphatase in BCG: Enrichment of ATP-Binding Proteins

With the objective of identifying the putative Ser/Thr kinase that phosphorylates isocitrate dehydrogenase, we tried to extract ATP-binding proteins (ABPs) from crude cell extracts using the ProteoEnrich ATP-Binders Kit. The experiment was carried out as described in section 2.2.1 of Materials and Methods.

The different fractions (flowthrough/wash/eluate), collected from the affinity column, were used to run an SDS-PAGE. Silver staining of the gel revealed many bands for the flowthrough and wash fractions but none for the eluate fraction. No differences were found between lysates derived glucose grown bacteria and acetate grown bacteria.

3.2 The Phosphoproteom of BCG: Purification of Phosphoproteins

To address the questions if i) ICD-1 and/or ICD-2 were phosphorylated at their amino acid residues serine and/or threonine and ii) the phosphorylation status was in dependence on the carbon source in the culture medium (glucose or acetate), we made use of the Phosphoprotein Purification Kit from Qiagen. The experiment was carried out as described in section 2.2.2 of Material and Methods.

The experiment was carried out with crude cell extracts of either glucose or acetate grown wt BCG. Additionally, the experiment was carried out with crude cell extract of the human lung adenocarcinoma cells (A549). We used these cells as a positive control since the kit was designed for eukaryotic cells.

The flowthrough, wash and eluate fractions were collected from the affinity column and used for Western transfer. Immunodetection of phosphorylated protein revealed i) many bands for the fractions containing the lysate and flowthrough; ii) no bands for the eluate fractions; and iii) overall no noticeable differences between the lysates derived from DS or AS grown bacteria. In case of the A549 cell line, no bands were detected in the flowthrough and wash fractions but by contrast, there were a few bands noticeable in the eluate fractions. This indicates that the procedure worked well in the case of eukaryotic cells. The reason why we were not able to purify phosphoproteins from BCG cell extracts is unclear.

3.3 Expression and Purification of M. tuberculosis ICD-1 and ICD-2 in E. coli

3.3.1 Small Scale Purification

The Gateway system was used for small scale purification of the *M. tuberculosis* proteins ICD-1 and ICD-2. Expression vectors were generated by recombination of a set of entry vectors containing one of the two target proteins (ICD-1 or ICD-2) with destination vectors carrying 8 different N-terminal fusion tags. All expression vectors shared a 6xHis-tag, an S-tag, the PreScission site and two restriction sites specific for integration of the gene of interest. The recombined vectors where directly transformed into the *E. coli* strain Tuner (DE3). The 8 different types of fusion proteins were expressed under the T7 promoter in the transformed cells. The procedure for protein expression is described in section 2.2.3.1 of Material and Methods. Ni-NTA spin columns, containing Ni-NTA silica, a metal chelate chromatography material with high affinity for 6xHis-tagged

proteins, were used to purify the target proteins. SDS-PAGE and Coomassie Blue staining allowed evaluation of the best suited fusion tag to express recombinant ICD-1 and ICD-2 at a high yield and in a predominantly soluble form.

From the different fractions (i.e. soluble protein/insoluble protein/eluted protein), the fraction of insoluble ICD-1 was very big with all fusion tags. Out of the 8 tags, only the *E. coli* N-utilization substance (NusA)-6xHis-S-tag led to a comparatively large amount of soluble protein. Performing gel filtration with ICD-1 fused to this particular tag resulted in a loss of most protein in the void volume. As a consequence, this construct was not considered as the appropriate one. The two fusion proteins containing either the *E. coli* thioredoxin (Trx)-6xHis-S-tag or the *Staphylococcus aureus* Protein A IgG binding double domain (ZZ)-6xHis-S-tag showed a small band on the gel, corresponding to the soluble fraction. Since the insoluble fraction for the ZZ-tag protein was much bigger than the one for the Trx-tagged protein, the latter one was used for continuation. Along with the small fraction of soluble protein obtained for all fusion proteins, the fraction with the eluted/purified protein was also found to be small, no matter which construct was used.

The small scale purification of ICD-2 fusion proteins resulted, in comparison to ICD-1, in a higher yield of soluble protein concerning several constructs. The biggest portion of soluble protein was obtained when ICD-2 was fused to the *E. coli* nonsecreted maltose binding protein (MBP)-tag. In addition, the insoluble fraction was much smaller then the soluble one. Insoluble and eluted fractions had about the same band intensity. This construct was chosen for continuation.

Taken together, the recombinant proteins used for the subsequent large scale purification, size exclusion chromatography and enzyme assay were: ICD-1 fused to a Trx-tag and an adjacent His- and S-tag; and ICD-2 fused to a MBP-tag and a flanking His- and S-tag. The molecular weight (M_w) of Trx was around 17 kDa and the one of MBP approximately 46 kDa. The M_w of ICD-1 (~49 kDa) and ICD-2 (~82 kDa) gave rise to recombinant proteins having a M_w of around 66 kDa and around 128 kDa, respectively. Although the profiles of these two constructs were both not optimal, *i.e.* soluble and purified protein fractions were small, they were the most suitable comparing all the 8 constructs with each other.

3.3.2 Large Scale Purification

Large scale purification was carried out with *E. coli* Tuner (DE3), transformed with ICD-1 fused to Trx-6xHis-S-tag (M_w ~66 kDa) and ICD-2 fused to MBP-6xHis-S-tag (M_w ~128 kDa), in 1 litre culture each. Purification was carried out as described in section 2.2.3.2 of Materials and Methods. The different fractions (flowthrough/wash/eluate) obtained from IMAC were collected and loaded onto a SDS gel. The flowthrough fraction appeared mostly as a big smeary band, which allowed us to assume that not all recombinant protein had been able to bind to the column. Loading the flowthrough a second, or even a third or fourth time onto the column, resulted in a remarkably higher yield of eluted protein. During the wash step much recombinant protein was lost as well. Performing a gradient step elution allowed us to chose the appropriate concentration of imidazole for the wash buffer. Forty mM of imidazole seemed to be suitable for the wash process in order to get rid of the majority of impurities and at the same time to prevent a

big loss of recombinant protein. The eluted fractions, which showed the highest colour conversion when mixed with Bradford reagent were combined and the protein concentration was measured using the Protein Quantification Kit from Pierce. This Kit is based on the reduction of Cu^{2+} to Cu^{1+} by protein in an alkaline medium. Colorimetric detection of the cuprous cation (Cu^{1+}) is carried out by using a reagent containing bicinchoninic acid (BCA). Using the GraphPad Prism software, we were able to estimate the protein concentration, which was ~1.19 mg/ml for ICD-1 and ~2.14 mg/ml for ICD-2. From 1 litre culture we extracted about 3 mg of recombinant ICD-1 and 5.4 mg of recombinant ICD-2. Figure 3.1 shows the combined eluted fractions, which were obtained by IMAC.

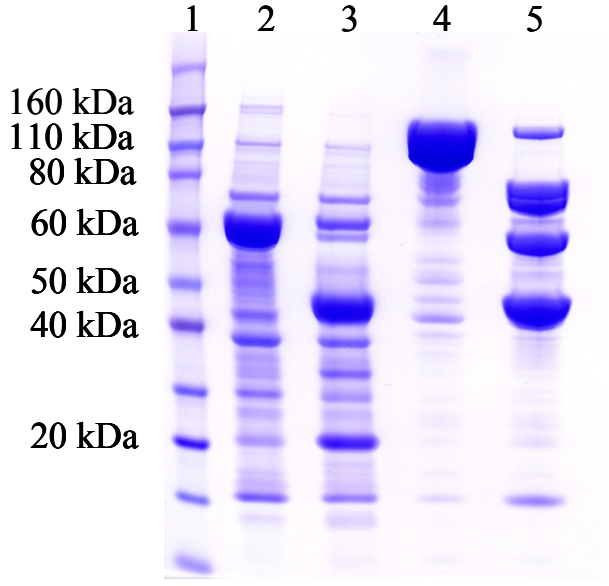

Figure 3.1 | **Purification and cleavage of recombinant ICD-1 and ICD-2.** ICD-1 fused to Trx-6xHis-S-tag and ICD-2 fused to MBP-6xHis-S-tag were purified with IMAC and subsequently cleaved in order to remove their tags. 1, Novex Sharp Protein Standard; 2, ICD-1 with Trx-6xHis-S-tag (M_w ~66 kDa) before cleavage process; 3, cleaved portion of ICD-1 (~49 kDa) and Trx-6xHis-S-tag (~17 kDa); 4, ICD-2 with MBP-6xHis-S-tag (M_w ~128 kDa) before cleavage process; 5, cleaved portion of ICD-2 (~82 kDa) and MBP-6xHis-S-tag (~46 kDa)

Separation of the Trx-6xHis-S-tag and the MBP-6xHis-S-tag from ICD-1 and ICD-2, respectively was achieved by a cleavage process performed with PreScission protease

(Figure 3.1). It has to be mentioned that the portion of uncleaved protein after the cleavage process remained usually quite high, even if an excess of PreScission protease was added to the protein sample (Figure 3.2 A an B).

Gel filtration (also dubbed size exclusion chromatography) allowed for separation of ICD-1 and ICD-2 from their specific tags based on differences in hydrodynamic volume. The theory behind that is the larger the proteins, the less overall volume to traverse over the length of the column and hence, the faster the elution. Proteins of the same size will elute together. Due to size separation it is desirable that the target proteins have a different size from their tags, in order to ensure their elution in different fractions.

When using gel filtration, we faced the problem that the highest absorbance was measured for the first two fractions, which represent the void volume (~1000 mAU for ICD-1 samples, ~500 mAU for ICD-2 samples). Running a gel showed that much of the cleaved target protein along with the yet uncleaved protein was found in this two fractions (Figure 3.2). Further, enzyme assays revealed that this portion of cleaved protein was inactive. The UV peak reflecting the cleaved, active protein was very small, i.e. ~200 mAU for ICD-1 and ~400 mAU for ICD-2.

Considering the efficiency of the purification process, we perceived that there little impurities found in the different fractions. Most impurities were found in the void volume (first two fractions). The remaining fractions consisted predominantly of uncleaved protein, cleaved protein and tag.

A

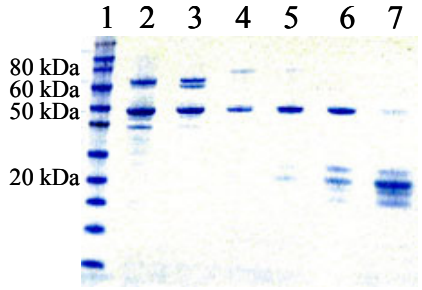

B

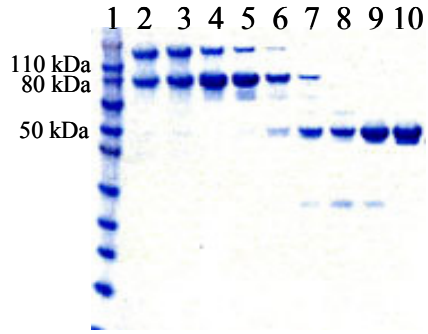

Figure 3.2 | **SDS-PAGE with the different fractions from gel filtration.** In order to separate ICD-1 and ICD-2 from their tags and from impurities, gel filtration was carried out. **A** | Gel filtration with ICD-1. 1, Novex Sharp Protein Standard; 2,3, void volume containing uncleaved ICD-1 (~66 kDa) and cleaved ICD-1 (~49 kDa).The cleaved portion turned out to be enzymatic inactive. 4,5,6, fractions containing cleaved ICD-1. These portions showed enzymatic activity. 6,7, fractions containing the Trx-6xHis-S-tag (~17 kDa).
B | Gel filtration with ICD-2. 1, Novex Sharp Protein Standard; 2,3, void volume containing uncleaved ICD-2 (~128 kDa) and cleaved ICD-2 (~82 kDa). The cleaved portions showed no enzymatic activity. 4,5,6, fractions containing cleaved and active ICD-2; 7,8,9,10, fractions containing the MBP-6xHis-S-tag (~46 kDa).

In order to improve the efficiency of the cleavage process and also to obtain a larger fraction of cleaved active protein, we changed many parameters of the whole large scale protein purification procedure. The modifications included replacing Tris-HCl buffer with sodium phosphate buffer; varying the concentration of imidazole in the wash buffer; changing amplitude, number of cycles and/or intervals of the cycles during the sonication step; introducing a cleavage buffer (50 mM Tris-HCl, 150 mM NaCl, 1 mM DTT, 1 mM EDTA, 0.01% Tween-80) and/or altering the duration of the cleavage process with PreScission protease. None of these changes resulted in a better profile for the active portion of cleaved ICD-1 and ICD-2. However, looking at enzymatic activity, both cleaved proteins revealed to be active.

3.4 Enzyme Assays with Purified ICD-1 and ICD-2

All the fractions containing cleaved ICD-1 and ICD-2 (Figure 3.2) were tested for their enzymatic activity by measuring the absorbance of NADPH (OD_{340}) at four different time points. The experimental procedure is described in section 2.2.4 of Materials and Methods. The fractions containing active enzyme where pooled. ICD-1 contained three fractions of active enzyme (Figure 3.2 A, column 4,5,6) and ICD-2 contained two fractions (Figure 3.2 B, column 4 and 5). The concentration of ICD-1 and ICD-2 was determined and found to be 3.76 μM and 8.61 μM, respectively. The pooled samples were divided into aliquots and stored at -80ºC.

In order to determine the activity of ICD-1 and ICD-2 we created a standard curve (Table 3.1), which depicted the concentration-dependent absorbance of NADPH. One mM NADPH was found to have an OD_{340} of about 1.56. Since we used 1 mM $NADP^+$ for the assays we could roughly estimate the conversion of $NADP^+$ to NADPH and thus, see whether the enzymes were active or not. In addition, a standard curve correlating NADPH absorbance with the percentage of NADPH produced was generated (Figure 3.3).

Enzyme assays were performed with the pooled fractions of ICD-1 and ICD-2. The measured NADPH absorbances during the assays were plotted in a graph (Figure 3.4).
This graph allowed us to estimate the time period in which the NADPH production showed a linear increase. Additionally, by using the standard curve (Figure 3.3) we were

able to estimate the percentage of NADPH produced from 1 mM $NADP^+$ at four different time points (Table 3.2).

Conc.of NADPH [µM]	OD_{340} of NADPH
1000.000000	1.56220
500.000000	0.81085
250.000000	0.41090
125.000000	0.19335
62.500000	0.11130
31.250000	0.06070
15.625000	0.03545
7.812500	0.01855
3.906250	0.00670
1.953125	0.00990
0.9765625	0.00000
0.4882813	0.00000

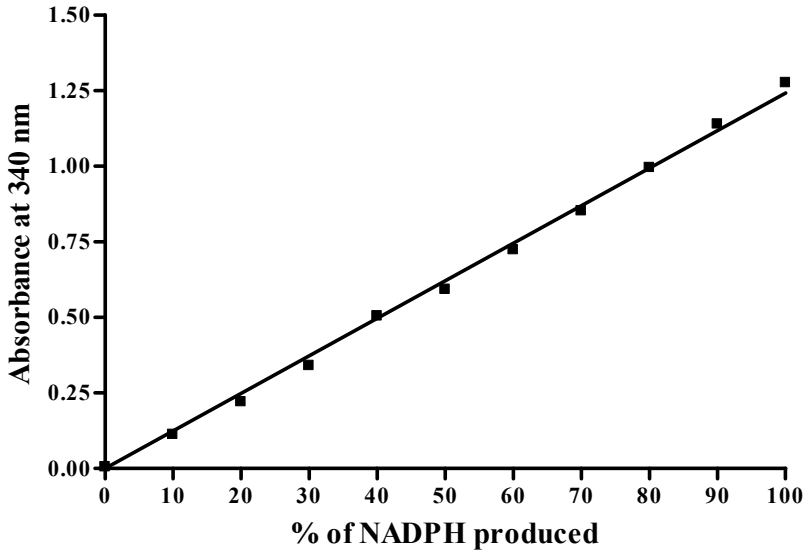

Table 3.1 | **Absorbance of NADPH at different concentrations.** This table was used to generate a standard curve that displayed the concentration-dependent absorbance of NADPH. Measuring the absorbance of NADPH during the enzyme assay and comparing the output values with the values from this table allowed to see whether the enzyme was active or not. Further, this table also allowed to roughly determine how much $NADP^+$ was converted to NADPH.

Figure 3.3 | **Production of NADPH in percentage.** The standard curve was used to link the absorbance of NADPH (OD_{340}) with the percentage of NADPH produced during the assay. 100 % NADPH corresponds to 1 mM NADPH.

We found that 120 min after the initiation of the enzymatic reaction, around 67% NADPH had been produced due to the reaction of ICD-1 with isocitrate. In the case of CD-2, around 34% of NADPH had been produced within the same timeframe.

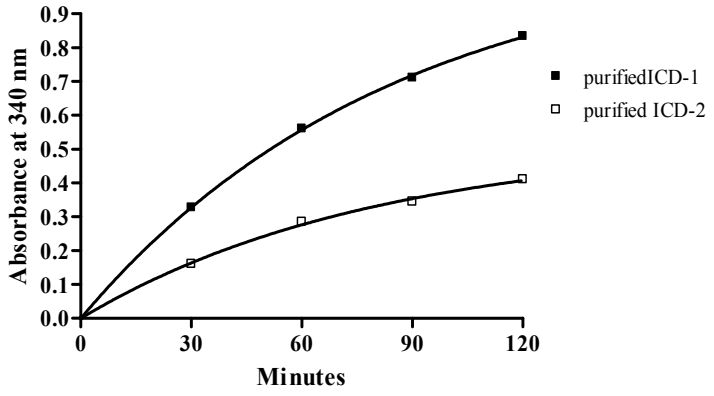

	% of NADPH produced	
	ICD-1	ICD-2
30 min	27	14
60 min	45	24
90 min	57	28
120 min	67	36

Figure 3.4 | **Enzymatic activity and the increase in absorbance of NADPH.** The figure shows the measured absorbance values for NADPH at four time points of the enzymatic assay. There is an increase in absorbance, the longer the assay is run. However, the linear increase of NADPH takes place within the first 30 min. Overall, this figure shows indirectly that the purified ICD-1 and ICD-2 were enzymatically active.

Table 3.2 | **Percentage of NADPH production.** The use of the standard curve (Figure 3.3) allowed us to determine the percentage of NADPH produced at the four different time points of the assay. It was found that the longer the duration of the assay, the more NADPH is produced.

Quantification of the NADPH absorbance values, measured during the linear phase of the assay, allowed us to determine the enzymatic activity U (Table 3.3). Here, one enzyme unit was defined as the amount of NADPH produced in pmol per minute. We found that the activity U for ICD-1 was around 900 and for ICD-2 around 463. Calculation of the specific activity, i.e. activity U per nmol of enzyme, showed how much NADPH was produced per minute per 1 nmol of enzyme. The specific activity for ICD-1 was found to be around 128,671 and for ICD-2 around 66,071.

Activity of purified ICD-1 and ICD-2

	NADPH produced, (pmole)	Activity, U (pmol/min)	Specific Activity, (U/nmol enzyme)
ICD-1	27,021	900	128,671
ICD-2	13,874	463	66,071

Table 3.3 | **Activity U of ICD-1 and ICD-2.** Quantification of the percentage of NADPH produced during the linear phase of the assay, allowed us to calculate the activity and the specific activity for ICD-1 and ICD-2.

In order to blank the assay we mixed the assay buffer with 2 mM final concentration of DL-isocitrate and 1 mM final concentration of $NADP^+$ but excluded the addition of the purified enzyme. The negative control, containing the assay buffer, $NADP^+$ and either ICD-1 or ICD-2 but no DL-isocitrate, showed no enzymatic activity. Conversely, the positive control, consisting of assay buffer along with DL-isocitrate, $NADP^+$ and 1 mM final concentration of NADPH, showed an absorbance of around 1.4.

3.5 Optimisation of E. coli Isocitrate Dehydrogenase

3.5.1 Subcloning of E. coli icd_{opt} into BCG and Determination of Phenotype

The *icd* gene from *E. coli* was modified in a way that i) it could exhibit its enzymatic function in BCG and ii) it could not get phosphorylated by the putative Ser/Thr kinase of BCG. Hence, the enzyme would be rendered in a permanently active state. The gene sequence and the modifications are described and illustrated in section 2.2.5.1 of Materials and Methods.

To accomplish the first condition, multiple adenines and thymidines of the *E. coli icd* gene sequence were replaced by guanines and cytosines (GCs). This was done due to the unusual feature of the *M. tuberculosis* genome. Its base composition shows a high and uniform GC content (65.6%) throughout the genome. Base exchange should allow expression and enzymatic activity of the modified *E. coli icd* gene in BCG. Regarding the second condition, much is known about the regulation of the branch point and its key players ICD, ICL, ICDK/P in *E. coli*. In contrast, little is known about this regulation in *M. tuberculosis*. Thus, the *E. coli icd* gene was chosen for inhibition of ICD phosphorylation since the mechanism behind is established. Overall, by overexpressing the modified *icd* gene, dubbed icd_{opt}, in BCG, we aimed to dysregulate the branch point and hence, proof the concept that the branch point in BCG is regulated in analogy to the one in *E. coli*.

Sequence alignment, carried out using NCBI BLAST, showed a sequence identity of 82% between *E. coli icd* and icd_{opt}. Importantly, the alignment also showed that no gaps were introduced.

The icd_{opt} gene was cloned into the final vector pMV306 and transformed into wt BCG before plated on 7H11 agar plates. Around three weeks after plating, we counted about the same number of colonies for plates containing either BCG with the empty pMV306 plasmid (control) or BCG transformed with pMV306 icd_{opt}. However, the colonies differed in their size. Colonies of the control strain were much bigger than the ones with the modified gene. This fact let us assume that the construct had a toxic effect on the cells, thus delaying cell growth. Further, since the number of colonies for both

transformants was about the same, we also assumed that *icd*$_{opt}$ had, at least phenotypically, no effect. The absence of phenotypical differences was also observed when we carried out growth assays and enzyme assays (for procedure refer to section 2.2.7 and 2.2.9) with wt BCG (control) and BCG pMV306 *icd*$_{opt}$. We found no major differences between them, neither in their growth behaviour (data not shown) nor in their enzymatic activity (Figure 3.5).

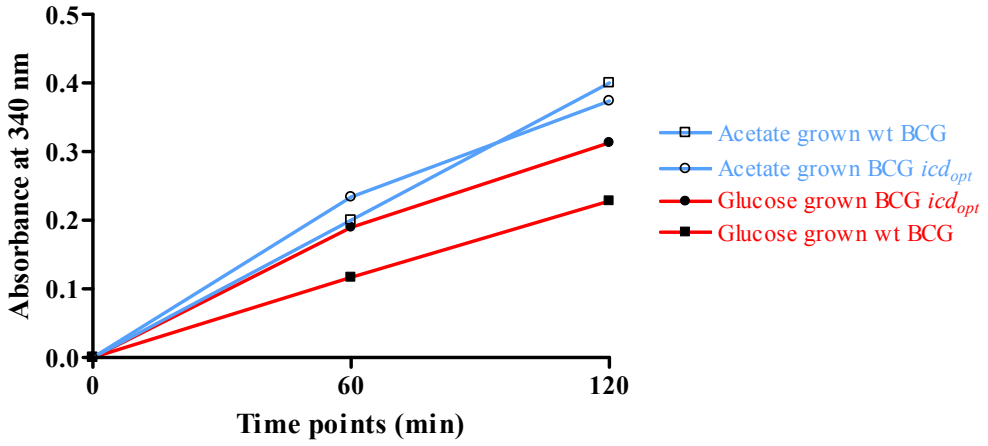

Figure 3.5 | **Enzyme assays with BCG *icd*$_{opt}$ (Ser113Ala).** Enzyme assays were carried out with BCG pMV306 *icd*$_{opt}$ and wt BCG (control). No major differences in enzymatic activity were found between the two constructs when grown either on glucose or on acetate.

3.5.2 Site Directed Mutagenesis of icd$_{opt}$

The introduction of a point mutation into the *icd*$_{opt}$ gene could possibly solve both problems: i) diminish the activity of the *icd*$_{opt}$ gene product (ICD$_{opt}$), and so reduce its toxicity to the cell; and ii) prohibit phosphorylation by substituting serine with alanine at position 113 of ICD$_{opt}$. As mentioned earlier, the isocitrate dehydrogenase of *E. coli* is phosphorylated/dephosphorylated by the ICDK/P at its serine 113. The procedure for

introducing a point mutation into *icd*$_{opt}$ is described in section 2.2.5.2 of Materials and Methods.

After subcloning the insert from pBSK into pMV262 and further into pMV306, wt BCG was transformed with either pMV306 alone (control) or pMV306 containing *icd*$_{opt}$ (Ser113Ala). As before, the number of colonies found on 7H11 plates were about the same for both strains. Additionally, the size of the colonies was about the same too.

We checked for proper insertion of *icd*$_{opt}$ (Ser113Ala) into pMV262 by designing appropriate primers. Further, from two clones, pMV306 *icd*$_{opt}$ (Ser113Ala) was digested with *XbaI* and *HindIII* in order to assure that *icd*$_{opt}$ had been inserted (Figure 3.6).

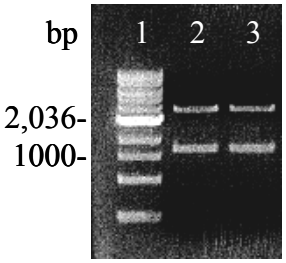

Figure 3.6 | **Confirmation of proper insertion of *icd*$_{opt}$ (Ser113Ala) into pMV306.** Two clones of pMV306 harbouring *icd*$_{opt}$ (Ser113Ala) were digested with *XbaI* and *HindIII*. 1, 1 Kb DNA ladder; 2, upper band displays the digested plasmid (2744 bp) and the insert *icd*$_{opt}$ (1251 bp) of clone 1; 3, clone 2, same appearance as clone 1.

In order to check for the site directed point mutation, and also to make sure that during the subcloning process no other mutation was introduced, we sequenced the whole gene *icd*$_{opt}$ (Ser113Ala) after insertion into pMV306. Using NCBI BLAST we found that the point mutation at position 323 (gene level) was present and further, no other mutation was introduced.

3.5.3 Determination of icd_{opt} (Ser113Ala) Phenotype: Growth Assays and Enzyme Assays

The two different assays, growth assay and enzyme assay, are described in section 2.2.7 and 2.2.9 of Materials and Methods. By carrying out these assays we found no major differences between the phenotypes of wt BCG and BCG pMV306 icd_{opt} (Ser113Ala). The growth assays (Figure 3.7) showed that BCG harbouring pMV306 icd_{opt} (Ser113Ala) grew about the same or somewhat slower than wt BCG, regardless of the type of carbon source used. BCG grown on acetate grew generally faster than BCG grown on glucose.

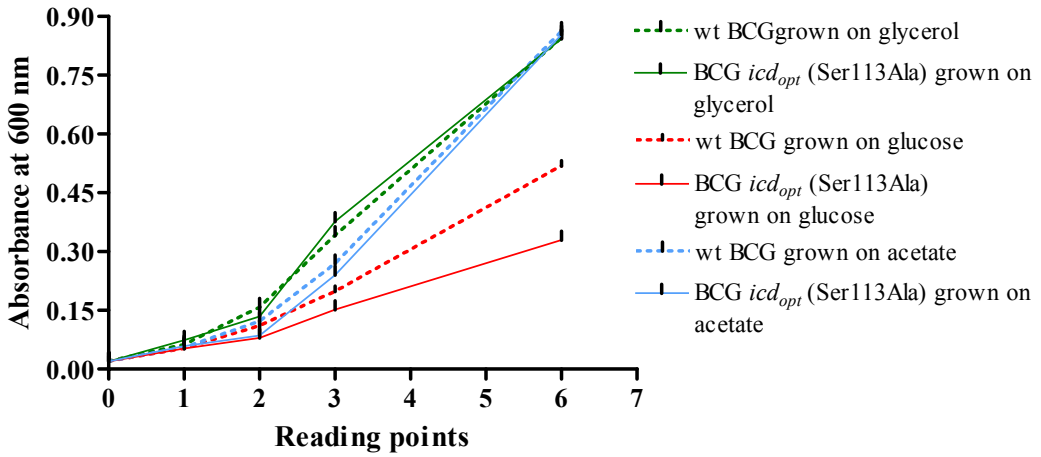

Figure 3.7 | **Growth assays with BCG icd_{opt} (Ser113Ala).** Growth assays were carried out with BCG icd_{opt} (Ser113Ala) and wt BCG (control). The figure shows that even after introduction of a point mutation into icd_{opt}, which would render the overexpressed enzyme in a permanent active state, no major phenotypic differences could be found between the transformed and the control strain.

The enzyme assays (Figure 3.8) showed that the activity of isocitrate dehydrogenase was higher when BCG expressing ICD_{opt} (Ser113Ala) was grown on acetate than on glucose. The same was observed with wt BCG that was used as a control. Generally, enzymatic activity was slightly lower in the transformed strain than in wt BCG.

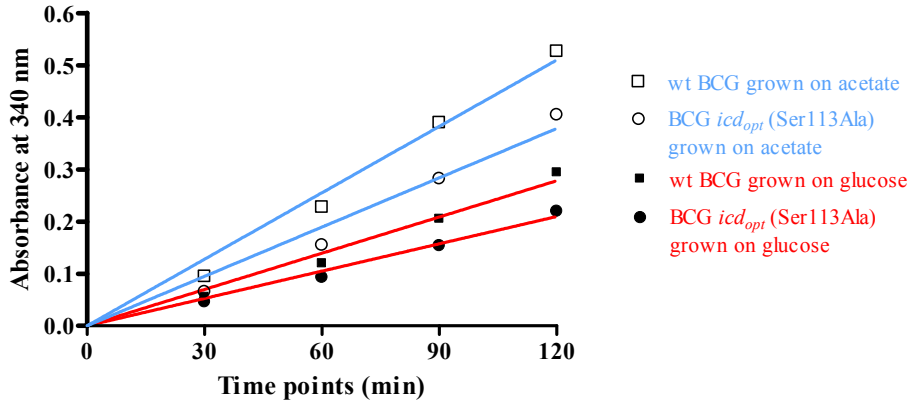

Figure 3.8 | **Enzyme assays with BCG *icd*$_{opt}$ (Ser113Ala).** Measuring the enzymatic activity of BCG *icd*$_{opt}$ (Ser113Ala) revealed only little differences in comparison to wt BCG. wt BCG showed a higher absorbance of NADPH than BCG *icd*$_{opt}$ in both type of media. Overall, a higher absorbance of NADPH was measured in acetate medium than in glucose medium.

However, the expression of ICD$_{opt}$ (Ser113Ala) in BCG did not lead to a dysregulation of the branch point since the growth of the recombinant and parental strains were comparable on glucose and on acetate. Therefore, we decided to stop further investigations at this point.

3.6 BCG Δicd-1 and Δicd-2 Knockout Mutants

Deletion of the BCG genes *icd-1* and *icd-2,* by replacing the internal gene sequence with a hygromycin resistance cassette, was carried out as described in section 2.2.6 of Materials and Methods.

As part of the vector construction, 5' and 3' fragments had to be generated and subcloned into a pCR2.1-TOPO plasmid vector. Concerning both knockout constructs, multiple

TOPO plasmid vectors had to be sent in for sequencing, in order to obtain 5'and 3' inserts without any point mutations.

All BCG transformants, generated by electroporation, were grown on 7H11 agar plates containing hygromycin, sucrose and X-gal, thus, allowing only transformants with a double-crossover to survive. Allelic exchange is only possible by homologous recombination with double crossover, which would insert the *hyg* gene but not the *sacB/lacZ* gene cassette into the mycobacterial genome. The counter-selectable marker *sacB* allowed for positive selection of the allelic exchange mutants, because the expression of the intact *sacB* gene would not allow growth on sucrose. Transformants that have undergone allelic exchange are hygromycin resistant, sucrose sensitive and white in their color since *sacB* and *lacZ* are forming a gene cassette. Often, transformants are first checked for hygromycin resistance and then screened for growth on sucrose. Here, they were subjected to hygromycin and sucrose at the same time, thus, creating a double selective pressure. This eventually led to a lower yield of putative double knockouts but allowed for a faster procedure of creating mutants since BCG is a slow growing bacterium and colonies are only visible on the plate after around 3 weeks.

In case of an allelic replacement for the *icd-1* gene, 10 colonies were observed on a total of four plates after around 3 week. In the same timespan, 15 putative knockouts of the *icd-2* gene were observed on a total of four plates. Some of the colonies were tested for allelic replacement by PCR. A knockout event was defined as successful, when the target gene was not detectable on an agarose gel but the 5' and the 3' flanking regions were present. As a control, genomic DNA of H37Rv was amplified by PCR using the same primers as for the knockouts. Amplification was visible for the gene of interest but not for

the flanking regions. Out of the 10 putative *icd-1* knockouts, 7 were subjected to PCR and gel electrophoresis and 5 revealed to be real. In case of *icd-2*, the 9 biggest colonies were picked from the plates and 3 were shown to be real knockouts. The knockout clones of either gene were pooled and kept as glycerol stock at -80ºC. *Icd-1* knockout mutants were also checked for the presence of the *icd-2* gene in their genome, and vice versa. The Figures 3.9 A and 3.9 B show that the genes *icd-1* and *icd-2* had been substituted with the resistance marker *hyg*.

A

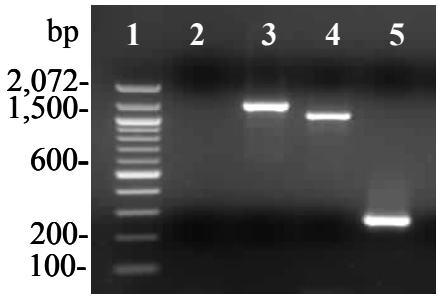

B

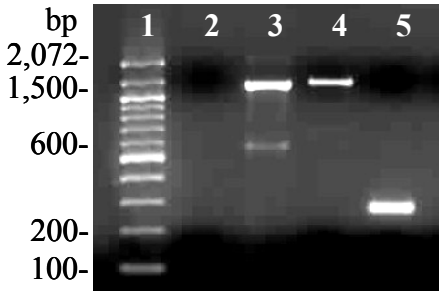

Figure 3.9 | **BCG *Δicd-1* and BCG *Δicd-2* knockout mutants.** The two agarose gels show the different amplified fragments, which indicate that an allelic replacement had taken place. The primers used for the generation of the different fragments are listed in Talbe 2.2.

A | BCG *Δicd-1* knockout mutant. 1, 100 bp DNA ladder; 2, deleted *icd-1* gene (internal fragment, 316 bp); 3, flanking region 5' end (+/-999 bp); 4, flanking region 3' end (+/-999 bp); 5, *icd-2* internal region (256 bp).

B | BCG *Δicd-2* knockout mutant. 1, 100 bp DNA ladder; 2, deleted *icd-2* gene (internal fragment, 256 bp); 3, flanking region 5' end (+/-999 bp); 4, flanking region 3' end (+/-999 bp); 5, *icd-1* internal region (316 bp).

3.7 Characterisation of the BCG Knockout Phenotypes

3.7.1 Growth Assays

Growth assays were carried out with the strains wt BCG, BCG *Δicd-1* and BCG *Δicd-2* and are described in section 2.2.7 of Materials and Methods. The objective of using this assay was to compare the growth behaviour of the different knockout mutants with wt BCG, combined with the effect of the culture medium. Three types of culture media were used: BCG culture medium with glycerol as main carbon source; BCG culture medium with glucose as sole carbon source; BCG culture medium with acetate as sole source of carbon.

As it is shown in Figure 3.10, the growth behaviour of wt BCG, BCG *Δicd-1* and BCG *Δicd-2* is about the same, independently from the carbon source in the culture medium.

A

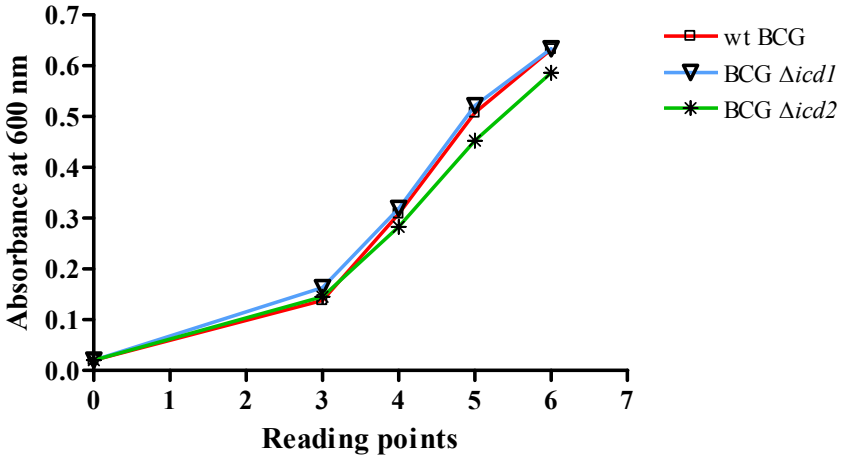

B

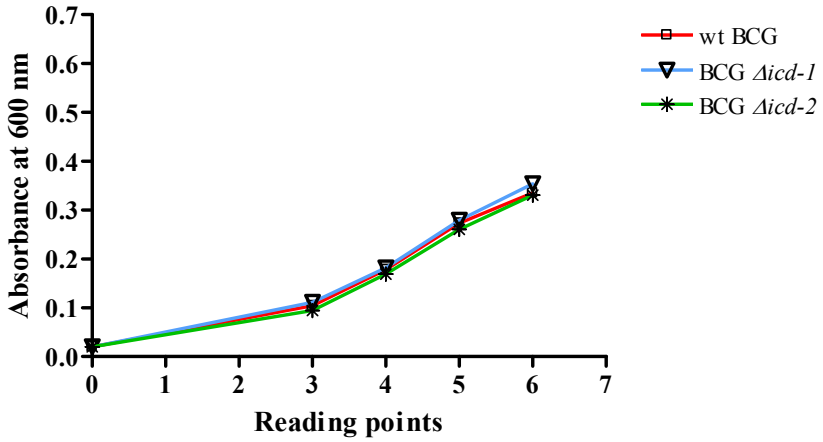

C

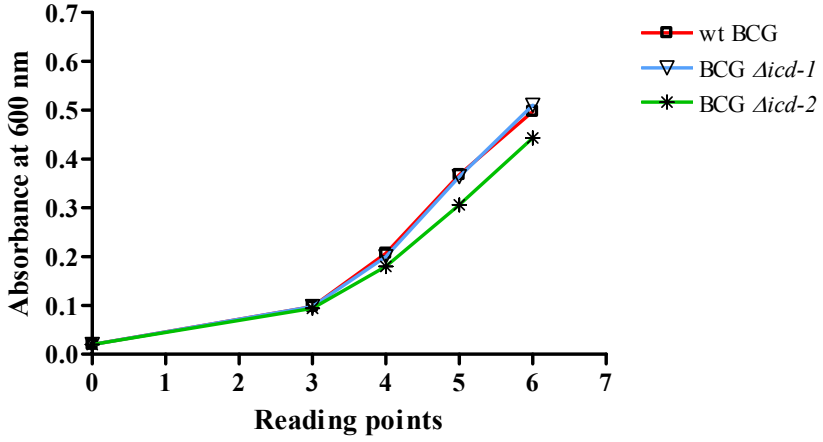

Figure 3.10 | **Growth assays with wt BCG, BCG *Δicd-1* and BCG *Δicd-2* on different carbon sources.** All the figures show that for each carbon source, the three different strains exhibit the same growth behavior. **A** | The strains were grown on glycerol. **B** | Bacteria were grown on glucose. **C** | Bacteria were grown on acetate.

3.7.2 Enzyme Assays

Enzyme assays were carried out with the cell extracts from wt BCG, BCG *Δicd-1* and BCG *Δicd*-2. The experimental procedure is described in section 2.2.9.2 of Materials and Methods.

For this type of assay bacteria were grown either on glucose or on acetate. Measuring NADPH absorbance we found that both, wt BCG and BCG *Δicd-1* were enzymatically active (Figure 3.11). Activity was about the same within one defined culture medium. Additionally, enzymatic activity was higher in lysates from bacteria grown on acetate than grown on glucose.

Surprisingly, for the BCG *Δicd-2* mutant no enzymatic activity was detected during the assay. This was independently from the carbon source used in the culture medium. Indirectly, this result suggests that ICD-1 is not enzymatically active in BCG. The enzymatic inactivity of this mutant is depicted in Figure 3.11 and 3.12.

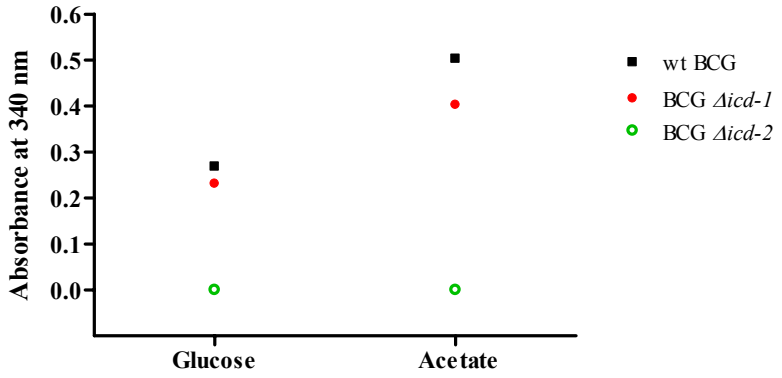

Figure 3.11 | **Enzymatic activity of wt BCG and the knockout mutants BCG *Δicd-1* and BCG *Δicd-2*.** ICD activity was comparable between the parental and BCG *Δicd-1* strains. The enzymatic activity was about the same within one defined medium. Activity was higher in acetate lysates than in glucose lysates. The BCG *Δicd-2* strain was completely deprived of ICD activity.

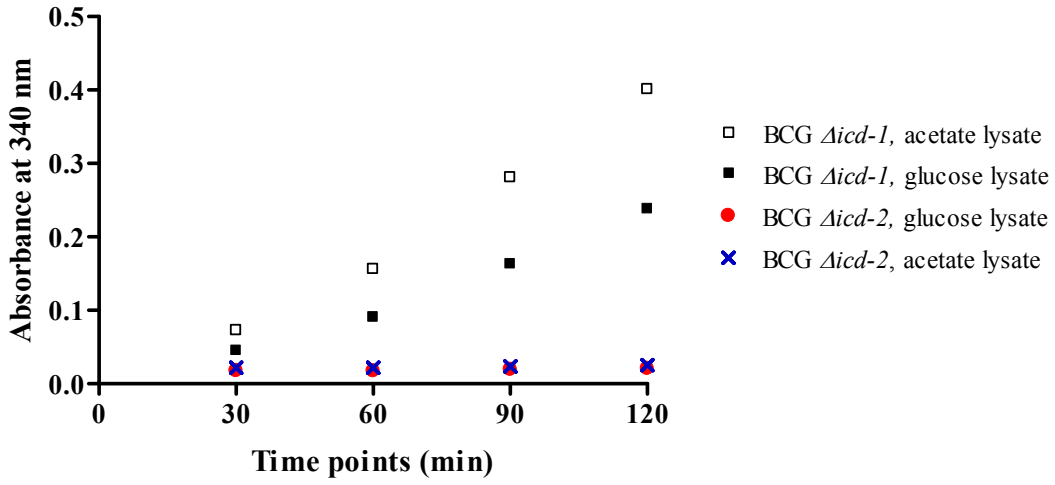

Figure 3.12 | **Enzymatic inactivity of BCG *Δicd-2*.** BCG *Δicd-2* showed no enzymatic activity, neither in lysate derived from glucose grown mycobacteria, nor in lysates derived from acetate grown mycobacteria. In comparison, BCG *Δicd-1* was found to be enzymatically active in both lysates.

3.7.3 The Carbon Flux is Diverted Through the Glyoxylate Shunt in BCG Δicd-2

The assays we have carried out so far led us to observe 1) comparable growth kinetics between all the three BCG strains, on all tested carbon sources and 2) no ICD enzymatic activity in BCG *Δicd-2*, which suggest that ICD-1 does not contribute to the overall isocitrate activity in BCG. If so, the TCA cycle in the BCG *Δicd-2* mutant would be disrupted at the point where isocitrate is converted by ICD to α-ketoglutarate. As a result, carbon flux would necessarily have to be diverted through the glyoxylate shunt in order to permit the bacteria to grow.

In order to test the importance of the glyoxylate shunt on the of growth of BCG *Δicd-2*, we inhibited ICL activity and thus, the operation of the glyoxylate shunt. Inhibition was achieved by carrying out MIC_{50} assays with the compound 3-nitropopionate (3-NP). This

compound is known for its inhibitory effect on ICL. In addition, MIC_{50} assays were carried out with the INH compound, whose inhibitory effect does not target the metabolism of BCG and thus, could be used as a control.

3.7.3.1 MIC_{50} Assays with Isoniazid and 3-Nitropropionate

MIC_{50} were carried out with wt BCG, BCG *Δicd-1* and BCG *Δicd-2*. The experimental procedure is described in section 2.2.8 of Materials and Methods.

Growing the different strains in the presence of different concentrations of INH resulted in an MIC_{50} that laid between ~ 0.19 and 0.35 µM. No major differences were found between the three strains or between the three different carbon sources (Table 3.4).

MIC_{50} in presence of the compound INH

	MIC_{50} [µM]		
Growth Medium	**wt BCG**	**BCG *Δicd-1***	**BCG *Δicd-2***
Glycerol medium	0.3323	0.3220	0.2285
Glucose medium	0.3165	0.3483	0.2216
Acetate medium	0.2090	0.1973	0.1971

Table 3.4 | **MIC_{50} in presence of INH.** Mycobacteria were exposed to INH and grown on glycerol, glucose or acetate medium. The concentration of the compound ranged from 5 µM to 0.02 µM. After 5

The concentration range for 3-NP used in the assays was from 1 mM to 1.95 µM. 3-NP had no inhibitory effect on wt BCG and BCG *Δicd-1* when grown on glycerol or on glucose. However, when these two strains where grown on acetate, 3-NP showed an inhibitory effect with an MIC_{50} around 20 µM for wt BCG and around 10 µM for BCG

Δicd-1. This result was expected since growth on acetate requires the operation of the glyoxylate shunt.

3-NP showed to have an inhibitory effect on BCG *Δicd-2*, no matter if the mutant was grown on glycerol, glucose or acetate. MIC_{50} for glycerol grown BCG *Δicd-2* was around 15 μM and dropped further down to around 3 μM when acetate was the sole source of carbon (Table 3.5).

MIC_{50} in presence of the compound 3-NP

	MIC_{50} [μM]		
Growth Medium	**wt BCG**	**BCG *Δicd-1***	**BCG *Δicd-2***
Glycerol medium	>300	>300	11.5
Glucose medium	>300	>300	15.9
Acetate medium	19.6	10.2	3.5

Table 3.5 | **MIC_{50} in presence of 3-NP**. Mycobacteria were exposed to 3-NP and grown on glycerol, glucose or acetate medium. The concentration of the compound ranged from 1 mM to 1.95 μM. After 5 days of incubation at 37 ºC, the OD_{600} was recorded and the MIC_{50} curve plotted using GraphPad.

These findings support our model that BCG *Δicd-2* is able to direct its carbon flux into the glyoxylate shunt, even when grown on glucose or glycerol. To further confirm our results, we tested whether the mutant strain is able to grow on medium lacking glutamic acid. This amino acid is produced by a reaction involving α-ketoglutarate, which in turn is required for the biosynthesis of amino acids, nucleotides and biological amines.

3.7.3.2 BCG Δicd-2 Strains are Auxotrophic for Glutamate

Growing the BCG *Δicd-2* mutant in 7H9 medium deprived of glutamic acid resulted in a restricted growth rate. In contrast, wt BCG showed no growth impairment when cultured in this medium. Supplementation of glutamic acid to the medium restored growth of BCG *Δicd-2*. As a consequence, BCG *Δicd-2* seems to be auxotrophic for glutamate. This result confirms that BCG *Δicd-2* exhibits no enzymatic activity and hence, cannot produce α-ketoglutarate. This means further that the entire carbon flux of this mutant is diverted into the glyoxylate shunt.

A

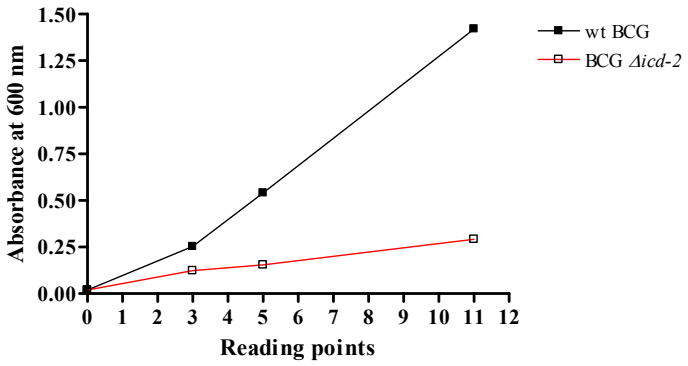

B

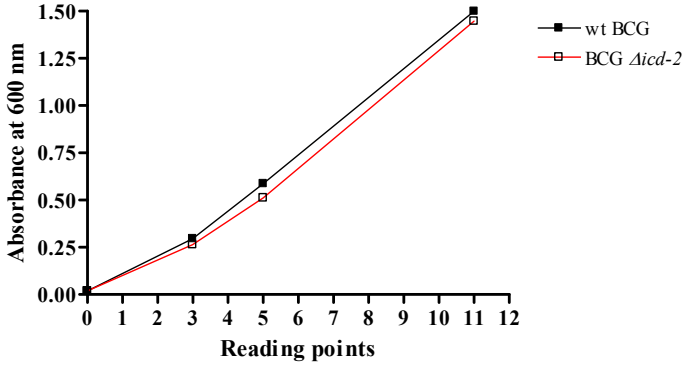

Figure 3.13 | **The dependence of the BCG *Δicd-2* mutant on glutamate.** Wt BCG and BCG *Δicd-2* were grown **A** | in medium deprived of glutamic acid, and **B** | in medium supplemented with glutamic acid. wt BCG grew well under both conditions, whereas growth of BCG *Δicd-2* was impaired in the absence of glutamic acid Growth was restored when glutamic acid was added to the medium.

Discussion

The prototrophic feature and metabolic flexibility of *M. tuberculosis* permit the bacilli to oxidise a variety of carbon substrates such as sugars, tricarboxylic acids, fatty acids and amino acids (Munoz-Elias and McKinney, 2006). This flexibility is necessary since this pathogen survives and persists within macrophages – immune cells, whose task is to kill microbes. Thus, the environment that is encountered by the bacilli within a phagosomal vacuole of a macrophage is very hostile (Smith, 2003). Nutrient starvation within the phagosome, forces the bacilli to shift their primary carbon source to fatty acids that are present in the endosomal-lysosomal network of the host cell (Boshoff and Barry, 2005). If this is true, then this could be an explanation for the high abundance of genes (>150) found in the genome of *M. tuberculosis*, which encode for enzymes involved in the β-oxidation of fatty acids (Honer zu Bentrup and Russell, 2001). The hypothesis, which proposes that host lipids are the preferred carbon source for *M. tuberculosis* during infection, is supported by the finding that bacteria harvested from infected tissues preferentially metabolise fatty acids over carbohydrates (Bloch and Segal, 1956). If host lipids are the main carbon source for *M. tuberculosis* during infection, then a high importance has to be given to the glyoxylate shunt; the pathway that allows bacteria to grow on fatty acids (Gould et al., 2006). In *E. coli* it is known that this bypass is mobilised when bacteria are grown on acetate or fatty acids. Whether the carbon flux is directed to the glyoxylate shunt or continues in the TCA cycle is determined at the branch point of these two cycles. There, isocitrate lyase and isocitrate dehydrogenase compete for their common substrate, isocitrate (Cozzone, 1998). That this pathway is also important in *M. tuberculosis* was supported by the findings that *icl-1* and *icl-2*, which showed to be essential when lipids are the sole source of carbon, are required for growth

in vivo (McKinney et al., 2000). Given that this shunt is absent in humans, and thus, making its enzymes attractive targets for the development of broad-spectrum antimicrobials, makes it even more important (Smith et al., 2004).

During this Master project we wanted to gain insight in the regulation of this branch point in BCG. Unfortunately, little is known about this anaplerotic bypass in *M. tuberculosis*, in contrast to *E. coli*, where this pathway is well studied. Since *E. coli* has only one ICL and one ICD, but *M. tuberculosis* does have two of each, it seems likely that the branch point might be differentially regulated. In addition, *M. tuberculosis* ICD-1 and ICD-2 have distinct phylogenetic affiliations (Banerjee et al., 2005), raising the possibility that they might have different roles in the regulation of the branch point. In the case of *M. tuberculosis* ICDs it has been predicted that the branch point is regulated by phosphorylation of ICD-1 (Singh and Ghosh, 2006).

The putative Ser/Thr kinase

In order to better understand the regulation of the branch point, we aimed in finding the so far unknown, putative *M. tuberculosis* ICDK/P. From studies in *E. coli* it is known that ICDK/P controls the partitioning of the carbon flux at this particular branch point by phosphorylation/dephosphorylation of ICD (Cozzone, 1998). Based on the fact that in *E. coli* the putative ICDK/P is a Ser/Thr kinase (STK) and also a Ser/Thr phosphatase (PstP), it may be possible that the putative kinase in *M. tuberculosis* is also a STK/PstP. To date, the family of eukaryotic-like protein kinases and phosphatases found in the genome of *M. tuberculosis* consists of 11 predicted STKs and at least one PstP (Cowley

et al., 2004). By using a kit specific for enrichment of ATP-binding proteins, we hoped to find the putative kinase in BCG. Unfortunately, we were not able to extract any kinase/phosphatase. One possible reason for the failure might be that this kit is designed for eukaryotic cells, though we applied it to BCG. Given that there are over 500 putative STKs or Tyr protein kinases expressed in humans and over 130 putative protein phosphatases (Greenstein et al., 2005), this kit might not have been sensitive enough to enrich the 11 STKs in BCG. Furthermore, we faced the problem that BCG cells could not be lysed the way it was described in the kit. This is due to the fact that the break down of the mycobacterial cell wall requires bead beating. Hence, the difference in obtaining cell extracts might have had an issue on the enrichment process. Possibly, one of the many parameters such as pH, temperature, reagents etc. might also have had an impact on the procedure.

Expression and Purification of M. tuberculosis ICD-1 and ICD-2 in E. coli

In association with the aim of identifying the putative ICDK/P, we expressed and purified *M. tuberculosis* ICD-1 and ICD-2 in *E. coli.* The two enzymes were thought to be in later use for the conformation of the expected role of the putative kinase/phosphatase. As described in the Results section we were able to purify ICD-1 and ICD-2 and further, show that both of them were active. As an incidental remark it is to mention that the problems faced during the purification process could possibly be solved by making use of the S-tag. This tag was a component of the whole N-terminal fusion tag. An S-tag allows another affinity approach in order to purify target proteins. Instead of using metal chelation chromatography, purification is achieved by the affinity interaction between S-

protein, immobilised on agarose beads, and S-tag. Further, extremely pure, intact target proteins can be obtained using a combination of N-terminal S-tag and C-terminal His-tag sequences (McCormick and Mierendorf, 1994).

For further investigations, these two purified enzymes could be used for identification of the probable ICDK/P. One possibility is to express and purify the 11 STKs from *M. tuberculosis* and to determine, which one can phosphorylate ICD-1 and ICD-2 *in vitro*. Kinase activity could be determined by using radioactive labelled phosphate. Important to mention is that the group of Pedro Alzari (Pasteur Institute, France) developed a panel of the 11 purified *M. tuberculosis* STKs that could be used for this purpose.

Alternatively, by tagging and immobilising the 11 STKs on a resin, they could be used in a pull down experiment. Detection of ICD-1 and ICD-2 in the eluate could be carried out with ICD-1 and ICD-2 specific antibodies or by using mass spectrometry.

The Phosphoproteom of BCG: Purification of Phosphoproteins

One further aspect in the regulation of the branch point involves the finding that in *E. coli* the ICD phosphorylation status is dependent on the carbon source encountered by the bacilli (Cozzone, 1998). Assuming that the regulation of the branch point in BCG would be in analogy to the one in *E. coli*, we hoped to identify proteins phosphorylated at their serine residue(s) when BCG was grown on acetate, but not when grown on glucose. As for the ATP-Binders Kit, we were not able to detect serine phosphorylated proteins by Western blotting, after they had been purified using the Phosphoprotein Purification Kit. Hence, there was no need to carry out 2D gel electrophoresis for analysing the phosphoproteom, derived from BCG grown on different carbon sources. Again, we can

only speculate about the failure. Since this kit was designed for eukaryotic cells, it is interesting to mention that when using eukaryotic cells (A549) , we were able to detect some bands after Western blotting and immunodetection with Ser/Thr antibodies. This could mean that there might be differences in the sensitivity of the kit, depending whether the purification of phosphoproteins is carried out with prokaryotic or eukaryotic cell lysates. Regarding prospective investigations, it shall be mentioned that Macek *et al.* have developed a high-accuracy, high sensitivity method to study the phosphoproteom of any species (Macek et al., 2008). They were able to analyse the Ser/Thr/Tyr phosphoproteom of *E. coli* K12 using this particular method. It involves high accuracy mass spectrometry in combination with phosphopeptide enrichment. For enrichment, strong cation exchange chromatography is used followed by titanium dioxide chromatography (Macek et al., 2008). This method could also be applied in order to obtain a site-specific, *in vivo* phosphoproteom of *M. tuberculosis*. In turn, this could help to elucidate various steps in the regulation of the bacterium's metabolism, possibly also the one involved in the regulation of the glyoxylate shunt/TCA cycle branch point.

Optimised Isocitrate Dehydrogenase

E. coli's isocitrate dehydrogenase was modified with the intension to dysregulate the branch point. However, BCG harbouring icd_{opt} (Ser113Ala) did not show any phenotypic conspicuity, compared to wt BCG, in the growth assays and enzyme assays we have performed. This finding was unexpected since the incapability of phosphorylating ICD_{opt} (Ser113Ala) should not have allowed the diversion of the carbon flux into the glyoxylate bypass. Hence, in presence of acetate, bacterial growth should have been reduced

significantly. The explanation behind this assumption is that the higher pool of unphosphorylated ICD_{opt} should have decreased the probability that ICL binds isocitrate due to the low affinity for the substrate.

However, transformed bacteria grew as fine on acetate as on glucose and further, no major difference in growth kinetics was found when compared to wt BCG. Further, since the enzymatic activity measured in presence and absence of the modified gene was about the same, it seems that somehow overexpression of the construct did not occur or was not sufficient.

The lack of dysregulation suggests a very high robustness of the branch point in mycobacteria. This robustness might be due to the presence of two *icd* genes, or alternatively by some fundamental differences in the regulation of the branch point between *E. coli* and mycobacteria.

Since dysregulation of the branch point could not be achieved using this model, we decided to stop further investigations here. Therefore, we constructed two knockout mutants, one with a disrupted *icd-1*, the other with a disrupted *icd-2* gene.

BCG Δicd-1 and Δicd-2 Knockout Mutants

By knocking out the two genes, whose proteins function at the branch point, we hoped to find alterations in the regulation of this site. Further, since both mutants display loss-of function phenotypes, we also hoped in gaining insight into the nature of ICD-1 and ICD-2.

We initially showed that there was no difference in the growth kinetic between the BCG parental strain, BCG *Δicd-1* and BCG *Δicd-2* on all carbon sources that were tested.

These observations suggested that the deletion of one of the ICD genes was not sufficient to compromise the regulation of the branch point.

However, when the enzyme assays were carried out with the cell free extracts of the mutant strains, we found that the BCG *Δicd-2* strain was completely deprived of ICD activity. The ICD activity was comparable between the parental and BCG *Δicd-1* strains. Taken together, these data suggested that ICD-1 is enzymatically not active in BCG and thus, the whole isocitrate dehydrogenase activity derives from ICD-2. In addition, these data suggested that the TCA cycle can be interrupted at the level of isocitrate dehydrogenase in BCG.

If ICD-1 is effectively enzymatically inactive, then there is need to explain why we did not observe differences in the growth kinetics between BCG *Δicd-2* and the other two strains. From what is known in *E. coli*, one should have expected a growth impairment for BCG *Δicd-2* in glycerol and glucose, and no growth on acetate (Helling and Adams, 1970). Thus, an interruption of the TCA cycle at the point, where isocitrate is converted to α-ketoglutarate, would have resulted in an impass in terms of energy production and a deficiency in amino acid synthesis (because α-ketoglutarate is an essential precursor intermediate for amino acid synthesis). Also to mention is that in *E. coli* the glyoxylate shunt is turned off, whenever there is access to a more easily metabolisable carbon source (*i.e.* glycerol or glucose) (Cozzone, 1998). However, a flux of carbon is theoretically possible if ICL and malate synthase would be expressed on glucose. To test this possibility, we used the specific ICL inhibitor 3-nitropropionate (3-NP) (Sharma et al., 2000). In *M. tuberculosis* wt, 3-NP inhibits the growth of the bacteria on acetate (Sharma

et al., 2000). As expected, there was no inhibitory effect of 3-NP for BCG *Δicd-1* and for the parental strain when grown on glucose or on glycerol. However, the BCG *Δicd-2* strain was found to be sensitive to 3-NP, not only when grown on acetate, but also when grown on glycerol or glucose. Importantly, the minimal inhibitory concentrations of 3-NP in BCG *Δicd-2* were similar in all media. From this, we concluded that the entire carbon flux in BCG *Δicd-2* is diverted through the glyoxylate shunt, and this independently from the carbon source present in the medium. If this is the case, then this might indicate that the glyoxylate bypass does not need the operation of the TCA cycle in terms of energy and carbon metabolism.

However, our observations do not explain how BCG *Δicd-2* can multiply as efficiently as the parental strain. If the entire carbon flux is directed through the glyoxylate shunt due to the interruption of the TCA cycle, then the question remains, how the bacteria obtain α-ketoglutarate and synthesise amino acids. α -ketoglutarate is normally produce in the NADP-dependent ICD reaction and is required for ammonium assimilation through the glutamine synthetase-glutamate synthase (GS-GOGAT) pathway. It is a key metabolite in the linkage of nitrogen and carbon metabolism. (Muro-Pastor et al., 1996).

This conflict was resolved by demonstrating that BCG *Δicd-2* is unable to multiply in the absence of glutamic acid in the culture medium. This auxotrophic phenotype suggests that α-ketoglutarate is not produced by BCG *Δicd-2*.

Quantification of α-ketoglutarate in cell lysates from the parental and BCG *Δicd-2* strains should lead to no detection of α-ketoglutarate in the mutant strain. In contrast, α-ketoglutarate should be detectable in the parental strain.

To resume, our results suggest that ICD-2 is the only isocitrate dehydrogenase enzyme active in BCG. The reason why ICD-1 is not enzymatically active is not clear, but could be explained by a lack of expression or by constitutive phosphorylation of the enzyme at the active site. That a differential expression of the two isoforms during differential stages and conditions of growth cannot be ruled out, even though the enzymes have identical enzymatic function, has further been mentioned by Banerjee *et al.* (Banerjee et al., 2005). Experiments with *Vibrio sp.* showed that ICD-1 and ICD-2 are differentially regulated *in vivo* by various growth conditions. ICD-1 was induced by acetate, while ICD-2 remained almost unchanged (Ishii et al., 1993). Thus, differential expression of isocitrate dehydrogenases has been found in other bacteria. Examine the transcriptom of BCG, in association of the possible differential expression of *icd-1* and *icd-2* (or the lack of expression of ICD-1) in dependence on carbon sources, could help in understanding the regulation of the branch point.

Since the measured enzymatic activities of purified ICD-1 and ICD-2 were similar, it seems reasonable that *in vivo* ICD-1 might be constitutively phosphorylated. Singh *et al.* demonstrated, using a modelling system that carbon flux through the glyoxylate shunt was only allowed when both, ICD-1 and ICD-2 where more than 70% inactivated (Singh and Ghosh, 2006). Having ICD-1 in a constitutively phosphorylated state would lower the threshold, which is required to direct the carbon flux through the glyoxylate bypass. Though, our finding that in BCG *Δicd-2* the glyoxylate shunt is operating also during growth on glycerol and glucose, suggests that the shunt is constitutively expressed.

Overall it seems that the glyoxylate shunt produces enough carbon and energy for the bacilli to survive.

Looking at BCG *Δicd-1* we found that it grows well in glucose and in presence of 3-NP. In other words, it seems that the TCA cycle is functioning and thus, ICD-2 enzymatically converts isocitrate to α-ketoglutarate. In presence of acetate and 3-NP growth is impaired due to the fact that fatty acids do require an operating glyoxylate shunt to generate some biomass. If ICD-1 is constitutively phosphorylated, the question remains how ICD-2 is regulated. Possibly, the regulation is based on allosteric effectors. In *E. coli* it has been found that ICD is strongly inhibited by glyoxylate plus oxaloacetate in combination (Cozzone, 1998). It would be interesting to investigate if ICD-2 is regulated allosterically.

Leaving the speculations about the nature and regulation of ICD-1 and ICD-2 aside and coming back to the putative ICDK/P, it seems that out of the 11 predicted STKs, a putative candidate could be PknG. In *E. coli* it was found that ICD showed to be dispersed in the cytoplasm (Yasutake et al., 2003). In *M. tuberculosis,* only two out of the 11 STKs are predicted to be located in the bacterial cytoplasm. One of them is PknG. The *pknG* gene is located in an operon with *glnH,* which encodes an extracellular glutamine-binding protein. In other bacteria, *glnH* was found to be induced under nitrogen-limiting conditions. This is interesting in terms of the findings from the experiments with *Vibrio sp*. (Ishii et al., 1993). Further, it has been hypothesised that the *M. tuberculosis* PknG participates in the metabolism of poly L-glutamate/glutamine (Cowley et al., 2004).

Overall, if PknG is the putative ICDK/P, deletion of the *pknG* gene in BCG *Δicd-2* should restore the enzymatic activity of ICD-1 and also render the strain insensitive towards 3-NP during growth on glucose and glycerol.

Taken together, our results suggest that ICD-2 is the only active isocitrate dehydrogenase enzyme in BCG. Further, the inactivity of ICD-1 requires a constantly operating glyoxylate shunt in order to permit growth of the BCG *Δicd-2* mutant. Thus, we predict that ICD-1 and ICD-2 differ in their function and possibly in the way they are regulated by the putative kinase/phosphatase.

Forthcoming investigations involving ICD-1 and ICD-2 could entail explanations why there are two isocitrate dehydrogenases in *M. tuberculosis*. Revelation of possible functional differences between the two isocitrate dehydrogenases could lead to the understanding of the branch point regulation. It could also allow to define the role of the putative ICDK/P in *M. tuberculosis*. This in turn might be supportive in finding the particular kinase/phosphatase.

Bibliography

Journals

ANDERSEN, P., MUNK, M. E., POLLOCK, J. M. & DOHERTY, T. M. (2000) Specific immune-based diagnosis of tuberculosis. *Lancet,* 356**,** 1099-104.

BANERJEE, S., NANDYALA, A., PODILI, R., KATOCH, V. M. & HASNAIN, S. E. (2005) Comparison of Mycobacterium tuberculosis isocitrate dehydrogenases (ICD-1 and ICD-2) reveals differences in coenzyme affinity, oligomeric state, pH tolerance and phylogenetic affiliation. *BMC Biochem,* 6**,** 20.

BETTS, J. C., LUKEY, P. T., ROBB, L. C., MCADAM, R. A. & DUNCAN, K. (2002) Evaluation of a nutrient starvation model of Mycobacterium tuberculosis persistence by gene and protein expression profiling. *Mol Microbiol,* 43**,** 717-31.

BLOCH, H. & SEGAL, W. (1956) Biochemical differentiation of Mycobacterium tuberculosis grown in vivo and in vitro. *J Bacteriol,* 72**,** 132-41.

BOSHOFF, H. I. & BARRY, C. E. (2005) A low-carb diet for a high-octane pathogen. *Nat Med,* 11**,** 599-600.

BOSHOFF, H. I. & BARRY, C. E., 3RD (2005) Tuberculosis - metabolism and respiration in the absence of growth. *Nat Rev Microbiol,* 3**,** 70-80.

BRENNAN, P. M., YOUNG, D. B. (2008) Handbook of anti-tuberculosis agents. Introduction. *Tuberculosis (Edinb),* 88**,** 85-6.

BROSCH, R., PYM, A. S., GORDON, S. V. & COLE, S. T. (2001) The evolution of mycobacterial pathogenicity: clues from comparative genomics. *Trends Microbiol,* 9**,** 452-8.

COLE, S. T., BROSCH, R., PARKHILL, J., GARNIER, T., CHURCHER, C., HARRIS, D., GORDON, S. V., EIGLMEIER, K., GAS, S., BARRY, C. E., 3RD, TEKAIA, F., BADCOCK, K., BASHAM, D., BROWN, D., CHILLINGWORTH, T., CONNOR, R., DAVIES, R., DEVLIN, K., FELTWELL, T., GENTLES, S., HAMLIN, N., HOLROYD, S., HORNSBY, T., JAGELS, K., KROGH, A., MCLEAN, J., MOULE, S., MURPHY, L., OLIVER, K., OSBORNE, J., QUAIL, M. A., RAJANDREAM, M. A., ROGERS, J., RUTTER, S., SEEGER, K., SKELTON, J., SQUARES, R., SQUARES, S., SULSTON, J. E., TAYLOR, K., WHITEHEAD, S. & BARRELL, B. G. (1998) Deciphering the biology of Mycobacterium tuberculosis from the complete genome sequence. *Nature,* 393**,** 537-44.

CORBETT, E. L., CHARALAMBOUS, S., MOLOI, V. M., FIELDING, K., GRANT, A. D., DYE, C., DE COCK, K. M., HAYES, R. J., WILLIAMS, B. G. & CHURCHYARD, G. J. (2004) Human immunodeficiency virus and the prevalence of undiagnosed tuberculosis in African gold miners. *Am J Respir Crit Care Med,* 170**,** 673-9.

COWLEY, S., KO, M., PICK, N., CHOW, R., DOWNING, K. J., GORDHAN, B. G., BETTS, J. C., MIZRAHI, V., SMITH, D. A., STOKES, R. W. & AV-GAY, Y. (2004) The Mycobacterium tuberculosis protein serine/threonine kinase PknG is linked to cellular glutamate/glutamine levels and is important for growth in vivo. *Mol Microbiol,* 52**,** 1691-702.

COZZONE, A. J. (1998) Regulation of acetate metabolism by protein phosphorylation in enteric bacteria. *Annu Rev Microbiol,* 52**,** 127-64.

COZZONE, A. J. & EL-MANSI, M. (2005) Control of isocitrate dehydrogenase catalytic activity by protein phosphorylation in Escherichia coli. *J Mol Microbiol Biotechnol,* 9**,** 132-46.

DANIEL, T. M. (2006) The history of tuberculosis. *Respir Med,* 100**,** 1862-70.

DYE, C. (2006) Global epidemiology of tuberculosis. *Lancet,* 367**,** 938-40.

DYE, C., WATT, C. J., BLEED, D. M., HOSSEINI, S. M. & RAVIGLIONE, M. C. (2005) Evolution of tuberculosis control and prospects for reducing tuberculosis incidence, prevalence, and deaths globally. *Jama,* 293**,** 2767-75.

EHRT, S. & SCHNAPPINGER, D. (2007) Mycobacterium tuberculosis virulence: lipids inside and out. *Nat Med,* 13**,** 284-5.

EL-MANSI, M., COZZONE, A. J., SHILOACH, J. & EIKMANNS, B. J. (2006) Control of carbon flux through enzymes of central and intermediary metabolism during growth of Escherichia coli on acetate. *Curr Opin Microbiol,* 9**,** 173-9.

FEDOY, A. E., YANG, N., MARTINEZ, A., LEIROS, H. K. & STEEN, I. H. (2007) Structural and functional properties of isocitrate dehydrogenase from the psychrophilic bacterium Desulfotalea psychrophila reveal a cold-active enzyme with an unusual high thermal stability. *J Mol Biol,* 372**,** 130-49.

FLYNN, J. L. & CHAN, J. (2001) Tuberculosis: latency and reactivation. *Infect Immun,* 69**,** 4195-201.

FRIEDEN, T. R., STERLING, T. R., MUNSIFF, S. S., WATT, C. J. & DYE, C. (2003) Tuberculosis. *Lancet,* 362**,** 887-99.

GOMEZ, J. E. & MCKINNEY, J. D. (2004) M. tuberculosis persistence, latency, and drug tolerance. *Tuberculosis (Edinb),* 84**,** 29-44.

GOULD, T. A., VAN DE LANGEMHEEN, H., MUNOZ-ELIAS, E. J., MCKINNEY, J. D. & SACCHETTINI, J. C. (2006) Dual role of isocitrate lyase 1 in the glyoxylate and methylcitrate cycles in Mycobacterium tuberculosis. *Mol Microbiol,* 61**,** 940-7.

GREENSTEIN, A. E., GRUNDNER, C., ECHOLS, N., GAY, L. M., LOMBANA, T. N., MIECSKOWSKI, C. A., PULLEN, K. E., SUNG, P. Y. & ALBER, T. (2005) Structure/function studies of Ser/Thr and Tyr protein phosphorylation in Mycobacterium tuberculosis. *J Mol Microbiol Biotechnol,* 9**,** 167-81.

HELLING, R. B. & ADAMS, B. S. (1970) Nalidixic acid-resistant auxotrophs of Escherichia coli. *J Bacteriol,* 104**,** 1027-9.

HONER ZU BENTRUP, K. & RUSSELL, D. G. (2001) Mycobacterial persistence: adaptation to a changing environment. *Trends Microbiol,* 9**,** 597-605.

ISHII, A., SUZUKI, M., SAHARA, T., TAKADA, Y., SASAKI, S. & FUKUNAGA, N. (1993) Genes encoding two isocitrate dehydrogenase isozymes of a psychrophilic bacterium, Vibrio sp. strain ABE-1. *J Bacteriol,* 175**,** 6873-80.

JAIN, M., PETZOLD, C. J., SCHELLE, M. W., LEAVELL, M. D., MOUGOUS, J. D., BERTOZZI, C. R., LEARY, J. A. & COX, J. S. (2007) Lipidomics reveals control of Mycobacterium tuberculosis virulence lipids via metabolic coupling. *Proc Natl Acad Sci U S A,* 104**,** 5133-8.

JONES, S. A., JORGENSEN, M., CHOWDHURY, F. Z., RODGERS, R., HARTLINE, J., LEATHAM, M. P., STRUVE, C., KROGFELT, K. A., COHEN, P. S. & CONWAY, T. (2008) Glycogen and maltose utilization by Escherichia coli O157:H7 in the mouse intestine. *Infect Immun,* 76**,** 2531-40.

KAUFMANN, S. H. E. (2001) How can immunology contribute to the control of tuberculosis?. *Nature Reviews Immunology* 1**,** 20-30.

KOUL, A., HERGET, T., KLEBL, B. & ULLRICH, A. (2004) Interplay between mycobacteria and host signalling pathways. *Nat Rev Microbiol,* 2**,** 189-202.

MACEK, B., GNAD, F., SOUFI, B., KUMAR, C., OLSEN, J. V., MIJAKOVIC, I. & MANN, M. (2008) Phosphoproteom analysis of E. coli reveals evolutionary conservation of bacterial Ser/Thr/Tyr phosphorylation. *Mol Cell Proteomics,* 7**,** 299-307.

MCKINNEY, J. D., HONER ZU BENTRUP, K., MUNOZ-ELIAS, E. J., MICZAK, A., CHEN, B., CHAN, W. T., SWENSON, D., SACCHETTINI, J. C., JACOBS, W. R., JR. & RUSSELL, D. G. (2000) Persistence of Mycobacterium tuberculosis in macrophages and mice requires the glyoxylate shunt enzyme isocitrate lyase. *Nature,* 406**,** 735-8.

MILLER, S. P., CHEN, R., KARSCHNIA, E. J., ROMFO, C., DEAN, A. & LAPORTE, D. C. (2000) Locations of the regulatory sites for isocitrate dehydrogenase kinase/phosphatase. *J Biol Chem,* 275**,** 833-9.

MUNNICH, A. (2008) Casting an eye on the Krebs cycle. *Nat Genet,* 40**,** 1148-9.

MUNOZ-ELIAS, E. J. & MCKINNEY, J. D. (2005) Mycobacterium tuberculosis isocitrate lyases 1 and 2 are jointly required for in vivo growth and virulence. *Nat Med,* 11**,** 638-44.

MUNOZ-ELIAS, E. J. & MCKINNEY, J. D. (2006) Carbon metabolism of intracellular bacteria. *Cell Microbiol,* 8**,** 10-22.

MURO-PASTOR, M. I., REYES, J. C. & FLORENCIO, F. J. (1996) The NADP+-isocitrate dehydrogenase gene (icd) is nitrogen regulated in cyanobacteria. *J Bacteriol,* 178**,** 4070-6.

ONYEBUJOH, P., RODRIGUEZ, W. & MWABA, P. (2006) Priorities in tuberculosis research. *Lancet,* 367**,** 940-2.

PETHE, K., SWENSON, D. L., ALONSO, S., ANDERSON, J., WANG, C. & RUSSELL, D. G. (2004) Isolation of Mycobacterium tuberculosis mutants defective in the arrest of phagosome maturation. *Proc Natl Acad Sci U S A,* 101**,** 13642-7.

PIETERS, J. (2001) Entry and survival of pathogenic mycobacteria in macrophages. *Microbes Infect,* 3**,** 249-55.

ROOK, G. A., DHEDA, K. & ZUMLA, A. (2005) Immune responses to tuberculosis in developing countries: implications for new vaccines. *Nat Rev Immunol,* 5**,** 661-7.

RUSSELL, D. G. (2001) Mycobacterium tuberculosis: here today, and here tomorrow. *Nature Reviews Molecular Cell Biology,* 2**,** 569-586

SHARMA, V., SHARMA, S., HOENER ZU BENTRUP, K., MCKINNEY, J. D., RUSSELL, D. G., JACOBS, W. R., JR. & SACCHETTINI, J. C. (2000) Structure of isocitrate lyase, a persistence factor of Mycobacterium tuberculosis. *Nat Struct Biol,* 7**,** 663-8.

SINGH, V. K. & GHOSH, I. (2006) Kinetic modeling of tricarboxylic acid cycle and glyoxylate bypass in Mycobacterium tuberculosis, and its application to assessment of drug targets. *Theor Biol Med Model,* 3**,** 27.

SMITH, C. V., HUANG, C. C., MICZAK, A., RUSSELL, D. G., SACCHETTINI, J. C. & HONER ZU BENTRUP, K. (2003) Biochemical and structural studies of malate synthase from Mycobacterium tuberculosis. *J Biol Chem,* 278**,** 1735-43.

SMITH, C. V., SHARMA, V. & SACCHETTINI, J. C. (2004) TB drug discovery: addressing issues of persistence and resistance. *Tuberculosis (Edinb),* 84**,** 45-55.

SMITH, I. (2003) Mycobacterium tuberculosis pathogenesis and molecular determinants of virulence. *Clin Microbiol Rev,* 16**,** 463-96.

STEWART, G. R., ROBERTSON, B. D. & YOUNG, D. B. (2003) Tuberculosis: a problem with persistence. *Nat Rev Microbiol,* 1**,** 97-105.

TUNDUP, S., AKHTER, Y., THIAGARAJAN, D. & HASNAIN, S. E. (2006) Clusters of PE and PPE genes of Mycobacterium tuberculosis are organized in operons: evidence that PE Rv2431c is co-transcribed with PPE Rv2430c and their gene products interact with each other. *FEBS Lett,* 580**,** 1285-93.

WENDISCH, V. F., DE GRAAF, A. A., SAHM, H. & EIKMANNS, B. J. (2000) Quantitative determination of metabolic fluxes during coutilization of two carbon sources: comparative analyses with Corynebacterium glutamicum during growth on acetate and/or glucose. *J Bacteriol,* 182**,** 3088-96.

WIRTH, T., HILDEBRAND, F., ALLIX-BEGUEC, C., WOLBELING, F., KUBICA, T., KREMER, K., VAN SOOLINGEN, D., RUSCH-GERDES, S., LOCHT, C., BRISSE, S., MEYER, A., SUPPLY, P. & NIEMANN, S. (2008) Origin, spread and demography of the Mycobacterium tuberculosis complex. *PLoS Pathog,* 4**,** e1000160.

YASUTAKE, Y., WATANABE, S., YAO, M., TAKADA, Y., FUKUNAGA, N. & TANAKA, I. (2003) Crystal structure of the monomeric isocitrate dehydrogenase in the presence of NADP+: insight into the cofactor recognition, catalysis, and evolution. *J Biol Chem,* 278**,** 36897-904.

ZAHRT, T. C. (2003) Molecular mechanisms regulating persistent Mycobacterium tuberculosis infection. *Microbes Infect,* 5**,** 159-67.

ZHU, G., GOLDING, G. B. & DEAN, A. M. (2005) The selective cause of an ancient adaptation. *Science,* 307**,** 1279-82.

Books

BERG, J. M., TYMOCZKO, J. L., STRYER, L. (2003) *Biochemie,* Heidelberg, Spektrum Akademischer Verlag.

DANIEL, T. M., BATES, J. H., DOWNES, K. A. (1994) History of Tuberculosis. IN BLOOM, B. R. (Ed.) *Tuberculosis: Pathogenesis, Protection, and Control.* Washington, DC, ASM Press.

DANNENBERG, A. M., ROOK, G. A. W. (1994) Pathogenesis of Pulmonary Tuberculosis: an Interplay of Tissue-Damaging and Macrophage-Activating Immune Response-Dual Mechanisms That Control Bacillary Multiplication. IN BLOOM, B. R. (Ed.) *Tuberculosis: Pathogenesis, Protection, and Control.* Washington, DC, ASM Press.

LEHNINGER, A. L., NELSON, D.L., COX, M. M. (1993) *Principles of Biochemistry,* New York, Worth Publishers.

WHEELER PAUL R., R. C. (1994) Metabolism of Mycobacterium tuberculosis. IN BLOOM, B. R. (Ed.) *Tuberculosis: Pathogenesis, Protection, and Control.* Washington, DC, ASM Press.

WHEELER, P. R., BLANCHARD, J. S. (2005) General Metabolism and Biochemical Pathways of Tubercle Bacilli. IN COLE, S. T., EISENBACH, D. K., MCMURRAY, D. N., JACOBS, W. R. (Ed.) *Tuberculosis and the Tubercle bacillus.* Washington, DC, ASM Press.

YOUNG, M., MUKAMOLOVA, G. V., KAPRELYANTS, A. S. (2005) Mycobacterial Dormancy and Its Relation to Persistence. IN PARISH, T. (Ed.) *Mycobacterium Molecular Microbiology.* Horizon Bioscience.

Electronic Sources

MCCORMICK, M., MIERENDORF, 1994. R. *S-Tag: A Multipurpose Fusion Peptide for Recombinant Proteins.* Novagen, Inc. Available from: www.emdbiosciences.com/docs/docs/LIT/inno01-001.pdf

MEXICO, T. U. O. N, 2008. *UNM Medical Library Introduces New Exhibit - Search for a Cure: Life at Valmora.* Available from: www.unm.edu/~market/cgi-bin/archives/002658.html

SWISS TROPICA INSTITUTE, 2006. *Infection Biology and Epidemiology.* Available from: http://www.infektionsbiologie.ch/

World Health Organization:

Global tuberculosis control: surveillance, planning, financing. WHO report 2006. Geneva, World Health Organization (WHO/HTM/TB/2006.362)

Global tuberculosis control: surveillance, planning financing. WHO report 2008. Geneva, World Health Organization (WHO/HTM/TB/2008.393)

Treatment of Tuberculosis: Guidelines for National Programmes. WHO 3rd. Edition 2003. Geneva, World Health Organization (WHO/CDS/TB/2003.313)

WORLD HEALTH ORGANIZATION, 2009. *Tuberculosis TB.* Available from: http://www.who.int/tb/en/